การแสดงออกและลักษณะสมบัติของคัลมอดุลินและโปรตีนคล้ายคัลมอดุลินจากข้าว

Oryza sativa L.

นายอำนาจ ชินพงษ์พานิช

EXPRESSION AND CHARACTERIZATION OF CALMODULIN AND

CALMODULIN-LIKE PROTEINS FROM RICE *Oryza sativa* L.

Mr. Aumnart Chinpongpanich

A Thesis Submitted in Partial Fulfillment of the Requirements
for the Degree of Master of Science Program in Biochemistry
Department of Biochemistry
Faculty of Science
Chulalongkorn University
Academic Year 2009

Thesis Title   Expression and characterization of Calmodulin and Calmodulin-
                like proteins from rice *Oryza sativa* L.
By   Mr. Aumnart Chinpongpanich
Field of Study Biochemistry
Thesis Advisor Assistant Professor Teerapomg Buaboocha, Ph.D.

Accepted by the Faculty of Science, Chulalongkorn University in Partial Fulfillment of the Requirements for the Master's Degree

…….…………………………...Dean of the Faculty of Science
(Professor Supot Hannongbua, Dr.rer.nat.)

THESIS COMMITTEE

…………………………………… Chairman
(Associate Professor Piamsook Pongsawasdi**,** Ph.D.)

…………………………………… Thesis Advisor
(Assistant Professor Teerapong Buaboocha, Ph.D.)

…………………………………… Examiner
(Associate Professor Tipaporn Limpaseni, Ph.D.)

…………………………………. Examiner
(Assistant Professor Kanoktip Packdibamrung, Ph.D.)

…………………………………. External Examiner
(Assistant Professor Kiattawee Choowongkomon, Ph.D.)

อำนาจ ชินพงษ์พานิช: การแสดงออกและลักษณะสมบัติของคัลมอดุลินและโปรตีนคล้ายคัลมอดุลินจากข้าว *Oryza sativa* L. (EXPRESSION AND CHARACTERIZATION OF CALMODULIN AND CALMODULIN-LIKE PROTEINS FROM RICE *Oryza sativa* L.) อ. ที่ปรึกษาวิทยานิพนธ์หลัก: ผศ. ดร.ธีรพงษ์ บัวบูชา, 124 หน้า.

คัลมอดุลิน (Calmodulin, CaM) เป็นโปรตีนรับสัญญาณแคลเซียมขนาดเล็กที่ประกอบด้วยส่วน EF hand ซึ่งเมื่อจับกับแคลเซียมจะเกิดการเปลี่ยนโครงรูปและการเปิดของบริเวณที่มีสมบัติ hydrophobic ทำให้สามารถจับและกระตุ้นโปรตีนเป้าหมายต่างๆ ในกลไกการตอบสนองต่อสภาวะแวดล้อมของพืช จากการศึกษาที่ผ่านมาพบกลุ่มยีน *Cam* และ *calmodulin-like protein (CML)* ขนาดใหญ่ในจีโนมข้าว (*Oryza sativa* L.) ในงานวิจัยนี้เป็นการศึกษาสมบัติของโปรตีนรีคอมบิแนนต์บริสุทธิ์ OsCaM และ OsCML ทั้งหมด 11 ชนิด โดยเริ่มจากการสร้างพลาสมิดรีคอมบิแนนต์ 3 ยีนของ OSCML9, OsCML11 และ OsCML13ใน pET-21a (+) รวมทั้ง 8 ยีนของ *OsCam* และ *OsCML* ที่ถูกสร้างไว้แล้ว และส่งถ่ายเข้าสู่ เซลล์ *E. coli* สายพันธุ์ BL21(DE3) หลังจากเหนี่ยวนำให้เกิดการสร้างโปรตีนด้วยการเติม IPTG พบว่า สามารถทำโปรตีนทั้งหมดยกเว้น OsCML9ให้บริสุทธิ์ได้ด้วยวิธี phenyl-Sepharose hydrophobic chromatography เมื่อนำโปรตีนบริสุทธิ์ที่ได้มาตรวจสอบโดยวิธี electrophoretic mobility shift พบว่า โปรตีนส่วนใหญ่สามารถจับกับแคลเซียม ซึ่งแสดงให้เห็นว่าโปรตีนเหล่านี้ทำหน้าที่รับสัญญาณแคลเซียม ภายในเซลล์ จากการตรวจสอบความสามารถในการจับกับเพปไทด์ของ CaMK II พบว่าโปรตีน CaM1 CaM2 และ CaM3 สามารถจับและเกิดเป็น peptide-protein complex ได้ แต่สำหรับโปรตีน CML ไม่ สามารถจับได้ ในการศึกษาการเปลี่ยนแปลงโครงสร้างทุติยภูมิโดยวิธี Circular dichroism (CD) พบว่าใน ภาวะที่มีแคลเซียมเข้าจับ โปรตีน OsCaM ทั้งหมด และโปรตีน OsCML บางชนิดมีค่า molar ellipticity เพิ่มขึ้นมากเมื่อเปรียบเทียบกับในภาวะที่ไม่มีแคลเซียม ซึ่งแสดงให้เห็นว่ามีการเพิ่มขึ้นของโครงสร้าง α helix ในภาวะที่โปรตีนจับกับแคลเซียม และจากการวัด ANS fluorescence spectroscopy พบว่าโปรตีน OsCaM และ OsCML เหล่านี้มีการเปลี่ยนแปลงของ emission spectrum ในภาวะที่มีแคลเซียม โดยมีค่า λ_{max} ลดลงและมีความเข้มเพิ่มขึ้น ซึ่งแสดงให้เห็นว่าโปรตีน OsCML เหล่านี้สามารถจับกับแคลเซียมและ ทำให้เกิดการเปิดบริเวณที่มีสมบัติ hydrophobic ออกมา จากผลการทดลองแสดงให้เห็นว่าโปรตีน CML เป็นโปรตีนรับสัญญาณที่มีลักษณะการทำงานทั้งที่คล้ายคลึงและแตกต่างจากโปรตีน CaM ซึ่งข้อมูลนี้จะ นำไปสู่ความเข้าใจในกลไกการทำงานและหน้าที่ของโปรตีนเหล่านี้ต่อไป

ภาควิชา......ชีวเคมี......... ลายมือชื่อนิสิต....................................

สาขาวิชา......ชีวเคมี......... ลายมือชื่อ อ.ที่ปรึกษาวิทยานิพนธ์หลัก..................

ปีการศึกษา.....2552...........

4972582723   : MAJOR BIOCHEMISTRY

AUMNART CHINPONGPANICH: EXPRESSION AND CHARACTERIZATION OF CALMODULIN AND CALMODULIN-LIKE PROTEINS FROM RICE *Oryza sativa* L. THESIS ADVISOR: ASST. PROF. TEERAPONG BUABOOCHA, Ph.D., 124 pp.

Calmodulin (CaM) is a small calcium receptor protein that contains Ca^{2+}-binding EF hand motifs. When CaMs bind Ca^{2+} ions, they undergo conformational changes revealing their hydrophobic surfaces, which bind to and alter the activities of target proteins that affect physiological responses to the vast array of specific stimuli received by plants. Previously, a large family of *Cam* and *calmodulin-like* (*CML*) genes has been identified in *Oryza sativa* L. Here, we examined properties of the purified recombinant proteins encoded by 11 *OsCam* and *OsCML* genes. Three *OsCML* genes, *OsCML9*, *OsCML11* and *OsCML13* were successfully cloned. The recombinant plasmids of these genes and eight other previously cloned genes of *OsCam* and *OsCML* were constructed in pET-21a (+) vector and introduced into *E. coli* BL21 (DE3). After protein production was induced by IPTG, it was shown that all OsCaM and OsCML proteins except OsCML9 could be purified by Ca^{2+}-dependent Phenyl-Sepharose hydrophobic chromatography. By electrophoretic mobility shift, most of them exhibited these characteristic when incubated with Ca^{2+} indicating that they are functional Ca^{2+}-binding proteins. To examine possible differential target binding, their ability to bind the peptide derived from CaM kinase II was assessed. All OsCaM proteins (OsCaM1, OsCaM2, and OsCaM3) displayed a peptide-protein complex but all OsCML proteins did not form complexes with CaMKII peptides. Changes in their secondary structure upon Ca^{2+}-binding through measurements by Circular dichroism (CD) were determined. All OsCaM and some OsCML proteins displayed a large increase in the molar elipticity when compared with the value in the absence of Ca^{2+}, which indicates that the helical content was highly increased in these proteins upon Ca^{2+} binding. The ANS fluorescence spectroscopy measurement showed that all proteins examined exhibited a change in the ANS spectrum as the λ_{max} for emission spectrum decreased and the fluorescence intensity increased in the presence of Ca^{2+}. These changes indicate that all proteins bind Ca^{2+} and expose hydrophobic patches on their surfaces. These results suggest that OsCMLs represent novel sensor proteins whose modes of action are probably different from or overlapping with those of OsCaMs and possibly serve distinct roles and will help us further investigate the molecular functions and physiological significance of these proteins.

Department: …….Biochemistry…   Student's Signature……………………………………

Field of Study: ..….Biochemistry….   Advisor's Signature……………………………………

Academic Year: ….2009…………..

ACKNOWLEDGMENTS

I would sincerely like to acknowledge the efforts of many people who contribute to this work. This thesis could not be achieved without their following assistance, my thesis advisor Assistant Professor Dr. Teerapong Buaboocha for his generous advice, skillful assistance, technical helps, guidance, encouragement, support, fruitful and stimulating discussion through the period of my study.

Sincere thanks and appreciation are due to Associate Professor Piamsook Pongsawasdi, Associate Professor Tipaporn Limpaseni, Assistant Professor Kanoktip Packdibamrung, and Assistant Professor Kiattawee Choowongkomon for serving as the member of the master thesis committee, for their useful comments and suggestions.

I would like to thank the graduate school, Chulalongkorn University for financially supporting the research through the thesis fund.

Special thanks are also extended to Srivilai Phean-o-pas, Mayura Thongchuang and other friends of the Biochemistry and Biotechnology programs for lending a helping hand whenever needed, sharing the great time in laboratory, for their friendships.

Finally, the warmest gratitude is extended to my family for their patience, understanding, help, encouragement, constant support and warmhearted love whilst I have spent many hours with this thesis rather than with them.

CONTENTS

Page

LIST OF TABLES

LIST OF FIGURES

Figure   **Page**

LIST OF ABBREVIATIONS

A	absorbance, 2′-deoxyadenosine (in a DNA sequence)
ANS	8-Anilino-1-naphthalenesulphonate
bp	base pairs
C	2′-deoxycytidine (in a DNA sequence)
^{O}C	degree Celsius
C-terminus	carboxyl terminus
Ca^{2+}	Calcium ion
CD	circular diohroism
cDNA	complementary deoxyribonucleic acid
cyt	cytosol
Da	Dalton
DNA	deoxyribonucleic acid
dNTP	2′-deoxynucleoside 5′-triphosphate
DTT	dithiothreitol
EGTA	ethylene glycol tetraacetic acid
EDTA	ethylene diamine tetraacetic acid
G	2′-deoxyguanosine (in a DNA sequence)
g	gram
HCl	hydrochloric acid
IPTG	isopropyl-thiogalactoside
kb	kilobase pairs in duplex nucleic acid, kilobases in single-standed nucleic acid
KCl	potassium chloride
kDa	kiloDalton
KOH	potassium hydroxide
l	liter
LB	Luria-Bertani
Mg^{2+}	magnesium ion

µg	microgram
µl	microliter
µM	micromolar
M	mole per liter (molar)
mA	milliampere
mg	milligram
min	minute
ml	milliliter
mM	millimolar
MW	molecular weight
N	normal
ng	nanogram
nm	nanometer
NMR	nuclear magnetic resonance
N-terminus	amino terminus
OD	optical density
PCR	polymerase chain reaction
pmol	picomole
Rpm	revolution per minute
SDS	sodium dodecyl sulfate
T	2′-deoxythymidine (in a DNA sequence)
Tris	tris (hydroxyl methyl) aminomethane
UV	ultraviolet
V	voltage
vir	virulence
v/v	volume by volume
w/w	weight by weight
X-Gluc	5-Bromo-4-chloro-3-indolyl-β-D-glucuronic acid

CHAPTER I

INTRODUCTION

Calcium signaling

Calcium (Ca^{2+}), a universal second messenger, acts as a mediator of stimulus-response coupling in the regulation of diverse cellular functions (Yang and Poovaiah, 2003). Intracellular calcium concentrations are modulated in a wide range of developmental processes and responses to hormonal and environmental signals such as salinity, cold, light, drought, symbiotic and pathogenic elicators. Cytosolic free Ca^{2+} ion is a convergence point for many disparate signaling pathways (Zhang and Tang Lu, 2003). It appears that different stimuli elicit specific calcium signatures, generated by altering the kinetics, magnitude, and cellular source of the influx (Malhó *et al.*, 1998; Allen *et al.*, 2000, 2001; Evans *et al.*, 2001; Rudd and Franklin-Tong, 2001). Ca^{2+} is important in maintaining the stability of the cell wall, membrane and membrane bound protein, due to its ability to bridge chemical residues among these structures (Nayyar, 2003). Research during the last two decades has clearly established that Ca^{2+} acts as an intracellular messenger in coupling a wild range of extracellular signals to specific responses (Reddy, 2001). The concentration of Ca^{2+} in the cytoplasm of plant cells is maintained low in the nanomolar range (100-200 nM) by being actively pumped into intracellular compartments and extracellular spaces where $[Ca^{2+}]$ is in the millimolar range (1-10 mM) as shown in Figure 1.1 (Reddy, 2001). The export of Ca^{2+} ions from the cytosol to the extracellular space or into intracellular organelles is achieved by ATP-driven Ca^{2+}-pumps and antiporters (Vetter and Leclerc, 2003).
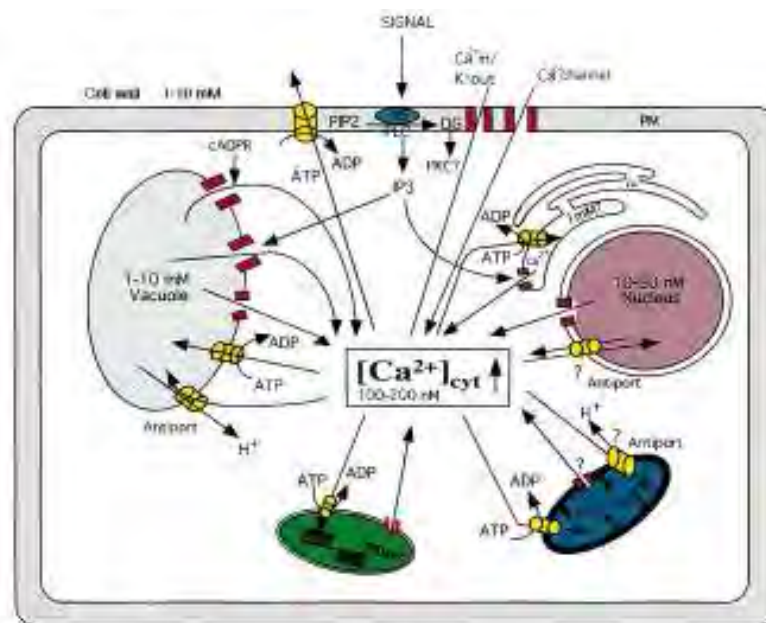
Figure 1.1 Schematic diagram illustrating the mechanisms by which plant cells elevate $[Ca^{2+}]_{cyt}$ in response to various signals and restore Ca^{2+} concentration to resting level. Ca^{2+} channels are shown in red, whereas Ca^{2+} ATPases and antiporters are indicated in yellow. Arrows indicate the direction of Ca^{2+} flow across the plasma membrane, and into and out of cellular organelles (vacuole, plastids, mitochondria, endoplasmic reticulum and nucleus). The estimated concentration of resting levels of Ca^{2+} in different organelles is indicated. Question marks indicate the lack of evidence. $[Ca^{2+}]_{cyt}$, cytosolic Ca^{2+}; PLC, phospholipase C; R, receptor; cADPR, cyclic ADP ribose; PIP_2, phosphotidyl inositol-4,5-bisphosphate; DG, diacylglycerol; PKC, protein kinase C; IP_3, inositol-1,4,5-trisphosphate; ER, endoplasmic reticulum; Mito, mitochondria; Plast, plastids; PM, plasma membrane (Reddy, 2001).

Different stimuli elicit Ca^{2+} transients which are distinct in their subcellular localization, amplitude, duration, frequency of oscillation and mode of spatial propagation (Snedden and Fromm, 2001). These properties are highly coordinated and regulated by the spatial distribution of Ca^{2+}-release channels throughout the cell. The influx of Ca^{2+} ions is generated by voltage- and ligand-gated Ca^{2+}-permeable channels on the plasma membrane. In addition, several intracellular organelles function as Ca^{2+} stores, which can release Ca^{2+} upon stimulation by, for instance, inositol-1, 4, 5-trisphosphate (IP_3) or cyclic ADP-ribose (cADPR). The endoplasmic reticulum (ER) is a major Ca^{2+} stores, but mitochondria and the nucleus also participate actively in the release of Ca^{2+} through the IP_3-receptor. An important feature of the role of Ca^{2+} as a signal is the presence of repetitive Ca^{2+} transients. These transients may be generated both by first-round second messengers and by signaling molecules such as abscisic acid that may themselves be produced as a result of cascades of early Ca^{2+} signals as shown in Figure 1.2. These rounds of signals may have quite different signaling consequences and, therefore, physiological meaning (Xiong *et al.*, 2002).

The EF-hand motif

The approximately 100-fold increase in free Ca^{2+} concentration upon stimulation of a cell allows Ca^{2+}-binding proteins to bind Ca^{2+} ions. Several hundred Ca^{2+}-binding proteins have been identified and most of them share a common Ca^{2+} binding motif. This motif comprises about 30 amino acids consisting of a helix-loop-helix where the two helices are arranged similar to the extended thumb and index finger of a hand: it is

commonly called the EF-hand motif as shown in Figure 1.3. In almost all Ca^{2+}-binding proteins two EF-hand motifs are in close proximity forming an EF-hand pair. This consists of four helices arranged in the form of a twisted four helix bundle.

The EF hands have the canonical 12-residue Ca^{2+} binding loop. Ca^{2+} is bound in a pentagonal bipyramidal geometry with seven sites of coordination occurring through interactions with six amino acids, those in position 1, 3, 5, 7, 9 and 12 (alternatively called +X, +Y, +Z, -Y, -X, and -Z) within the region designated as +X*+Y*+Z*-Y*-X**-Z, in which * represents an intervening residue as shown in Figure 1.4. All of these amino acids interact with Ca^{2+} through side chain oxygens, except residue seven, which acts through its main chain oxygen. Three ligands for Ca^{2+} coordination are provided by carboxylate oxygens from residues 1 (+X), 3 (+Y) and 5 (+Z), one from a carbonyl oxygen from residue 7 (-Y), and two from carboxylate oxygens in residue 12 (-Z). The seventh ligands is provided either by a carboxylate side chain from residue 9 (-X), or from a water molecule received via the side chain or carbonyl oxygen of residue 9. Thus, there are strong preferences for specific amino acids within the Ca^{2+}-binding loop. The +X position is almost exclusively filled with aspartate (D); +Y is usually aspartate (D) or asparagine (N); +Z is aspartate (D), asparagine (N), or serine (S); the -Y position tolerates a variety of amino acids; -X also varies, but is usually aspartate (D), asparagine (N), or serine (S); and -Z, which contributes two coordination sites, is nearly invariably glutamate (E). Glycine (G) at position 6 is highly conserved and is thought to provide the ability for forming a sharp turn within the loop. The cysteine (C) residue in position 7 of the first EF hand is common among plant calmodulins (Zielinski, 1998), but uncommon

Signal $\longrightarrow$ **Primary sensor** $\longrightarrow$ Ca^{2+} $\longrightarrow$ **Secondary Signal Molecules** $\longrightarrow$ Receptor $\longrightarrow$ Ca^{2+}

$\downarrow$ $\downarrow$ $\downarrow$

$\downarrow$ $\downarrow$ $\downarrow$

Output 1 **Output 2** **Output 3**
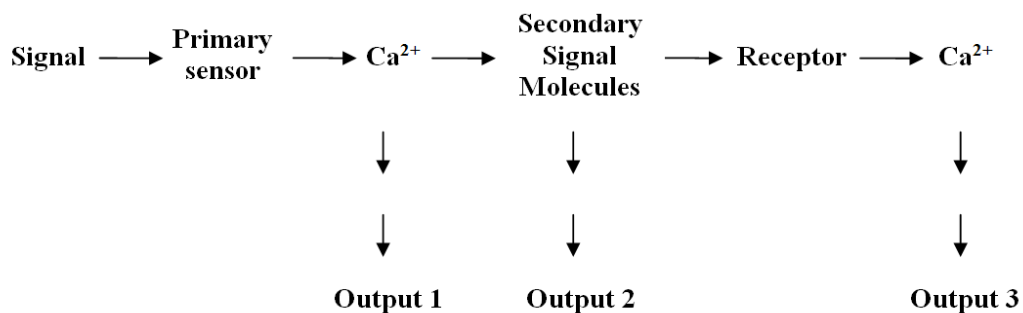
Figure 1.2 Repetitive Ca^{2+} transients upon the perception of a primary signal. The primary increase in cytosolic Ca^{2+} facilitates the generation of secondary signaling molecules, which stimulate a second round of transient Ca^{2+} increases, both locally and globally. These second Ca^{2+} transients may feedback regulate each of the previous steps (not shown). Ca^{2+} transients from different sources may have different biological significance and result in different outputs, as shown. Secondary signaling molecules such as ROS can also directly regulate signal transduction without Ca^{2+} (Output 2) (Xiong *et al.*, 2002).
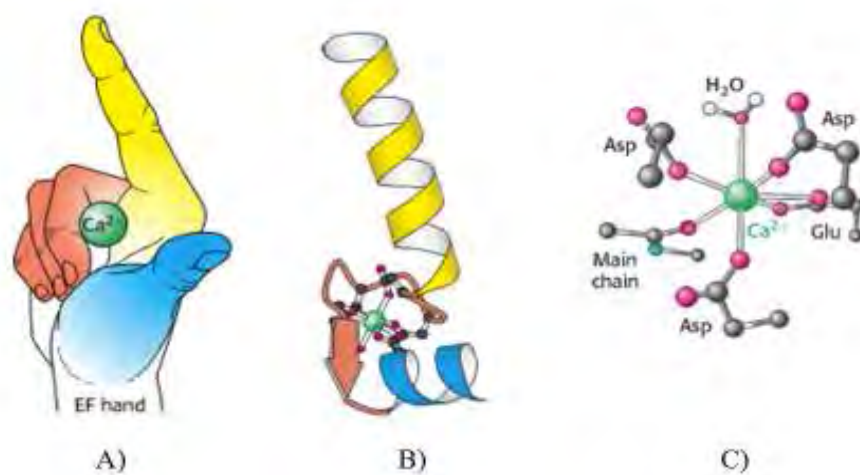
Figure 1.3 The tertiary structure of EF hand motif. (A) A symbolic representation of the EF-hand motif. The helix E winds down the index finger, where as the helix F winds up the thumb of a right hand, (B) helix-loop-helix; E helix, loop and F helix are displayed in yellow, orange and blue respectively, (C) the geometry of Ca^{2+} ligands that interact with six amino acids and a water molecule within the loop (Tymoczko and Stryer, 2001).

```
                - - - - - Loop - - - -
   - - - Helix E - - - -                    - - - Helix F - - -

                 X   Y   Z  -Y  -X    -Z
   E n x x n n x x n D x D x D G x I D x x E L x x n n x x n
                 N i E D g L E      D I
                 S l N N p V N         V
                   v S Q   M Q         M
                   f T H   C S         F
                   y G R     T         Y
                   w   K     A         W
                               G
                               C
```

Figure 1.4 Consensus sequence for EF-hands. (Harmon, 2003). "n" represents hydrophobic amino acids and "x" represents any amino acid.

in nonplant CaMs. Finally, position 8 is most often isoleucine (I), which can form hydrogen bonds with the other EF loop in a pair.

The E helix generally starts with a glutamate (E); both the E and F helices flanking the Ca^{2+}-binding loop are generally each 9 amino acids long. There is a regular distribution of hydrophobic amino acids in the E helices with a pattern of 'nxxnnxxn' where 'n' represents hydrophobic amino acids and 'x' represents any amino acid. In CaMs, the pattern is similar for the F helices of hands 1 and 3, but diverges slightly in hands 2 and 4. The Ca^{2+}-binding domains are numbered I through IV, beginning from the amino-terminus.

Ca^{2+}-binding proteins

The involvement of Ca^{2+} as a second messenger in a wide variety of cellular and physiological processes is well documented (Zhang *et al*., 2002). To respond appropriately to a specific calcium concentration in cytosol perturbation, a cell must activate a unique combination of Ca^{2+}-binding proteins. These Ca^{2+} sensor proteins can be grouped into four major classes as shown in Figure 1.5. These include (A) Ca^{2+}-dependent protein kinase (CPK) that contains CaM-like Ca^{2+} binding domains and a kinase domain in a single protein. Each individual CPK protein is expected to detect the changes in the Ca^{2+} parameters and translate these changes into the regulation of a protein kinase activity (Roberts and Harmon, 1992), (B) Calmodulin (CaM) which contains four EF-hand domains but has no enzymatic activity themselves and functions by interacting with their target proteins (Zielinski, 1998), (C) other EF-hand motif-containing Ca^{2+}-

binding proteins and Calcineurin B-like (CBL) proteins that are similar to both the regulatory B subunit of calcineurin and the neuronal Ca^{2+} sensor (NCS) in animals (Klee *et al.*, 1998) and (D) Ca^{2+}-binding proteins without EF-hand motifs.

Members of the first three classes of Ca^{2+} sensor proteins bind Ca^{2+} using the EF hand, which binds a single Ca^{2+} molecule with high affinity (Strynadka and James, 1989). However, different Ca^{2+}-binding proteins differ in the number of EF-hand motifs and their affinity to Ca^{2+} with dissociating constants (K_ds) ranging from 10^{-5} to 10^{-9} M. Binding of Ca^{2+} to a Ca^{2+} sensor causes a conformational change in the sensor resulting in modulation of its activity or its ability to interact with and modulate function/activity of other proteins (Reddy, 2001).

Calmodulin

Calmodulin (CaM) is a ubiquitous Ca^{2+} sensor protein. It is a small (16 to 18 kDa), highly conserved, soluble, intracellular Ca^{2+}-binding protein ubiquitously found in animals, plants, fungi and protozoa. CaM has no catalytic activity but, upon binding Ca^{2+}, its conformation is changed leading to activation of its target proteins involved in various cellular processes. Many proteins involved in Ca^{2+} signal transduction alter their activity in response to changes in free Ca^{2+} levels, but are themselves not able to bind Ca^{2+} ions. Some of these proteins utilize CaM as a sensor and mediator of the initial Ca^{2+} signal. CaM is multifunctional protein because of its ability to interact and regulate the activity of a number of other proteins as shown in Figure 1.6. CaM has four EF-hands that function in pairs. CaM relays the Ca^{2+} signal by binding free Ca^{2+} ions to its C- and N-
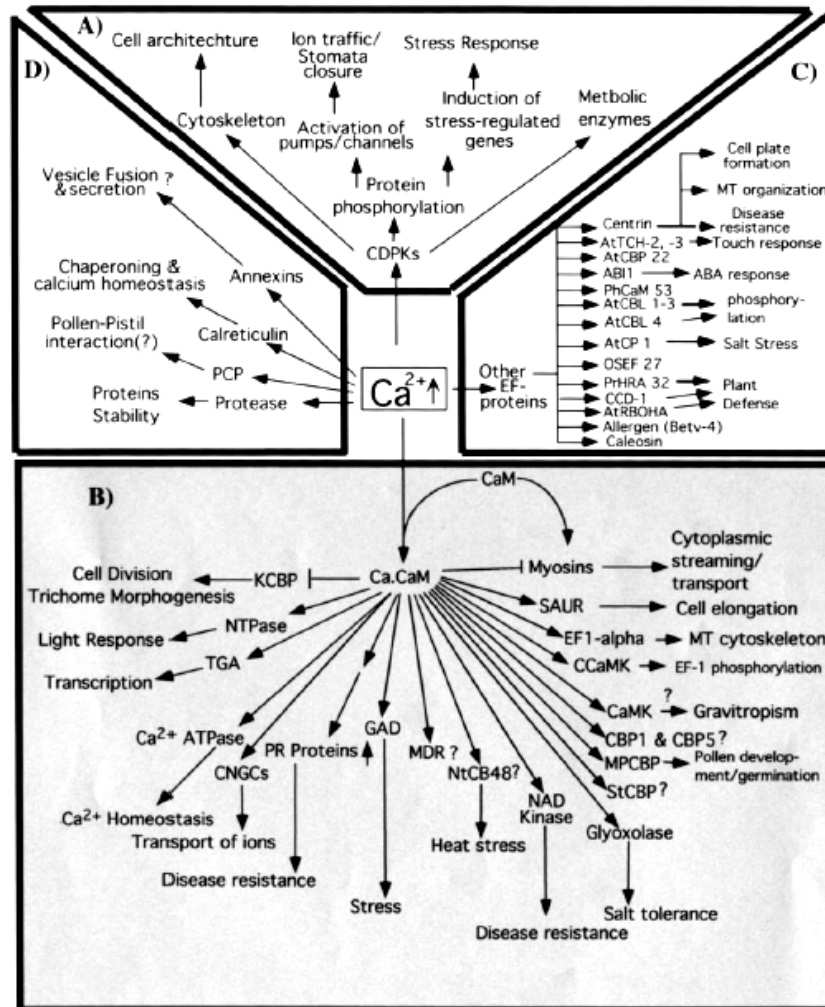
Figure 1.5 Ca^{2+} sensing proteins and their functions in plants. Four major groups of Ca^{2+} sensors (indicated in four boxes) have been described in plants: (A) Ca^{2+}-dependent protein kinase (CDPK or CPK), (B) Calmodulin (CaM), (C) other EF-hand motif-containing Ca^{2+}-binding proteins and Calcineurin B-like (CBL) protein, (D) Ca^{2+}-binding proteins without EF-hand motifs (Reddy, 2001).

terminal EF-hand pairs, which causes a conformational change and enables Ca^{2+}/CaM to bind to specific CaM-binding domains. The binding of Ca^{2+}/CaM to its target proteins alters their activity in a calcium dependent manner.

Ca^{2+}-bound-calmodulin-mediated signal transduction in plants is shown in Figure 1.7. Biotic and abiotic signals are perceived by receptors, resulting, in some cases, in transient changes in Ca^{2+} concentrations in the cytosol and/or organelles (e.g. nucleus). Increases in free Ca^{2+} concentrations originating from either extracellular pools or intracellular stores are capable of binding to Ca^{2+}-modulated proteins including CaM and CaM-related proteins. Structural modulations of these proteins enable them to interact with numerous cellular targets that control a multitude of cellular functions, such as metabolism, ion balance, cytoskeleton and protein modifications. In addition, Ca^{2+} and CaM might also regulate the expression of genes by complex signaling cascades or by direct binding to transcription factors. Rapid changes in cellular functions result from direct interactions of CaM and CaM-related proteins with their targets (within seconds to minutes) while slower responses require gene transcription, RNA processing and protein synthesis (variable times from minutes to days).

The EF hands in CaM are organized into two distinct globular domains, each of which contains one pair of EF hands. Each pair of EF hands is considered the basic functional unit. Pairing of EF hands is thought to stabilize the protein and increase its affinity toward Ca^{2+}. Although each globular domain binds Ca^{2+} and undergoes conformational changes independently, the two domains act in concert to bind target proteins. Upon increase of Ca^{2+} concentration to submicromolar or low micromolar
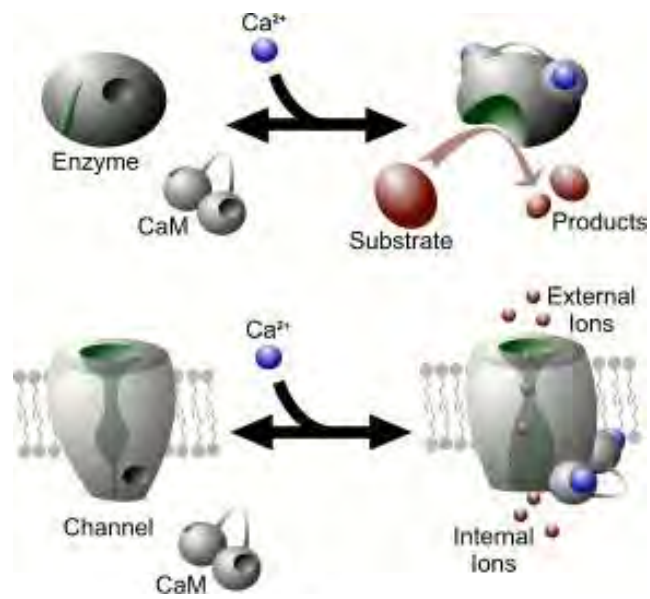
Figure 1.6 Calmodulin acts as a multifunctional protein (Boonpurapong, 2006).
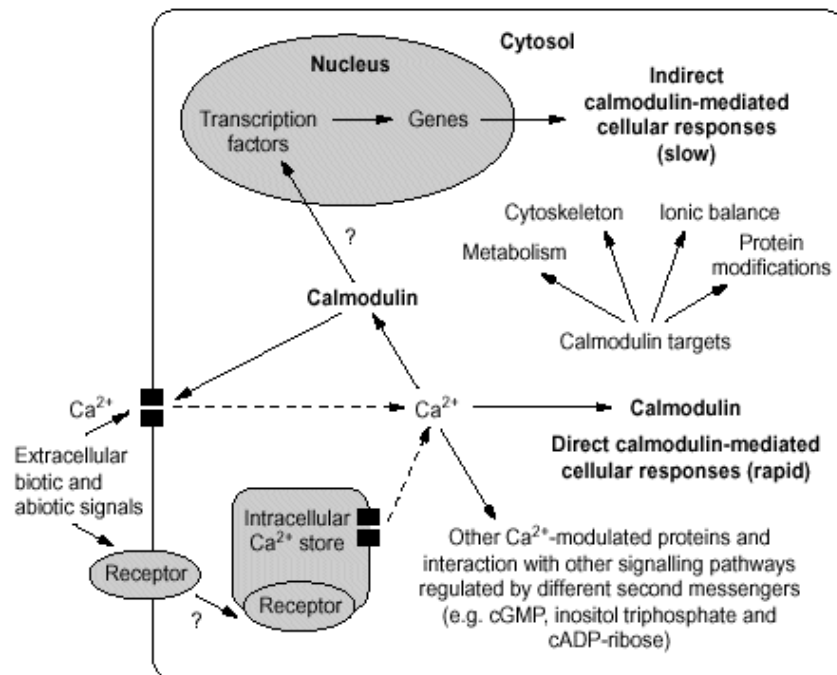
Figure 1.7 The Ca^{2+}-bound-calmodulin-mediated signal transduction in plants. Broken arrows denote Ca^{2+} fluxes from extracellular or intracellular stores, and question marks signify unknown signal transduction intermediates (Snedden and Fromm, 1998).

levels, all CaM molecules are activated. Cooperative binding is required for this "on/off" mechanism to function efficiently. The cooperativity of Ca^{2+} binding ensures that full activation of the CaM occurs in a narrow region of calcium concentration during a signaling event.

The selectivity of CaM toward Ca^{2+} also is an important factor in effective transduction of the Ca^{2+} signal. CaMs bind Ca^{2+} selectively in the presence of high concentrations of Mg^{2+} and monovalent cations in the cell. The cation selectivity is achieved by optimization in the structure folds of the binding loop. For example, discrimination between Ca^{2+} and Mg^{2+} is accomplished through reduction in the size of the binding loop. Binding of Mg^{2+} ions would collapse the EF-hand loop, thereby reducing the distance between negatively charged side chains and destabilizing the CaM/Mg^{2+} complex (Falke *et al.*, 1994). Even small changes in the chemical properties of the Ca^{2+} binding loop (e.g., Glu-12→Gln) can drastically reduce the binding affinity to Ca^{2+} (Beckingham, 1991; Haiech *et al.*, 1991). The Glu-12→Gln mutation changes the carboxylate side chain into carboxylamide, which removes the oxygen ligand for Ca^{2+}. Together, structural analyses in combination with site-directed mutagenesis established that CaMs (and other EF hand–containing proteins, including CBLs) have evolved as highly specific Ca^{2+} sensors (Luan *et al.*, 2002).

The overall structure of Ca^{2+}/CaM is dominated by two EF-hand pairs forming the C- and N- terminal lobes and a long α-helix connecting the two lobes. In vertebrate CaM, the two EF-hand pairs share 48% sequence identity and 75% sequence similarity and the peptide backbone of the two lobes can be superimposed with a mean square

derivation of ~0.7 A° (Vetter and Leclerc, 2003). Figure 1.8 show the crystal structure of *Rattus rattus* calmodulin by X-Ray crystallography which this protein adopts an open conformation and exposes a large hydrophobic cleft in each half of the molecule in the Ca^{2+}-bound state. Although X-ray crystallographic structures of Ca^{2+}-CaM depict the central linker as a helix (Babu *et al*., 1988; Chattopadhyaya *et al*., 1992), the NMR spectroscopy has been used to show that the central linker of Ca^{2+}-CaM is flexible in solution (Brokx *et al*., 2004). Structural analysis of the Ca^{2+}-free and Ca^{2+}-bound states of CaM proteins reveals the conformational changes induced by Ca^{2+} binding as shown in Figure 1.9. In the Ca^{2+}-free state, CaM adopts a closed conformation. Ca^{2+} binding triggers a conformational change, and the protein adopts an open conformation with nearly perpendicular interhelical angles between the globular domains. This open conformation exposes a hydrophobic surface within each globular domain and permits the binding of protein targets (Babu *et al.*, 1988; Kuboniwa *et al.*, 1995, Zhang *et al.*, 1995).

Ca^{2+}/CaM bind and regulate the activity of a wide range of proteins that are not necessarily related in structure. How can Ca^{2+}/CaMs bind to so many different proteins? More specifically, the plasticity of the Ca^{2+}/CaM structure must accommodate the variation in both the molecular size and the composition of the target proteins. This issue has been addressed by structural analyses of Ca^{2+}/CaM and target-bound Ca^{2+}/CaM. Figure 1.9C shows that the two globular domains of Ca^{2+}/CaM are connected by a flexible tether that can accommodate peptides of varying sizes. The binding of CaM-binding peptides is largely driven by hydrophobic interactions between hydrophobic anchor residues of the
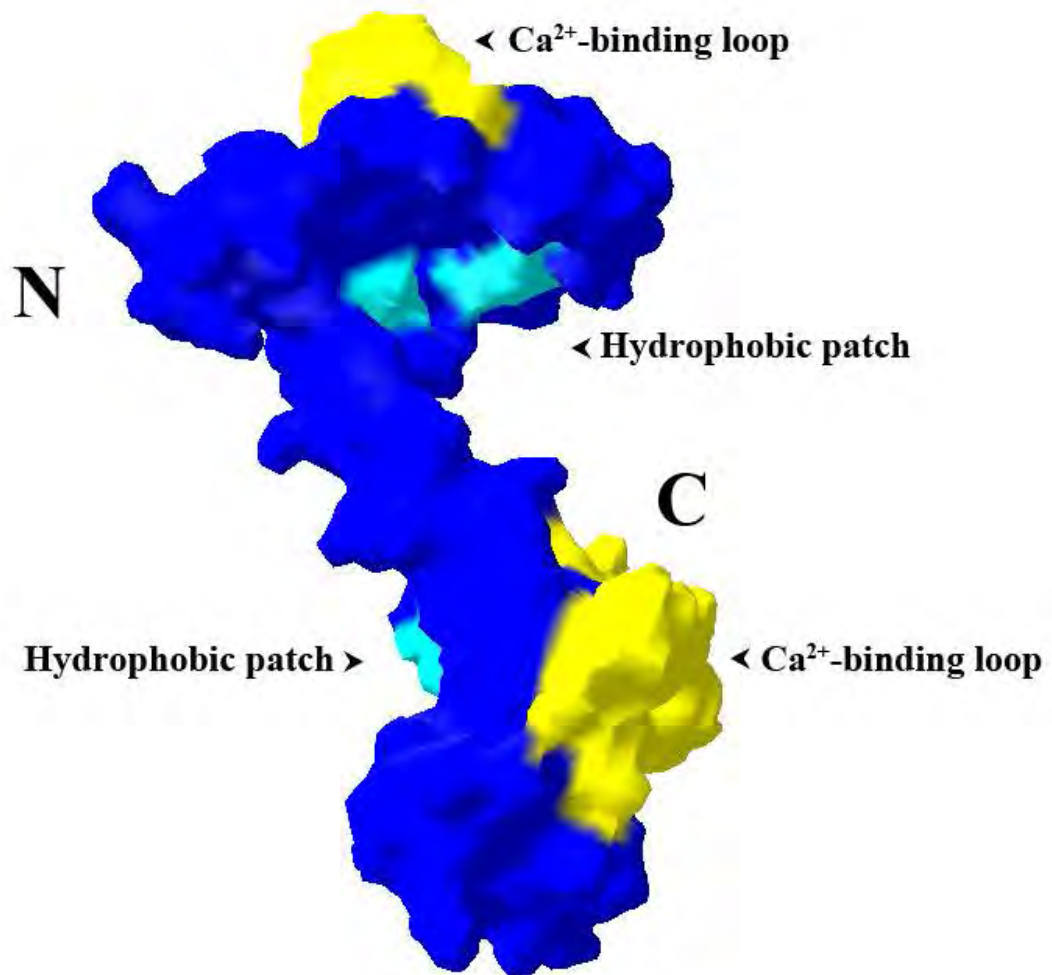
Figure 1.8 Molecular surface of *Rattus rattus* calmodulin structure. The four Ca^{2+}-binding domains in calmodulin have a typical EF hand conformation (helix-loop-helix). A hydrophobic patch is formed on the surface of each of the two lobes. The hydrophobic patches and the Ca^{2+}-binding loops are colored in light blue and yellow, respectively.
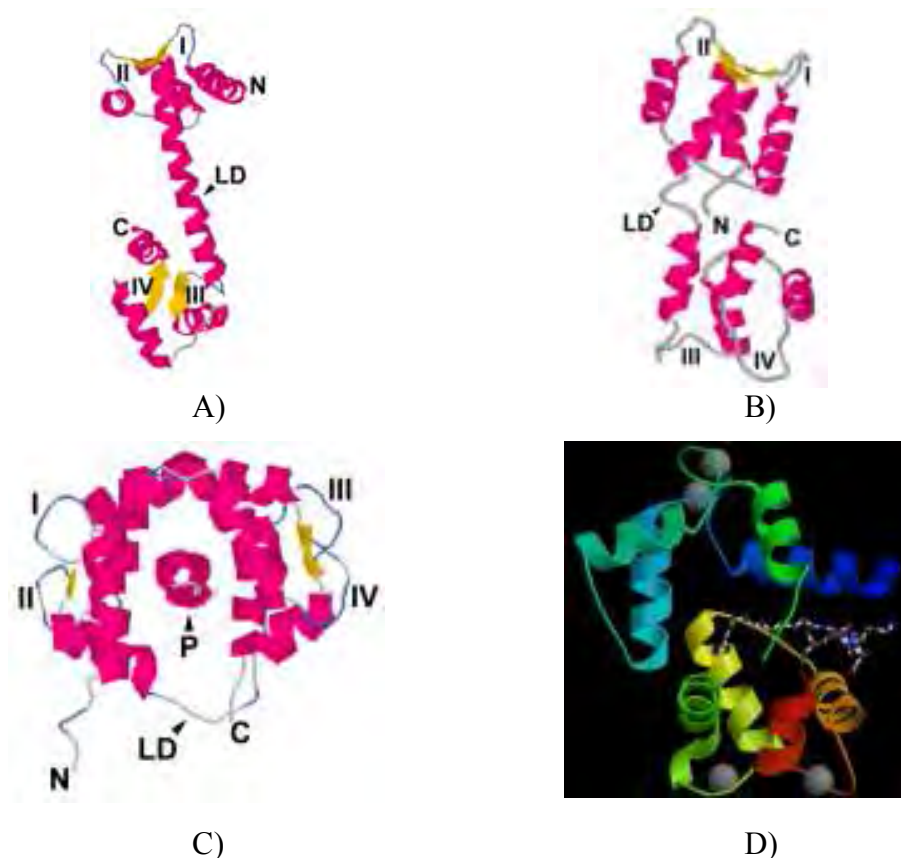
Figure 1.9 Ribbon presentations of calmodulin. (A) Ca^{2+}/CaM determined by X-ray crystallography, (B) globular domain of CaM (apo-CaM) determined by NMR spectroscopy, (C) and (D) Ca^{2+}/CaM-target peptide interaction; Peptide binding causes disruption of the flexible tether, bringing the globular domains closer to form a channel around the peptide. The majority of contacts between Ca^{2+}/CaM and target peptide are nonspecific van der Waals bonds made by residues in the hydrophobic surfaces. For (A) to (C), I-IV, Ca^{2+}-binding loops in the EF-hands; N, amino-termini of the CaM; C, carboxy-termini of the CaM; LD, central linker domain and P, target peptide. The α-helix, loop and β-sheet are colored in red, blue and yellow, respectively (Zielinski, 1998).

peptide with the hydrophobic surface cavities of CaM. Methionine residues, unusually abundant in CaM, play a particularly important role in the binding of target peptides. The methionine side chains are very flexible and the sulfur atom has a larger polarizability than carbon, resulting in stronger van der Waals interactions. The hydrophobic patches of each lobe are surrounded by several charged residues, creating charged binding channel outlets. The C-terminal end of the peptide-binding channel has a negatively charged rim, whereas the N-terminal hydrophobic patch has clusters of negatively and positively charged residues. This charge distribution on the molecular surface contributes to peptide binding via electrostatic interactions and determines the relative binding orientation of CaM-binding peptides. Basic residues at the N-terminus of the peptide form salt bridges with acidic residues surrounding the peptide-binding channel of the C-terminal lobe of CaM. Together, the structures of CaM illustrate how this class of proteins can function as extremely efficient Ca^{2+} sensors and on/off switches, allowing them to transduce Ca^{2+} signals with high efficiency and accuracy.

In plants, there are multiple *Cam* genes that code for either identical proteins or proteins containing a few conservative changes. These small changes in amino acid composition of CaM isoforms may contribute to differential interaction of each CaM isoform with target proteins. The striking example for differential regulation of CaMs comes from the studies with soybean CaM isoforms. In soybean there are five CaM isoforms (SCaM1 to -5). SCaM1, -2 and -3 are highly conserved compared to other plant CaM isoforms including Arabidopsis CaM isoforms whereas SCaM4 and -5 are divergent and show differences in 32 amino acids with the conserved group (Lee *et al.*, 1995). Soybean isoforms show differences in their relative abundance *in vivo*. The

conserved isoforms are relatively abundant in their expression compared to divergent forms. Surprisingly, these divergent CaM isoforms are specifically induced by fungal elicitors or pathogen (Heo *et al.*, 1999). These results provide evidence for the differential regulation of CaM isoforms in plants. Differential regulation of enzymes by soybean divergent and conserved CaM isoforms has also been reported (Lee *et al.*, 2000). All SCaM isoforms activate phosphodiesterase (PDE) but differ in their activation of NAD kinase, calcineurin and nitricoxide synthase indicating Ca^{2+}/CaM specificity between CaM isoforms and target proteins (Lee *et al.*, 1997). Although SCaM isoforms show similar patterns in protein blot overlay assays, they differ in their relative affinity in interacting with CaM binding proteins (Lee *et al.*, 1999). In another sample, two divergent CaM isoforms that are found in Arabidopsis do not interact with proteins that bind to conserved CaM isoforms (Kohler and Neuhaus, 2000). These studies suggest that conserved and divergent CaM isoforms may interact with different target proteins.

There is considerable evidence to indicate that *Cam* genes are differentially expressed in response to different stimuli indicating that different CaM isoforms are involved in mediating a specific signal (Zielinski, 1998). Three of the six Arabidopsis *Cam* genes (*Cam*1, -2 and -3) are inducible by touch stimulation (Zielinski, 1998) indicating the presence of different *cis*-regulatory elements in their promoters. In potato, only one of the eight CaM isoforms (PCaM1) is inducible by touch (Takezawa *et al.*, 1995). Taken together, these results indicate that the presence of multiple CaM isoforms adds further complexity to the Ca^{2+} mediated network. Even though a large family of genes encoding CaM and closely related proteins from several plants has been identified, with the exception of Arabidopsis and rice, families of genes

encoding CaM and related proteins have not been extensively conducted in a whole-genome scale. In Arabidopsis, McCormack and Braam have characterized members of Groups IV and V members from the 250 EF-hand encoding genes identified in the Arabidopsis genome. Seven loci are defined as *Cam* genes and 50 additional genes are CaM-like (*CML*) genes, encoding proteins composed mostly of EF-hand Ca^{2+}-binding motifs (McCormack and Braam, 2003, McCormack *et al.* 2005). The high complexity of the CaM and related calcium sensor proteins in Arabidopsis suggests their important and diverse roles of calcium signaling.

Calmodulin-like protein

In plant several classes of EF-hand-containing Ca^{2+}-modulated proteins were identified. Like CaM, calmodulin-like proteins (CMLs) are composed mostly of EF-hand Ca^{2+}-binding motif, with no other identifiable functional domains. A large family of 50 *CML* genes in Arabidopsis (*AtCML*) was identified. Amino acid comparison enables the separation of the AtCMLs into nine groups based on apparent divergence from CaM. The CML family does not include proteins, such as the Ca^{2+}-dependent protein kinase (CPKs) and calcineurin B-like proteins (CBLs), which have EF-hand motifs and additional functional domains. All but one (AtCML1) of the CMLs have at least two identifiable EF hand-like motifs (McCormack and Braam, 2003). Most AtCMLs have four predicted EF hands but AtCML12 has six EF hands (Sistrunk *et al.*, 1994). Owing to the diverse functions of CMLs, one of the first CMLs identified, AtCML24 was recently shown to play a role in ion homeostasis, photoperiod-response, and abscisic acid (ABA)-mediated inhibition of germination and seeding growth (Delk *et al.*, 2005). Three proteins (AtCML37, AtCML38 and

AtCML39) were shown to play important roles as sensors in Ca^{2+}-mediated developmental and stress response pathways (Vanderbeld and Snedden, 2007). In addition, CML43 and CML18 from Arabidopsis have been implicated in pathogen response (Chiasson *et al*., 2005) and salinity tolerance (Yamaguchi *et al*., 2005), respectively. These reports suggest that CMLs likely function to interpret Ca^{2+} signals during development and stress response. However, the vast majority of Arabidopsis CMLs remain uncharacterized. In the case of *Oryza sativa* L., OsCaM and OsCML proteins were classified by Boonpurapong and Buaboocha (Boonpurapong and Buaboocha, 2007). A summary of their characteristics is shown in Table 1.1. They were named according to their percentages of amino acid identity with OsCaM1 which were calculated by dividing the number of identical residues by the total number of residues that had been aligned to emphasize the identical amino acids. These proteins are small proteins consisting of 145 to 250 amino acid residues and sharing amino acid identity between 30.2% to 84.6% with OsCaM1. When the full-length amino acid sequences of OsCaM and OsCML proteins were subjected to phylogenetic analysis using the neighbor-joining method and bootstrap analysis performed with ClustalX, a consensus tree which is depicted in Figure 1.10 was generated. This analysis led to separation of these proteins into six groups: 1-6. All the CML proteins in group 2 share more than 60% of amino acid sequence identity with OsCaM1. The CML proteins in groups 3, 4, and 5 have identities with OsCaM1 that average 48.2%, 46.9%, and 43.8%, respectively. By the bootstrapped phylogenetic tree based on amino acid sequence similarity of these proteins, group 6 CML proteins were separated into five subgroups: 6a-6e. These proteins share identities no more than 40.7% with OsCaM1 that average at 35.6% with the exception

of OsCML10 (45.6%). All members of groups 6b and 6e contain three EF-hand motifs though with different configurations (Boonpurapong and Buaboocha, 2007).

Some important CaM functional features were found existing only in a few OsCML proteins. The characteristic cysteine (C) at residue 7(-Y) of the first EF hand, a hallmark of higher plant CaM sequences is absent in all CaM-like proteins with the exception of three highly conserved CML proteins, which are OsCML4, OsCML5 and OsCML6. Based on multiple sequence alignment, OsCML4, OsCML5, OsCML7 OsCML10, OsCML17, OsCML18, and OsCML28 are the only CaM-like proteins that contain lysine at a position equivalent to the Lys116 of CaMs. These features may be indicators of proteins that serve similar *in vivo* functions with those of CaMs. OsCML4 and OsCML5 are the only CaM-like proteins that possess both of these signature characteristics. However, another important determinant of CaM function, which is a high percentage of methionine (Met) residues, has been found in most of the OsCML proteins. The average percentage of Met residues among OsCMLs is 4.6% compared with 6.0% in OsCaMs. Considering the usually low percentage found in other proteins, the Met-rich feature in CMLs is likely an indication of their relatedness to CaMs and possibly similar mechanisms of action i.e. exposure of hydrophobic residues caused by conformational changes upon Ca^{2+} binding. Nonetheless, some newly attained characteristics specific to CMLs probably allow them to fine-tune their Ca^{2+}-regulated activity to more specialized functions.

Of these proteins, three OsCMLs contain an extended C-terminal basic domain and a CAAX (C is cysteine, A is aliphatic, and X is a variety of amino acids) motif, a putative prenylation site (CVIL in OsCML1 and CTIL in OsCML2 and 3). OsCML1,

also known as OsCaM61 was identified as a novel CaM-like protein (Xiao *et al.*, 1999). The CML protein was reported to be membrane-associated when it is prenylated and localized in the nucleus when it is unprenylated (Dong *et. al.,* 2002). A similar protein called CaM53 previously found in the petunia also contains an extended C-terminal basic domain and a CAAX motif which are required for efficient prenylation in response to specific changes in carbon metabolism (Rodriguez-Concepcion *et. al.,* 1999). Similar subcellular localization of CaM53 depending on its prenylation state was reported. To locate another possible modification, all proteins were analyzed by the computer program, Myristoylator (Bologna *et. al.,* 2004). As a result, OsCML20 was predicted to contain a potential myristoylation sequence. No other potential myristoylated glycines either terminal or internal were found among the rest of the OsCML proteins. In addition, to determine the possible localization of the OsCML proteins, their sequences were analyzed by targetP (Emanuelsson *et. al.,* 2000). OsCML30 was predicted to contain an endoplasmic reticulum signal sequence and OsCML21 was predicted to be an organellar protein. For OsCaMs and other OsCMLs, no targeting sequence was present, thus, they are probably cytosolic or nuclear proteins.

In order to elucidate the functional mechanism of calmodulin, structural studies have been undertaken on plant calmodulin. The crystal structure of potato calmodulin PCM6 has been solved. It has a dumbbell-like structure, consisting of an N-lobe, a C-lobe and a long bent central helix. There are a total of seven alpha helices connected by four Ca^{2+}-binding loops and two outstretched loops, which form four EF-hand motifs. A hydrophobic patch is formed on the surface of each of the two lobes and within the patch there is a hydrophobic cavity that can hold a hydrophobic

group as large as the side chain of tryptophan. Three Methionine residues are located in each hydrophobic patch and around the patch there are two clusters of acidic amino-acid residues (Yun *et al*., 2003). The hydrophobic patches are very important for target-peptide binding by CaM and methionine residuces have been proposed to be important in the adaptation of CaM to different kinds of target peptides as their long unbranched side chains can undergo certain conformational changes to best fit the shape and nature of the target peptide (Ikura *et al*., 1992; Kurokawa *et al*., 2001) In addition, the Ca^{2+}-loaded from of the N-terminal domain of a CML34 protein from *Arabidopsis thaliana* (Ca-nCML) has been determined by NMR spectroscopy. The interhelical angles of Ca-nCML indicate that the conformation of the first EF-hand is 'open', whereas that of the second EF-hand is 'closed'. Thus Ca-nCML differs from the N-terminal domain of Ca-CaM in which both hands are 'open' (Song *et al*., 2004).

Although the broad significance of these proteins can be postulated to be important in distinguishing between the Ca^{2+} signals from different stimuli and thus aid in eliciting the correct response, the actual significance is, however, not clearly understood, but nevertheless accumulating evidence suggests that each of the different *Cam* and *CML* genes may have distinct and significant functions. Until now, there is no detailed information on *Cam* and *CML* gene products in rice, which is considered a model plant for monocots. Thus, the objective of this study is to determine the characteristics of OsCaM and OsCML protein by assessing their Ca^{2+} and target peptide binding ability and their conformational changes upon Ca^{2+}-binding through measurements by circular dichroism (CD) and fluorescence spectroscopy using 8-anilino-1-naphthalene-sulfonic acid (ANS).

Table 1.1 Characteristics of *OsCam* and *OsCML* genes and the encoded proteins (Boonpurapong and Buaboocha, 2007).

Name	Locus[1]	Chr[2]	cDNA length[3]	Amino Acids[4]	EF hands[5]	% of Met[6]	Identity to OsCaM1(%)[7]	Cys 27[8]	Lys 116[9]	Prenyl-ation[10]	Myristo-ylation[11]	References
OsCam1-1	LOC_Os03g20370	3	450	149	4	6.0	100.0	+	+			[10]
OsCam1-2	LOC_Os07g48780	7	450	149	4	6.0	100.0	+	+			
OsCam1-3	LOC_Os01g16240	1	450	149	4	6.0	100.0	+	+			
OsCam2	LOC_Os05g41210	5	450	149	4	6.0	98.7	+	+			[10]
OsCam3	LOC_Os01g17190	1	450	149	4	6.0	98.7	+	+			
OsCML1	LOC_Os01g59530	1	564	187	4	4.3	84.6			+		[8, 9, 10]
OsCML2	LOC_Os11g03980	11	552	183	4	4.9	70.3			+		
OsCML3	LOC_Os12g03816	12	552	183	4	4.9	68.9			+		
OsCML4	LOC_Os03g53200	3	465	154	4	6.5	68.9	+	+			
OsCML5	LOC_Os12g41110	12	501	166	4	4.8	62.2	+	+			
OsCML6	LOC_Os11g37550	11	513	170	4	6.5	53.9	+				
OsCML7	LOC_Os08g02420	8	447	148	2	2.8	47.7		+			
OsCML8	LOC_Os10g25010	10	576	191	4	5.2	47.0					
OsCML9	LOC_Os05g41200	5	468	155	1	3.2	46.1					
OsCML10	LOC_Os01g72100	1	558	185	4	4.3	45.6		+			
OsCML11	LOC_Os01g32120	1	636	211	4	1.4	44.1					
OsCML12	LOC_Os01g41990	1	750	249	4	2.8	43.9					
OsCML13	LOC_Os07g42660	7	510	169	4	5.3	43.6					
OsCML14	LOC_Os05g50180	5	522	173	4	4.6	43.3					
OsCML15	LOC_Os05g31620	5	606	201	4	4.0	40.7					
OsCML16	LOC_Os01g04330	1	546	181	4	3.9	40.5					
OsCML17	LOC_Os02g39380	2	495	164	4	4.9	37.7		+			
OsCML18	LOC_Os05g13580	5	477	158	4	5.7	37.7		+			
OsCML19	LOC_Os01g72550	1	441	146	3	7.5	37.2					
OsCML20	LOC_Os02g50060	2	525	174	4	4.0	35.3				+	
OsCML21	LOC_Os05g24780	5	594	197	3	4.6	35.3					
OsCML22	LOC_Os04g41540	4	753	250	4	3.6	35.2					
OsCML23	LOC_Os01g72540	1	456	151	3	7.9	35.1					
OsCML24	LOC_Os07g48340	7	594	197	3	3.0	33.9					
OsCML25	LOC_Os11g01390	11	450	149	3	6.7	33.6					
OsCML26	LOC_Os12g01400	12	450	149	3	6.7	33.6					
OsCML27	LOC_Os03g21380	3	573	190	3	3.2	33.3					
OsCML28	LOC_Os12g12730	12	519	172	4	4.8	33.1		+			
OsCML29	LOC_Os06g47640	6	513	170	3	4.1	33.1					
OsCML30	LOC_Os06g07560	6	711	236	4	2.1	32.8					
OsCML31	LOC_Os01g72530	1	456	151	3	5.3	31.6					
OsCML32	LOC_Os08g04890	8	591	196	3	2.6	30.2					

[1] The Institute of Genomics Research (TIGR) gene identifier number.
[2] Chromosome number in which the gene resides.
[3] Length of the coding region in base pairs.
[4] Number of amino acids of the deduced amino acid sequence.
[5] Number of EF hands based on the prediction by InterPro Scan.
[6] Percentage of methionine (M) residues in the deduced amino acid sequence.
[7] Number of identical residues divided by the total number of amino acids that have been aligned expressed in percentage.
[8] Presence of a cysteine equivalent to Cys26 of typical plant CaMs at residue 7(-Y) of the first EF-hand.
[9] Presence of a lysine equivalent to Lys115 of typical plant CaMs.
[10] Presence of a putative prenylation site.
[11] Presence of a putative myristoylation site.
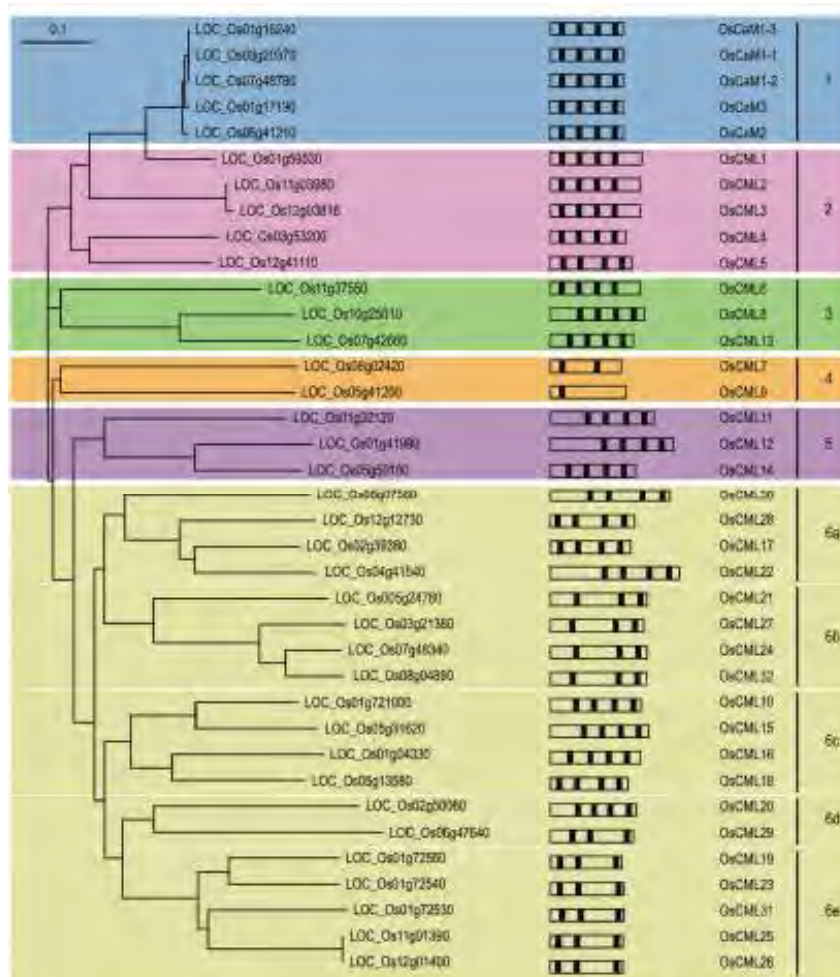
Figure 1.10 Neighbor-joining tree based on amino acid similarities among OsCaM and OsCML proteins. Tree construction using the neighbor-joining method and bootstrap analysis was performed with ClustalX. The TIGR gene identifier numbers are shown and the resulting groupings of CaM and CaM-like proteins designated as 1-6 are indicated on the right. Schematic diagrams of the OsCaM and OsCML open reading frames show their EF hand motif distribution (Boonpurapong and Buaboocha, 2007).

CHAPTER II

MATERIALS AND METHODS

2.1 Materials

2.1.1 Instruments

Autoclave: Labo Autoclave MLS-3020 (Sanyo Electric)

Automatic micropipette: pipetman P2, P20, P100, P1000 (Gilson Medical Electronics S.A.)

Balance: Sartorius CP423s (Scientific Promotion)

Centrifuge 5417C (Eppendorf)

-20 °C Freezer (Sharp)

-80 °C Freezer (Forma)

Gel Doc™ (Syngene)

Gel mate 2000 (Toyobo)

Incubator: BM-600 (Memmert Gambh)

Incubator shaker: Innova™ 4000 (New Brunswick Scientific)

Laminar flow: HS-124 (International Scientific Supply)

Luminescence Spectrometer LS55 (PerkinElmer)

Magnetic stirrer: Fisherbrand (Fisher Scientific)

Magnetic stirrer and heater: cerastir (Clifton)

Microcentrifuge: PMC-880 (Tomy Kogyo)

Microwave Oven (Panasonic)

Orbital Shaker: LD-40 (Lacinco)

pH meter: pH900 (Precisa)

PCR workstation Model P-036 (Scientific)

Power supply: Power PAC 1000 (Bio-RAD Laboratories)

Refrigerated centrifuge 5804R (Eppendorf)

Sonicator: Vibra cell^{Tm} (SONICS & MATERIALS)

Spectrophotometer: DU$^{®}$640 (Beckman Coulter)

Spectropolarimeter J-715 (Jasco)

Thermo cycler: Mastercycler gradient (eppendorf)

UV transilluminator: 2001 microvue (San Gabriel California)

Vortex mixer: Model K 550-GE (Scientific)

Water bath: Isotemp210 (Fisher Scientific)

2.1.2   Materials

Centrifugal Filters (10,000 Daltons molecular weight cut-off) (Amicon)

Filter paper: Whatman No.1 (Whatman International)

Microcentrifuge tube 0.6 and 1.5 ml (Axygen)

0.22µm Millipore membrane filter (Millipore)

Nipro disposable syringe (Nissho)

PCR: Mastercycler gradient (Eppendorf)

PCR Thin wall microcentrifuge tube 0.2 ml (Eppendorf)

Pipette tips10, 100, 1000 µl (Axygen)

2.1.3   Chemicals and reagents

Absolute ethanol (BDH)

Acetic acid glacial (BDH)

Agarose: Seakem LE Agarose (FMC Bioproducts)

Ammoniun sulfate (Sigma Chemical Company)

Ammonium persulfate (Sigma Chemical Company)

Ampicillin (Sigma Chemical Company)

8-Anilino-1-naphthalenesulfonic acid (ANS, Sigma)

Bacto agar (DIFCO)

Bacto tryptone (Scharlau)

Bacto yeast extract (Scharlau)

Bovine serum albumin (Sigma Chemical Company)

5-Bromo-4-chloro-3-indole-beta-D-galactopyranoside; X-gal

(Sigma Chemical Company)

Bromophenol blue (Merck)

Chloroform (Merck)

100mM dATP, dCTP, dGTP, and dTTP (Promega)

Dithiothreitol (Sigma Chemical Company)

Ethidium bromide (Sigma Chemical Company)

Ethylene diamine tetraacetic acid (EDTA) (Carlo Erba Reagenti)

Ethylene diamine tetraacetic acid (EDTA) disodium salt dehydrate

(Carlo Erba Reagenti)

Ethylene glycol tetraacetic acid (EGTA) (Carlo Erba Reagenti)

Glycerol (BDH)

Glacial acetic acid (Carlo Erba Reagenti)

Hydrochloric acid (Merck)

Isoamylalcohol (Merck)

Isopropanol (Merck)

Iso-1-thio-β-D-thiogalactopyranoside: IPTG (Serva)

Lamda DNA (Promega)

Magnesium sulfate (Sigma Chemical Company)

Methanol (Merck)

Methylene blue (Carlo Erba Reagenti)

Ni-Sepharose resins Amersham Biosciences (Piscataway)

Oligo dT (Promega)

Phenol Solution (Sigma Chemical Company)

Phenyl-Sepharose resin Amersham Biosciences (Piscataway)

Polyvinyl pyrrolidone (Sigma Chemical Company)

Potassium acetate (Merck)

Potassium nitrate (BDH)

Sodium acetate (Carlo Erba Reagenti)

Sodium chloride (Carlo Erba Reagenti)

Sodium dodecyl sulfate (Sigma Chemical Company)

Sodium dihydrogen orthophosphate (Carlo Erba Reagenti)

di-Sodium dihydrogen orthophosphate anhydrous (Carlo Erba Reagenti)

Sodium hydroxide (Carlo Erba Reagenti)

Triethanolamine (Sigma Chemical Company)

Tris-(hydroxyl methyl)-aminomethane (Fluka)

Triton X-100 (Merck)

Xylene cyanol FF (Sigma Chemical Company)

2.1.4 Enzymes and Restriction enzymes

Peptide derived from CaMKII (Sigma)

Restriction endonucleases: *Hind* III, *Nde* I, *Xho* I (Biolabs)

RNase A (Promega)

T4 DNA ligase (Biolabs)

Taq DNA Polymerase (Fermentus)

Vent DNA Polymerase (Biolabs)

2.1.5   Microorganisms

Escherichia coli

strain XLl-Blue (F′:: Tn*10 proA$^+$B$^+$lacl^q Δ(lacZ)M15/recA1*

endA1 gyrA96 (Nal^r) thi hsdR17 (r$_k$$^-$ m $_k$$^+$) supE44 relA1 lac)

strain BL21(DE3) F$^-$ *dcm ompT hsdS*(r$_B$$^-$ m$_B$$^-$) *gal* λ(DE3)

2.1.6   Kits and Plasmids

Geneaid^{TM} Gel/PCR DNA Fragment Extraction kit (Geneaid)

Geneaid^{TM} High-Speed Plasmid Mini kit (Geneaid)

pET-21a vector system (Promega), a vector for expression

(Appendix A)

Pierce BCA protein assay kit (Pierce, USA)

pTZ-57R vector system (Promega), a vector for cloning

(Appendix A)

2.1.7   Oligonucleotide primers

The oligonucleotide primers were synthesized by Operon

Biotechnologies (GmbH)(Cologne, Germany).

2.1.8   Antibiotics

Ampicilin (Sigma Chemical Co., USA)

2.2   Bacterial growth medium

Luria-Bertani broth (LB medium) (Maniatis et al., 1982)

LB medium containing 1% peptone, 0.5% NaCl and 0.5% yeast extract was prepared and adjusted pH to 7.2 with NaOH. For agar plate, the medium was supplemented with 1.5% (w/v) agar. Medium was steriled for 20 minutes at 121° C. If needed, a selected antibiotic drug was then supplemented.

2.3   Methods

2.3.1   Sequence analysis

Nucleotide and amino acid sequences of calmodulin and calmodulin-like proteins were obtained from GenBank databases via the National Center for Biotechnology Information (NCBI) (http://www.ncbi.mlm.nih.gov) and the rice databases via the Rice Genome Annotation Project (http://rice.plantbiology.msu.edu/) at Michigan State University and the Rice Annotation Project Database (RAP-DB) (http://rapdb.dna.affrc.go.jp/) at the National Institute of Agrobiological Sciences (NIAS). Sequencing of cDNA clones was carried out at Macrogen, Korea. Multiple

sequence alignment was performed using ClustalW2 (http://www.ebi.ac.uk/Tools/ clustalw2/) at the European Bioinformatics Institute (EBI).

2.3.2   Cloning of the *OsCML* genes into cloning vector (pTZ57R/T)

2.3.2.1)   Primer design

The oligonucleotide primers were designed on the *OsCML* cDNA sequences. The genes (and their GenBank Accession numbers) used were as follows: *OsCML7* (AK059891.1); *OsCML9* (AK105230.1); *OsCML11* (AK072726.1); and *OsCML13* (AK074019.1). Base on the *OsCML* cDNA sequence, a pair of primers for amplifying the coding region of the *OsCML* genes was designed with *Nde*I and *Hin*dIII restriction sites engineered at the 5′ and 3′ ends, respectively. The sequence and the length of the all oligonucleotide primers are shown in Table 2.1.

2.3.2.2)   PCR amplification

The coding regions of *OsCML7*, *OsCML9, OsCML11,* and *OsCML13* genes were amplified from the *OsCML* cDNA clones which were obtained from the DNA Bank of the National Institute of Agrobiological Science (NIAS) as template. The amplification reactions were performed in a 50-μl reaction containing 1X *Vent* DNA polymerase buffer, 2.5 mM $MgCl_2$, 50-100 ng of DNA template, 200 μM each of dATP, dCTP, dGTP and dTTP, 1 μM of each primer and 5 units of *Vent* DNA polymerase (BioLab, Inc., USA). PCR amplification was performed as follows: pre-denaturation at 94 ºC for 5 minutes, 30 cycles of denaturation at 94°C for 3 minutes,

annealing for *OsCML7*, *OsCML9,* and *OsCML11* genes at 60°C or for *OsCML13*

gene at 55°C for 1 minute and extension at 72°C for 1 minute. In the final extension

step, five units of *Tag* DNA polymerase (Fermentus, Inc., USA) were added and

Table 2.1 The sequence and the length of oligonucleotide primers used for PCR

amplification in this work.

Gene	Primer	Sequence	Length
OsCML7	Forward	5' -CATATGGGGGGGAAGGAGCT- 3'	20
	Reverse	5' -ATGACAAGCTTTTTGGCGACGATGC- 3'	25
OsCML9	Forward	5' -CATATGGCGGCCAAGCTGAC- 3'	20
	Reverse	5' -AAGCTTCTTGTTGTTCATCAACACC- 3'	25
OsCML11	Forward	5' -CATATGAGCGAGCCGGCCAC- 3'	20
	Reverse	5' -AAGCTTGGAGAAGATGTTGTCAAATGC- 3'	27
OsCML13	Forward	5' -CTCCCATATGTCTACTGTCAAG- 3'	22
	Reverse	5' -AAGCTTGTAACCATATCCAGTC- 3'	22

reactions were continued at 72 ºC for 20 minutes. PCR products were separated by agarose gel electrophoresis and visualized by ethidium bromide staining.

2.3.2.3) Agarose gel electrophoresis

Agarose gel electrophoresis was used to separate, identify, and purify DNA fragments. The concentration of agarose gel used varies with the size of the DNA fragments to be separated. Generally, 1.0-1.8% agarose gel was used and the DNA samples were run in Tris-acetate-EDTA (TAE) buffer. To prepare samples, DNA was mixed with 10% (v/v) DNA gel loading buffer (0.1 M EDTA/NaOH pH 7.5, 50% (v/v) of glycerol, 1% (w/v) of SDS, 0.5 (w/v) of xylene cyanol FF, and 0.5 (w/v) of Bromophenol blue) and loaded into agarose gel. Electrophoresis was performed at a constant voltage of 100 volts until the bromphenol blue migrated to an appropiate distance through the gel. After electrophoresis, the gel was stained with ethidium bromide solution (5-10 μg/ml in distilled water) for 5 minutes and destained with distilled water for 10 minutes. DNA fragments on agarose gel were visualized on the gel documentation and photographed. The concentration and molecular weight of DNA sample was determined by comparison of band intensity and relative mobility with those of the standard λ/*Hin*dIII DNA markers.

2.3.2.4) Extraction of DNA fragment from agarose gel

The amplification products generated by PCR were purified from agarose gel by using Geneaid gel extraction protocol (Geneaid, USA). After electrophoresis, the desired DNA fragment was excised as gel slice from an agarose gel using a scalpel and transferred to a microcentrifuge tube. Five hundred microliters of DF buffer were added to the gel and incubated for 10 minutes at 55-60°C or until the gel slice has been completely dissolved. During incubation, the tube was inverted every 2-3 minutes. The mixture was transferred into a DF column and centrifuged at 12,000 rpm for 1 minute. The flow through solution was discarded. Then 400 µl of W1 buffer was added, centrifuged at 12,000 rpm for 1 minute and the flow through was discarded. Six hundred µl of Wash buffer was then added to the DF column.The column was let standing for 1 minute, centrifuged at 12,000 rpm for 1 minute and the flow through was discarded. The DF column was centrifuged again for 3 minutes to remove a trace element of the Wash buffer. The DF column was then placed into a sterile 1.5 ml microcentrifuge tube. DNA was eluted by an addition of 15-50 µl of sterile water to the center of the DF column and the column was let standing for 2 minutes, and then centrifuged at 12,000 rpm for 2 minutes. DNA concentration was determined by agarose gel electrophoresis.

2.3.2.5) Ligation of *CML* genes product to pTZ57R/T

The purified PCR products were ligated to pTZ57R/T vector (see in Appendix A). A suitable molecular ratio between vector and inserted DNA in a mixture of cohesive-end ligation is usually 1:3. To calculate the appropriate amount of PCR product (insert) used in ligation reaction, the following equation was used:

$$\frac{\text{ng of vector} \times \text{kb size of insert}}{\text{kb size of vector}} \times \text{ insert: vector molar ratio } = \text{ ng of insert}$$

The 20 μl of ligation mixture contained appropriate amount of vector DNA and gene fragment, 1x ligation buffer and 10 U of T4 DNA ligase. The reaction was incubated overnight at 16$^{\text{o}}$C. The ligation product was then electrotransformed into *E. coli* XL1-Blue.

2.3.2.6) Transformation of ligated products to *E. coli* host cells by CaCl$_2$ method

a) Preparation of *E. coli* competent cells

Competent *E. coli* strain XL1-Blue was prepared according to the method of Sambrook *et al.* (1989). A single colony of *E. coli* strain XL1-Blue was inoculated in 3 ml LB broth (1% (w/v) tryptone, 0.5% (w/v) yeast extract, and 1% (w/v) NaCl, pH 7.2) and incubated at 37 ºC with shaking at 250 rpm overnight. Fifty milliliters of LB medium were inoculated with two percents of the starter culture and incubated at 37 ºC with shaking at 250 rpm for 3-4 hours until the optical density at 600 nm (OD$_{600}$) of culture reached 0.45-0.55. The cell was chilled on ice slurry for 15-30 minutes and harvested by centrifugation at 8,000 xg, 4 ºC for 10 minutes. After the culture supernatant was decanted, the cell pellet was washed with 25 ml of fresh ice 150mM CaCl$_2$, resuspended by gently mixing and centrifuged at 8,000 xg, 4 ºC for 10 minutes. After the supernatant was discarded, the cell was resuspended with 25 ml of fresh ice 150mM CaCl$_2$ and incubated on ice for 30 minutes, then centrifuged at 8,000

xg, 4 °C for 15 minutes. The supernatant was discarded and finally, the cells were resuspended in 1 ml of fresh ice-cold 150 mM CaCl$_2$ and incubated on ice for 1 hour. These cells were used immediately as freshly prepared competent cells (50 µL aliquot is sufficient for a transformation).

b) Transformation by CaCl$_2$ method

In this study, the recombinant plasmids were introduced into competent cells by CaCl$_2$ method. Sixty microliters of competent cells were mixed well with 10 µl of the ligation mixture and then placed on ice for 30 minutes. The mixture was heat-shocked for 90 minutes in a water bath set to 42 °C and the cells were quickly returned to the ice for 5 minutes. Five microliters of LB medium were then added to the cell suspension and incubated at 37 °C with shaking at 250 rpm for 1 hour. The cells were spun down to retain 200 µl, spread onto the LB agar plates containing 100 µg/ml ampicillin, 10 µl of 0.1 M Iso-1-thio-β-D-thiogalactopyranoside (IPTG), and 50 µl of 20 mg/ml 5-Bromo-4-chloro-3-indole-beta-D-galactopyranoside (X-gal) and incubated at 37 °C overnight. The white colonies which contain potential recombinant plasmids were selected and checked for the plasmids by restriction enzyme digestion.

2.3.2.7) Analysis of recombinant plasmids

a) Plasmid DNA isolation by alkaline lysis method

A single colony of recombinant cells was selected and grown in 5 ml of LB broth (1% (w/v) tryptone, 0.5% (w/v) yeast extract, and 1% (w/v) NaCl) containing 100 µg/ml of ampicillin overnight at 37 °C with shaking at 250 rpm. The cells were

spun in a microcentrifuge at 8000×g for 10 minute at 4 ℃. The cells were resuspended in 300 µl of Lysis buffer (50 mM of Tris base, 10 mM of Na$_2$EDTA.H$_2$O and 100 µg/ml of RNaseA) and mixed by vortex (see in Appendix C). Allow the suspension to strand for 5 minutes at room temperature then 300 µl of Alkaline-SDS solution (200mM NaOH and 1% SDS) was added and the suspension was inverted gently several times to mix and allowed to stand on ice of 5 minutes, the solution should be clear considerably. Three hundred microliters of High salt solution (3M of potassium acetate) was added to the mixture and the suspension was mixed gently and allowed to stand for 10 minutes on ice. The insoluble salt-genomic DNA precipitate was then removed by centrifugation at 14,000 rpm, 4℃ for 15 minutes. The supernatant was transferred to a fresh microcentrifuge tube and the nucleic acid was precipitated by adding 480 µl (0.6 volumes) of isopropanol. The sample was mixed thoroughly and immediately centrifuged for 20 minutes to collect the precipitated DNA. The DNA pellet was resuspended in 90 µl of sterile water and the suspension was vortexed gently. Ten microliters of 3M sodium acetate, pH7 and 300 µl of cold absolute ethanol were added to the mixture, mixed and chilled on ice for 30 minutes. DNA was collected by centrifuging at 14,000×g for 20 minutes at 4 ℃. The pellet was rinsed with 300 µl of 70% ethanol and allowed to dry for 10-15 minutes. The plasmid DNA was resuspended with 30 µl of sterile water and stored at -20 ℃.

b) Restriction enzyme analysis

Restriction endonuclease was used to cut double-stranded or single stranded DNA at specific recognition nucleotide sequence. The condition of digestion was

performed as recommended by the enzyme manufacturer. The recombinant plasmids isolated by alkaline lysis method were analyzed for the presence of the interested cloned fragments by digestion with appropriate restriction endonucleases. The *OsCML* recombinant plasmids were digested with *Nde*I and *Hin*dIII. Each of the reactions was carried out in 10 μl mixture at 37 ℃. The products were analyzed by 1% agarose gel electrophoresis. The size of DNA insert is compared with λ / *Hin*dIII marker.

2.3.3)   Cloning of *OsCML* genes into expression vector (pET-21a)

2.3.3.1)   Vector DNA preparation

The *E. coli* XL-1 Blue, which contained pET-21a plasmid was grown in 5 ml LB medium containing 100 μg/ml ampicillin at $37^{o}C$ with shaking at 250 rpm for 16 hours. The pET-21a vector was extracted using Alkaline lysis method as describe above. The expression vector pET-21a was linearized with *Nde*I and *Hin*dIII digestion using the conditions recommended by the enzyme manufacturer. The reaction was incubated at $37^{o}C$ for 3-4 hours. The linear pET-21a was harvested from agarose gel using Geneaid gel extraction protocol.

2.3.3.2)   *OsCML* genes fragment preparation

After the *OsCML* genes were cloned into pTZ57R/T and the recombinant clones were checked with restriction enzymed. The recombinant plasmids that

contained *OsCML* genes were extracted by Alkaline lysis method as describe above. The *OsCML* genes were digested with *Nde*I and *Hin*dIII using the condition of digestion recommended by the enzyme manufacturer. The reactions were incubated at 37°C overnight. The *OsCML* gene fragments were harvested from agarose gel using Geneaid gel extraction protocol and DNA insert sizes were determined by comparing with the λ / *Hin*dIII marker.

2.3.3.3) Ligation of *CML* genes product to pET-21a

The gene fragment was ligated to the pET-21a vector. A suitable molecular ratio of 1:5 between vector and inserted DNA in a mixture was used. The 20 μl of ligation mixture containing an appropriate amount of the vector DNA and the gene fragment, 1x ligation buffer and 10 U of T4 DNA ligase was incubated overnight at 16°C. The mixture was then used for transformation.

2.3.3.4) Transformation of ligated products to *E. coli* XL-1Blue cell by CaCl₂ method

Competent cells were prepared following the protocol described above. The ligation mixtures were mixed with competent cells and then placed on ice for 30 minutes. The cells were heat-shocked for 90 minutes in a water bath set to 42 °C and quickly incubated on ice for 5 minutes. Five hundred μl of LB medium was added, then the cell suspension was incubated at 37 °C with shaking at 250 rpm for 1 hour and spun down to retain 200 μl. Finally, the cell suspension was spread onto LB agar

plates containing 100 μg/ml ampicillin and incubated at 37 ºC overnight. The recombinant clones which contained pET-21a vector could grow on LB agar plates containing ampicillin. A single colony was selected and checked by restriction enzyme digestion.

2.3.3.5)   Analysis of recombinant plasmids

A single colony of recombinant cells was selected and grown in 5 ml of LB broth (1% (w/v) tryptone, 0.5% (w/v) yeast extract, and 1% (w/v) NaCl) containing 100 μg/ml of ampicillin overnight at 37 ºC with shaking at 250 rpm. The recombinant plasmids were extracted by alkaline lysis method. The recombinant plasmids were digested with *Nde*I and *Hin*dIII. The reaction was incubated at 37°C overnight and the products were analyzed by 1% agarose gel electrophoresis. The size of DNA insert was compared with the λ / *Hin*dIII marker.

2.3.4)   Nucleotide and amino acid sequences analysis

The recombinant plasmids were extracted by High Speed plasmid Mini kit (Geneaid, USA) (see in Appendix B) and nucleotide sequences of the inserts were determined. DNA sequencing was carried out at Macrogen, Korea. The sequencing primers, T7 promoter and T7 terminator were used. The molecular weights of OsCML7, OsCML9, OsCML11 and OsCML13 were calculated from the deduced amino acid sequences using the program Compute Mw (http://expasy.org/tools/ pi_tool.html).

2.3.5)   Expression of the *OsCam and OsCML* genes

Previously, the *OsCam* and *OsCML* genes including *OsCam1*, *OsCam2*, *OsCam3*, *OsCML1*, *OsCML3*, *OsCML4*, *OsCML5* and *OsCML8* were cloned into the expression vector pET-21a. Together with the OsCML7, OsCML9, OsCML11, OsCML13 genes that were cloned in this study, they were expressed in *E. coli* BL21(DE3) using the protocols described below.

2.3.5.1)   Preparation of *E. coli* cells

The recombinant pET-21a plasmids containing *OsCML* genes were transformed into *E. coli* strain BL21(DE3) cell by heat shock method. Competent cells were prepared following the protocol described above. The recombinant plasmids were mixed with the competent cells and the mixture was then placed on ice for 30 minute. The cells were heat-shocked for 90 minutes in a water bath set to 42 $^{\circ}$C and quickly incubated on ice for 5 minutes. Five hundred µl of LB medium was then added to the cell suspension and incubated at 37 ºC with shaking at 250 rpm for 1 hour Finally, fifty microliters of the cell suspension were spread onto the LB agar plates containing 100 µg/ml ampicillin and incubated at 37 ºC overnight.

2.3.5.2)   Optimization for *OsCam* and *OsCML* genes expression

A single colony of recombinant cells was grown overnight at 37°C in 5 ml of LB medium, pH 7.0, containing 100 µg/ml ampicillin. Then, 2.0% of the cell culture

was inoculated into 200 ml of the same medium and was incubated at 37°C with shaking for 3-4 hours until the optical density at 600 nm (OD$_{600}$) of the cell culture reached 0.6. Production of recombinant proteins was induced by IPTG at a final concentration of 0, 0.1, 0.3, 0.5, or 0.8 mM and the incubation was continued at 37°C for 4 hours. The cells were harvested by centrifugation at 8000xg for 15 minutes, then washed twice in cold wash buffer (50 mM Tris-HCl, pH 7.5) and collected by centrifugation. The cell pellet was stored at -80°C until it was sonicated. In crude extract preparation, the cell pellet was resuspended in 10 ml of cold lysis buffer (50 mM Tris-HCl, pH 7.5, 1 mM EDTA, and 1 mM DTT), incubated on ice for 30 minutes and then the cells were broken by sonication on ice. Unbroken cells and cell debris were removed by centrifugation at 20000xg for 30 minutes. The supernatant was kept at 4°C until it was used.

2.3.6) Determination of protein concentration

Protein concentration was determined by the modified method of Bradford, M. M. (1976). The reaction contained 100 μl of protein sample and 1 ml of Bradford solution, which was prepared as described in Appendix C. The solution was mixed by vortexing. Then, the protein concentration was monitored by measuring the absorbance at 595 nm after letting the mixture stand at room temperature for 5 minutes but before 1 hour after mixing and calculated from the standard curve of protein standard (0-20 μl of 1 mg/ml BSA).

2.3.7) SDS-polyacrylamide gel electrophoresis

The SDS-PAGE system was performed according to the method of Bollag *et al*., 1996. The slab gel system consisted of 0.1% SDS (W/V) in 12.5% separating gel and 3.9% stacking gel. Tris-glycine (25 mM Tris, 192 mM glycine and 0.1% SDS), pH 8.3 was used as electrode buffer. The gel preparation was described in Appendix C. The protein samples were mixed with 5x sample buffer (60 mM Tris-HCl pH 6.9, 79% glycerol, 2% SDS, 0.1% bromophenol blue and 14.4 mM β-mercaptoethanol) by the ratio 5:1 and boiled for 10 minutes before loading to the gel. The electrophoresis was run from the cathode towards the anode at a constant current (20 mA) per gel at room temperature. The molecular weight marker proteins containing β-galactosidase (116,000 Da), bovine serum albumin (66,200 Da), ovalbumin (45,000 Da), lactate dehydrogenase (35,000 Da), restriction endonuclease Bsp98I (25,000 Da), β-lactoglobulin (18,400 Da) and lysozyme (14,400 Da) were used. After electrophoresis, the gel was stained with Coomassie blue.

2.3.8) Protein staining

The gel was transferred to a box containing Coomassie staining solution (0.25% Coomassie Blue R-250, 50% methanol, and 7% glacial acetic acid). The gel was stained for 1 hour at room temperature with gentle shaking. After staining, the stain solution was poured out, and the gel was briefly rinsed with water and incubated with Coomassie destaining solution (10% methanol and 7% glacial acetic acid). The gel was gently destained several times until protein bands were readily visible.

2.3.9) Purification of the OsCaM and OsCML proteins

2.3.9.1) Crude extract preparation

For the large scale protein expression, a single colony of recombinant cells was grown overnight at 37°C for 16 hours in 25 ml of LB medium, pH 7.0, containing 100 μg/ml ampicillin. Then, 2.0% of the cell culture was inoculated into 1,000 ml of the same medium and was incubated at 37°C with shaking for 3-4 hours until the optical density at 600 nm (OD_{600}) of the cell culture reached 0.6. Production of recombinant proteins was induced by IPTG at the final concentration of 0.3 mM and the incubation was continued at 37°C for 4 hours. The cells were harvested by centrifugation at 8000xg for 15 minutes, and then washed twice in cold wash buffer (50 mM Tris-HCl, pH 7.5) and collected again by centrifugation. The cell pellet was stored at -80°C until it was sonicated. In crude extract preparation, the cell pellet was resuspended in 50 ml of cold lysis buffer (50 mM Tris-HCl, pH 7.5, 1mM EDTA, and 1mM DTT), incubated on ice for 30 minutes and then the cells were broken by sonication on ice. Unbroken cell and cell debris were removed by centrifugation at 20000xg for 30 minutes. The supernatant was kept at 4°C until it was used. In the case of OsCML9 protein extract preparation, the cell pellet was resuspended in 50 ml of cold binding buffer (20 mM Sodium phosphate, pH 7.4, 30 mM imidazole and 0.5 M NaCl) instead.

2.3.9.2) OsCaM and OsCML protein purification by Phenyl-Sepharose column or Ni-Sepharose column

The Phenyl-Sepharose was packed into a small column and washed with deionized water several times. After that the column was equilibrated with Equilibration buffer (50 mM Tris-HCl, pH 7.5, 1 mM $CaCl_2$ and 0.5 mM DTT) about 20 column volumes. Before applying the crude protein sample to the Phenyl-Sepharose column, $CaCl_2$ was added to a final concentration of 5 mM to the crude protein sample and the mixture was incubated at room temperature for 10 minutes. The crude protein sample was applied to the Phenyl Sepharose column, then the column was washed with Equilibration buffer until the absorbance at 280 nm was around 0.01. After that the column was washed with Wash buffer I (50 mM Tris-HCl, pH 7.5, 1 mM $CaCl_2$, 0.5 mM DTT and 200 mM NaCl) until the absorbance at 280 nm was near zero. Then proteins were eluted with Elution buffer I (50 mM Tris-HCl, pH 7.5, 5 mM EGTA and 0.5 mM DTT). In the case of the OsCML9 protein purification, Ni-Sepharose was equilibrated with Binding buffer (20 mM sodium phosphate, pH 7.4, 30 mM imidazole and 0.5 M NaCl). The crude protein sample was applied to the Ni-Sepharose column, and then the column was washed with Binding buffer of about 30 column volumes. After that the column was washed with Wash buffer II (20 mM sodium phosphate, pH 7.4, 150 mM imidazole and 0.5 M NaCl) of about 10 column volumes. Then the protein samples were eluted with Elution buffer II (20 mM sodium phosphate, pH 7.4, 500 mM imidazole and 0.5 M NaCl) of about 10 column volumes. The eluted proteins were analyzed by SDS-polyacrylamide gel electrophoresis as described above. The fractions containing OsCaM or OsCML proteins were pooled and dialyzed against sufficient EGTA to remove calcium ions

with 100 volumes of Dialysis buffer (1mM Tris-HCl, pH 7.5, 1mM KCl) for at least 4 hours 3 times. All proteins were concentrated using Centrifugal Filters (10000 Daltons molecular weight cut-off) (Amicon).

2.3.9.3) Determination of protein concentration by BCA protein assay

The BCA protein assay is a detergent-compatible formulation based on bicinchoninic acid (BCA) for the colorimetric detection and quantitation of total protein. In this study, protein concentration was determined using The Pierce BCA protein assay kit (Pierce, USA). In the first step, BCA working reagent was prepared by mixing 50 parts of reagent A with 1 part of reagent B. The second step, 25 μl of each standard BSA or protein sample was pipetted into a microplate well, then 200 μl of working reagent was added to each well and the plate was mixed thoroughly and incubated at 37 ^{0}C for 30 minutes. After that, the plate was cooled to room temperature and the absorbance at 540 nm was measureed on a microplate reader.

2.3.10) Characterization of OsCaM and OsCML proteins

2.3.10.1) Ca^{2+} binding properties of OsCaM and OsCML proteins

One of the characteristics of CaM is its ability to bind Ca^{2+} in the presence of SDS. To perform the electrophoresis mobility assay of each protein, 1 mM of CaCl$_2$ or 3 mM of EGTA in the final concentration was added to each protein sample, the sample was then mixed and let stand at room temperature for 15 minutes prior to

electrophoresis in a 12% (w/v) SDS-polyacrylamide gel. After electrophoresis, the gel was stained with Coomassie blue.

2.3.10.2) CaMKII peptide binding properties of OsCaM and OsCML proteins

To examine the properties of the OsCaM and OsCML proteins, its ability to bind the peptide derived from CaM kinase II (CaMKII) was assessed by gel mobility shift assay. The 100 picomoles of recombinant proteins in the presence of 1 mM Ca^{2+} or 3 mM EGTA were mixed with different amounts of the peptide derived from CaMKII (Sigma) and incubated for 1 hour at room temperature and then fractionated in 12.5% (w/v) polyacrylamide gel containing 4 M urea. The slab gel system consisted of 4 M urea in 12.5% seperating gel and 3.9% stacking gel. Tris-glycine (25 mM Tris, 192 mM glycine), pH 8.3 was used as electrode buffer. The gel preparation was described in Appendix C. The protein samples were mixed with 5x sample buffer (60 mM Tris-HCl pH 6.9, 79% glycerol, 0.1% bromophenol blue) by the ratio 5: 1. The electrophoresis was run from the cathode towards the anode at a constant current (20 mA) per gel at room temperature and the proteins were detected by Coomassie blue staining.

2.3.10.3) Analysis of structural changes from circular dichroism spectroscopy

Circular dichroism (CD) spectroscopy was carried out at 25 ^{o}C with constant N_2 flushing, using a CD instrument (Jasco J-715 Spectropolarimeter). The far UV CD

spectra of the OsCaM and OsCML proteins were measured from 190 to 250 nm in 1 mM Tris-HCl buffer, pH 7.5 and 1 mM KCl in the presence of 1 mM $CaCl_2$ or 1 mM EGTA. The final concentration of each protein used in far-UV CD analysis was 10 μM. All measurements were performed 30 min after sample preparation, using a 1-mm path length quartz cell and the parameter settings: response time 1 s; sensitivity 50 millidegrees; scan speed 50 nm/min; 2.0 nm spectral band widths, and average of three scans.

2.3.10.4) 8-Anilino-1-naphthalenesulphonate (ANS) fluorescence measurments

To examine Ca^{2+}-induced exposure of the hydrophobic surfaces of the recombinant OsCaM and OsCML proteins, fluorescence emission spectra of 8-Anilino-1-naphthalenesulfonic acid (ANS, Sigma) in the presence of these proteins were performed on a LS55 Luminescence Spectrometer (PerkinElmer, UK) at 25 °C. Fluorescence emission spectra were monitored with excitation set at 370 nm and scan emission spectra in the range 400-650 nm. All measurements were performed using 1 μM of each protein in 1 mM Tris-HCl buffer, pH 7.5 and 1 mM KCl; and ANS at a final concentration 100 μM in the presence of 1 mM $CaCl_2$ or 3 mM EGTA.

CHAPTER III

RESULTS

3.1   Cloning of *OsCML* genes

Four *OsCML* genes: *OsCML7*, *OsCML9*, *OsCML11* and *OsCML13* were cloned. Based on the *OsCML* cDNA sequences obtained from the National Institute of Agrobiological Sciences, Japan, a pair of primers for amplifying each coding region of the *OsCML* genes was designed with the restriction endonuclease sites for *Nde*I and *Hin*d*III* engineered at its 5′- and 3′-ends, respectively. The amplified PCR products of approximately 0.46, 0.47, 0.64 and 0.52 kb, which were the expected sizes of the *OsCML7*, *OsCML9*, *OsCML11* and *OsCML13* genes, respectively were obtained. Figure 3.1 shows the separation by agarose gel electrophoresis of the *OsCML* gene products obtained from PCR amplification using various annealing temperatures. The amounts of the PCR products of all *OsCML* genes were high from all temperatures and did not change with the increase of annealing temperature. Because no significant amount of non specific amplified DNA was detected for all *OsCML* genes, the PCR products of all annealing temperatures could be used for further cloning.

The amplified *OsCML* gene fragments were extended by adding dA at the 3′ end using *Taq* DNA polymerase. After each DNA fragment was purified using the Geneaid gel extraction kit, it was ligated into pTZ57R/T by T4 DNA ligase. Competent *E. coli* XL1-Blue cells were transformed with the ligation reactions and the transformants were selected by blue/white colony screening on ampicillin agar plates containing X-gal and IPTG. White colonies were randomly picked and cultured

in 5 ml LB broth containing 100 µg/ml of ampicillin at 37 °C overnight and the cultures were subjected to plasmid extraction. To verify insertion of the PCR products into pTZ57R/T vectors, the potential recombinant plasmids containing the *OsCML* genes were digested with *Nde*I and *Hin*dIII at 37 °C overnight and analyzed by 1.0% agarose gel electrophoresis. The results show that, in addition of the pTZ57R/T fragment of 2.9 kb, DNA fragments of approximately 0.46, 0.47 and 0.64 kb in length were obtained as expected for the restriction patterns of the recombinant plasmids harboring *OsCML7*, *OsCML9* and *OsCML11* as shown in Figures 3.2, 3.3 and 3.4 (lanes 2), respectively. For the DNA fragment of *OsCML13*, which contained an *Nde*I site in its coding sequence, when its potential recombinant plasmid was digested with *Nde*I and *Hin*dIII, the result shows that the DNA fragment of *OsCML13* was digested once in the coding sequence as expected producing two bands of approximately 0.26 and 0.25 kb in length as shown in Figure 3.5 (lane 2). The resulting recombinant plasmids were called pTZ-OsCML7, pTZ-OsCML9, pTZ-OsCML11 and pTZ-OsCML13, accordingly.

To clone the *OsCML* genes into the pET-21a expression vector, the recombinant pTZ57R/T plasmids containing *OsCML* genes were extracted and digested with *Nde*I and *Hin*dIII. The *Nde*I and *Hin*dIII-digested *OsCML* fragments were then ligated into the same restriction sites in the pET-21a vector. The ligation products were transformed to *E. coli* strain XL1-Blue. The transformants were selected by ampicillin resistance on LB agar. *E. coli* XL1-Blue single colonies were ramdomly picked for plasmid extraction and the plasmids were digested with *Nde*I and *Hin*dIII. After digestion, a linear pET-21a of 5.4 kb and the inserted *OsCML* gene fragments were obtained as shown in Figures 3.2, 3.3, 3.4 and 3.5 (lanes 5) for the
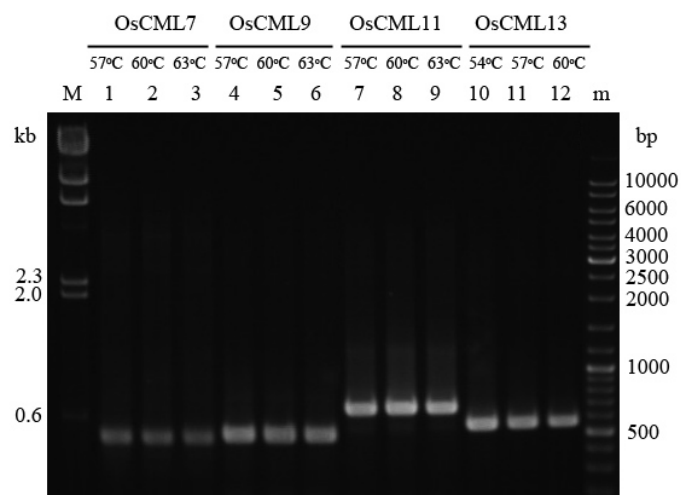
Figure 3.1 PCR products using various DNA templates and annealing temperatures

Lane M   = λ/*Hin*dIII standard DNA marker

Lane 1   = PCR product of *OsCML7* gene using annealing temperature of 57$^{\rm o}$C

Lane 2   = PCR product of *OsCML7* gene using annealing temperature of 60$^{\rm o}$C

Lane 3   = PCR product of *OsCML7* gene using annealing temperature of 63$^{\rm o}$C

Lane 4   = PCR product of *OsCML9* gene using annealing temperature of 57$^{\rm o}$C

Lane 5   = PCR product of *OsCML9* gene using annealing temperature of 60$^{\rm o}$C

Lane 6   = PCR product of *OsCML9* gene using annealing temperature of 63$^{\rm o}$C

Lane 7   = PCR product of *OsCML11* gene using annealing temperature of 57$^{\rm o}$C

Lane 8   = PCR product of *OsCML11* gene using annealing temperature of 60$^{\rm o}$C

Lane 9   = PCR product of *OsCML11* gene using annealing temperature of 63$^{\rm o}$C

Lane 10   = PCR product of *OsCML13* gene using annealing temperature of 54$^{\rm o}$C

Lane 11   = PCR product of *OsCML13* gene using annealing temperature of 57$^{\rm o}$C

Lane 12   = PCR product of *OsCML13* gene using annealing temperature of 60$^{\rm o}$C

Lane m   = 100 bp standard DNA marker

Figure 3.2 Restriction patterns of the recombinant plasmids pTZ-OsCML7 and pET21-OsCML7

Lane M   =   λ/*Hin*dIII standard DNA marker

Lane 1   =   undigested pTZ-OsCML7

Lane 2   =   *Nde*I/*Hin*dIII-digested pTZ-OsCML7

Lane 3   =   *Nde*I/*Hin*dIII -digested pET-21a

Lane 4   =   undigested pET-OsCML7

Lane 5   =   *Nde*I/*Hin*dIII -digested pET-OsCML7

Lane 6   =   PCR product of *OsCML7* gene

Lane m   =   100 bp standard DNA marker

Figure 3.3 Restriction patterns of the recombinant plasmids pTZ-OsCML9 and pET21-OsCML9

Lane M   =   λ/*Hin*dIII standard DNA marker

Lane 1   =   undigested pTZ-OsCML9

Lane 2   =   *Nde*I/*Hin*dIII -digested pTZ-OsCML9

Lane 3   =   *Nde*I/*Hin*dIII -digested pET-21a

Lane 4   =   undigested pET-OsCML9

Lane 5   =   *Nde*I/*Hin*dIII -digested pET-OsCML9

Lane 6   =   PCR product of *OsCML9* gene

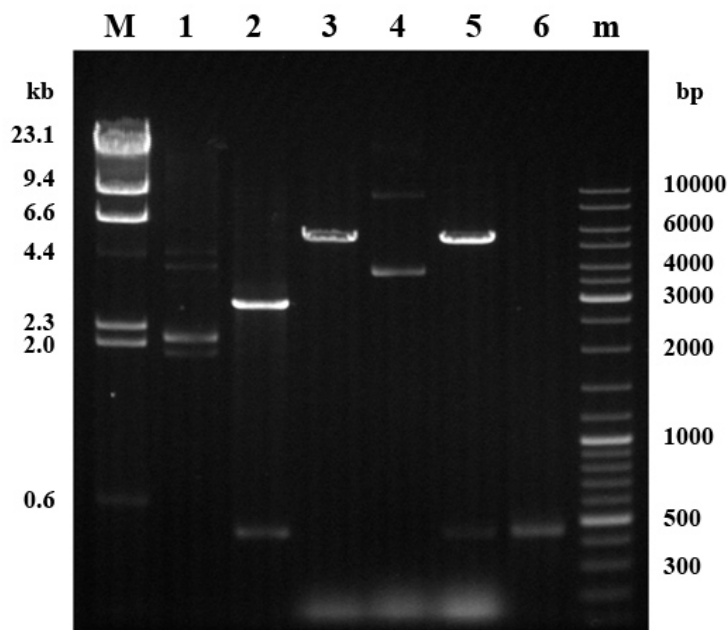Lane m   =   100 bp standard DNA marker

Figure 3.4 Restriction patterns of the recombinant plasmids pTZ-OsCML11 and pET21-OsCML11

Lane M   =   λ/*Hin*dIII standard DNA marker

Lane 1   =   undigested pTZ-OsCML11

Lane 2   =   *Nde*I/*Hin*dIII -digested pTZ-OsCML11

Lane 3   =   *Nde*I/*Hin*dIII -digested pET-21a

Lane 4   =   undigested pET-OsCML11

Lane 5   =   *Nde*I/*Hin*dIII -digested pET-OsCML11

Lane 6   =   PCR product of *OsCML11* gene

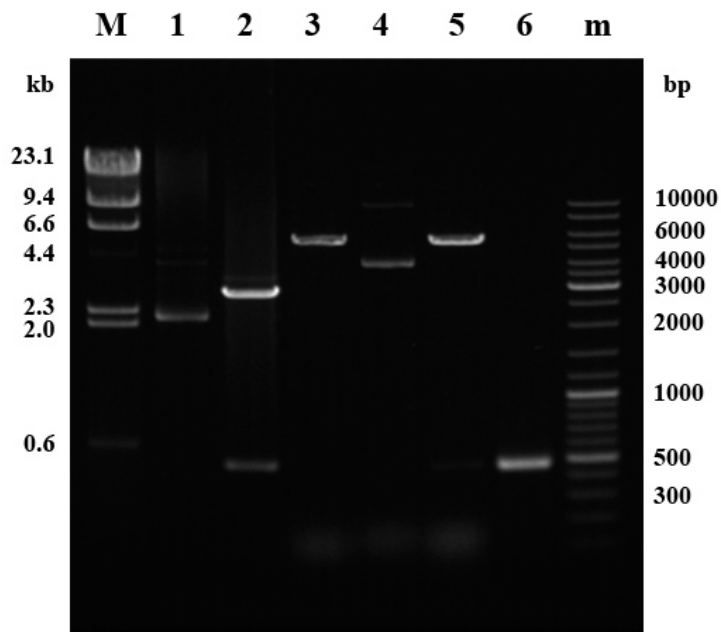Lane m   =   100 bp standard DNA marker

Figure 3.5 Restriction patterns of the recombinant plasmids pTZ-OsCML13 and pET21-OsCML13

Lane M = λ/*Hin*dIII standard DNA marker

Lane 1 = undigested pTZ-OsCML13

Lane 2 = *Nde*I/*Hin*dIII -digested pTZ-OsCML13

Lane 3 = *Nde*I/*Hin*dIII -digested pET-21a

Lane 4 = undigested pET-OsCML13

Lane 5 = *Nde*I/*Hin*dIII -digested pET-OsCML13

Lane 6 =   PCR product of *OsCML13* gene
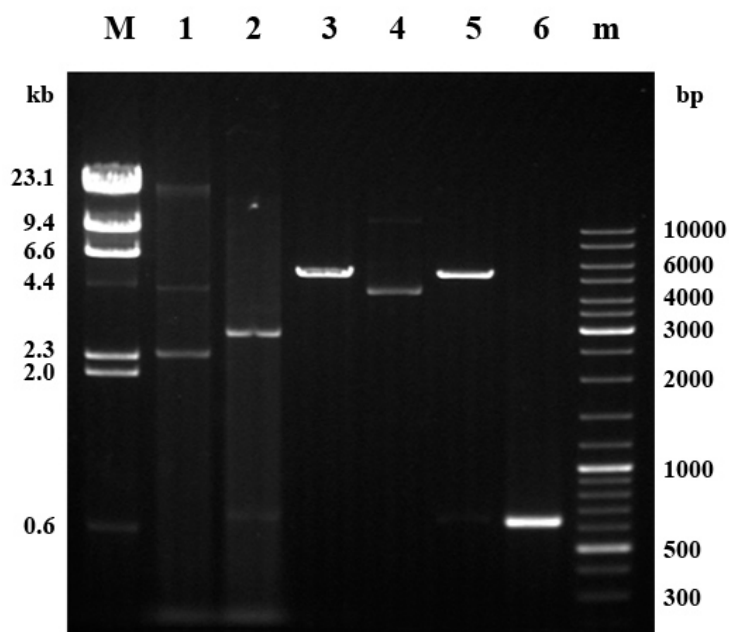
Lane m = 100 bp standard DNA marker
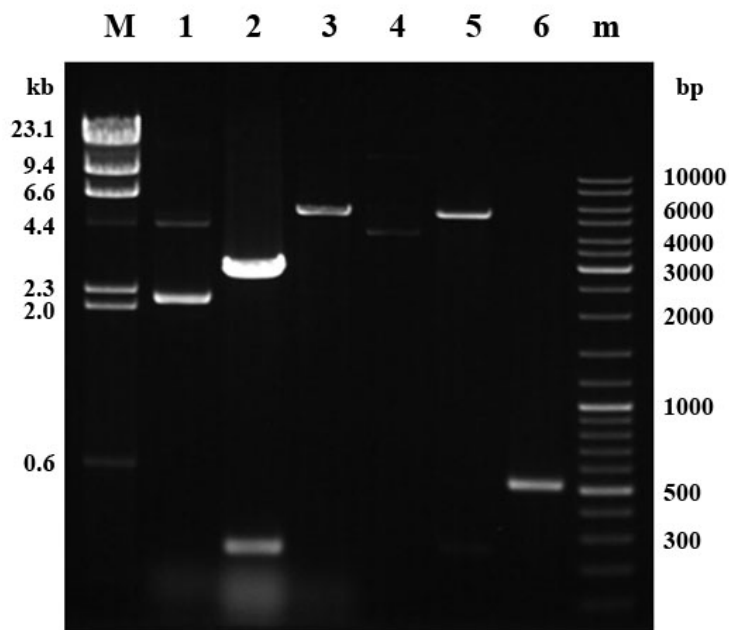
restriction patterns of the recombinant plasmids harboring *OsCML7*, *OsCML9*, *OsCML11* and *OsCML13*, respectively. With the exception of *OsCML13*, the sizes of the inserted fragment were the same as those of the PCR products (lanes 6). The resulting recombinant plasmids are called pET21-OsCML7, pET21-OsCML9, pET21-OsCML11 and pET21-OsCML13, accordingly.

To confirm the nucleotide sequences of the *OsCML* genes inserted into pET-21a, the recombinant plasmids were subjected to DNA sequencing using T7 promoter and T7 terminator primers. The results show that sequences of the *OsCML*7, *OsCML9*, *OsCML11* and *OsCMl13* genes in the recombinant plasmids share 100 % identity with their respective cDNA sequences as shown in Figure 3.6, 3.7, 3.8 and 3.9, respectively. The coding regions of the *OsCML* genes were engineered to lose its stop codon and fuse in frame with the 6x His tag coding sequence from pET-21a for further use in purification of the recombinant proteins**.** Direction of the *OsCML* genes inserted into pET-21a is shown in Figure 3.10. The molecular weights of the recombinant OsCML7, OsCML9, OsCML11 and OsCML13 calculated from their deduced amino acid sequences are 18.2, 18.1, 24.5 and 20.9 kDa, respectively.

3.2   Induction of OsCML protein expression

The *E. coli* BL21(DE3) transformants containing each of the four *OsCML* genes were grown and induced by IPTG at a final concentration of 0, 0.1, 0.3, 0.5 or 0.8 mM for 4 hours before cells were harvested as described in 2.3.5.2. Protein concentration of the crude extracts from each recombinant protein was determined by Bradford method as described in 2.3.6 and 20 μg proteins from the crude extracts were subjected to electrophoresis on 12 % SDS-polyacrylamide gel. The results in

Figure 3.11-3.13 show protein expression patterns of the recombinant *E. coli* cells harboring *OsCML9*, *OsCML11* and *OsCMl13* genes, respectively. For the cells harboring *OsCML7* gene, no recombinant protein was detected by all final concentrations of IPTG (data not shown). In the case of OsCML9 and OsCML11, they were clearly expressed in the presence of IPTG. The expression of OsCML9 was only detected in the presence of IPTG and its levels were similar in all concentrations while the OsCML11 expression was also detected in the absence of IPTG and its level was highest at 0.1 mM IPTG. For OsCML13, the expression was observed in the culture without IPTG induction, however, no obvious band was detected by SDS-PAGE in the culture with IPTG induction.

3.3   Purification of recombinant OsCaM and OsCML proteins

Crude proteins of the recombinant OsCMLs prepared from 1 liter of LB medium as described in section 2.3.9.1, were loaded into a phenyl-Sepharose column prepared as described in section 2.3.9.2. Unbound proteins were eluted from the column by Wash buffer I and the proteins were eluted by Elution buffer I. Proteins from each step of purification were analyzed by SDS-PAGE as described in section 2.3.7. All recombinant OsCaM and OsCML proteins (OsCaM1, OsCaM2, OsCaM3, OsCML1, OsCML3, OsCML4, OsCML5, OsCML8, OsCML11 and OsCML13) except OsCML9 could be purified by Ca^{2+}-dependent Phenyl-Sepharose hydrophobic chromatography. Figure 3.14 shows representative protein patterns of OsCML13 during purification. The molecular weight of OsCML13 was estimated to be 19.6 kDa by its mobility in SDS-PAGE when compared with those of standard proteins. Purification of the recombinant OsCML11 was similarly carried out and its molecular

GGATCGAGATCTCGATCCCGCGAAATTAATACGACTCACTATAGGGGAATTGTGAGCGGATA
ACAATTCCCCTCTAGAAATAATTTTGTTTAACTTTAAGAAGGAGATATACATATGGGGGGGA

                    M G G

AGGAGCTGAGCGAGGAGCAGGTGGCGTCGATGCGGGAGGCGTTCTCCCTCTTCGACACCGAC
K E L S E E Q V A S M R E A F S L F D T D

GGCGACGGCCGGATCGCGCCGTCGGAGCTCGGCGTCCTGATGCGCTCCCTCGGCGGGAACCC
G D G R I A P S E L G V L M R S L G N P

CACCCAGGCGCAGCTCCGCGACATCGCCGCGCAGGAGAAGCTCACCGCGCCCTTCGACTTCC
T Q A Q L R D I A A Q E K L T A P F D F

CGCGCTTCCTCGACCTCATGCGCGCCCACCTCCGCCCCGAGCCCTTCGACCGCCCGCTCCGC
P R F L D L M R A H L R P E P F D R P L R

GACGCCTTCCGCGTCCTCGACAAGGACGCCTCCGGCACCGTCTCCGTCGCCGATCTCCGCCA
D A F R V L D K D A S G T V S V A D L R H

CGTCCTCACCTCCATCGGCGAGAAGCTCGAGCCCCACGAGTTCGACGAGTGGATCCGCGAGG
V L T S I G E K L E P H E F D E W I R E

TCGACGTCGCCCCCGACGGCACCATCCGCTACGACGACTTCATCCGCCGCATCGTCGCCAAA
V D V A P D G T I R Y D D F I R R I V A K

AAGCTTGCGGCCGCACTCGAGCACCACCACCACCACCACTGAGATCCGGCTGCTAACAAGCC
K L A A A L E H H H H H H

CGAAGAAGCNNNNNNN

Figure 3.6 Nucleotide and deduced amino acid sequences of the *OsCML7* gene in the recombinant pET-21a. The red bold letters indicate start and stop codons. The green letters show a partial nucleotide sequence of the T7 promoter and the blue letters show the nucleotide sequence of the 6x His tag.

NNNNNNNNN NTCCCNTCTTAGAATATTTTGGTTTAACTTTAAGGAAGGGAGATATGACAT**ATG**

                                                                                M

GCGGCCAAGCTGACCCAAGAACAGGTGGACGAGTGCCGAGAAATCTTCGACCTGTTCGACAG

  A   A   K   L   T   Q   E   Q   V   D   E   C   R   E   I   F   D   L   F   D   S

CGACGAGGACGGTCGCATCGCCGCCGGCGAGCTCGTGACGGCGCTGCGGTCGCTGGGCCAGA

    D   E   D   G   R   I   A   A   G   E   L   V   T   A   L   R   S   L   G   Q

ACGTCGACGAGGCCGAGGCGCGGCGGTTCCTGGCGGACGCCACCGCCAGCGGCGGCGGCGGC

  N   V   D   E   A   E   A   R   R   F   L   A   D   A   T   A   S   G   G   G

GGAGGCGGCGGAGACATCGACTTCGCGGCGTTCCTGTCGGTGGCGGCGCGCAAGATGAGGCG

    G   G   G   G   D   I   D   F   A   A   F   L   S   V   A   A   R   K   M   R   R

CGGGGCGACGGAGAAGGAGCTCGCGGCGTGCTTGGACGTGTTCGACGACGCGCGGAGCGGGG

    G   A   T   E   K   E   L   A   A   C   L   D   V   F   D   D   A   R   S   G

TGATCCCGGCGGAGCAGCTCCGGCAGGCGATGGTGTCCCACGGCGACCGGCTGACGGAGGAG

  V   I   P   A   E   Q   L   R   Q   A   M   V   S   H   G   D   R   L   T   E   E

GAGGCCGACGAGATGGTGCGCAAGGCGGATCCCGCCGGCGAGGGCCGCGTCGAGTACAAGGA

  E   A   D   E   M   V   R   K   A   D   P   A   G   E   G   R   V   E   Y   K   E

GTTCGTCAAGGTGTTGATGAACAACAAGAAGCTTGCGGCCGCACTCGAGCACCACCACCACC

    F   V   K   V   L   M   N   N   K   K   L   A   A   A   L   E   H   H   H

ACCAC**TGA**GATCCGGCTGCTAACAAAGCCCGAAAGGAAGCTGAGTTGGCTGCTGCCACCGCT

H H

GAGCAATAACTAGCATAACCCCTTGGGGCCTCTAAACGGGTCTTGAGGGGTTTTTTGCTGAA
AGGAGGAACTATATCCGGATTGGCGAATGGGACGCGCCCTGTAGCGGCGCATTAAGCGCGGC

Figure 3.7 Nucleotide and deduced amino acid sequences of the *OsCML9* gene in the recombinant pET-21a. The red bold letters indicate start and stop codons. The green letters show a partial nucleotide sequence of the T7 promoter and the blue letters show the nucleotide sequence of the 6x His tag.

Figure 3.8 Nucleotide and deduced amino acid sequences of the *OsCML11* gene in the recombinant pET-21a. The red bold letters indicate start and stop codons. The green letters show a partial nucleotide sequence of the T7 promoter and the blue letters show the nucleotide sequence of the 6x His tag.

NNNNGNNNANATTTCCCCTCTAGAATAATTTTGTTTAACTTTAAGAAGGAGATATACAT**ATG**

                                                      M

TCTACTGTCAAGGGACAGACCAGGAGGGAGAGGCCTAGAGGAGCTCGCCCTCATGGATTGAC
  S T V K G Q T R R R E R P R G A R P H G L T

GAAGCAGAAGAGGCAGGAAATAAAGGAGGCGTTTGATCTGTTCGACACAGATAACTCTGGAA
  K Q K R Q E I K E A F D L F D T D N S G

CCATTGATGCCAAAGAGTTGAATGTTGCCATGAGAGCCTTGGGATTTGAGATGACAGAAGAA
  T I D A K E L N V A M R A L G F E M T E E

CAAATTAACCAGATGATTGCTGATGTGGACAAAGATGGTAGTGGATCCATAGATTATGAGGA
  Q I N Q M I A D V D K D G S G S I D Y E E

GTTTGAGCATATGATGACTGCTAAGATTGGAGAGAGAGACAGTAAAGAAGAACTTACGAAAG
  F E H M M T A K I G E R D S K E E L T K

CATTCAGTATTATCGACCAAGATAAAAATGGGAAGATATCAGATGTTGATATTCAGCGAATT
  A F S I I D Q D K N G K I S D V D I Q R I

GCCAAGGAATTAGGTGAAAACTTCACTTATCAAGAGATTCAAGAAATGGTGCAAGAGGCAGA
  A K E L G E N F T Y Q E I Q E M V Q E A D

TCGAAATGGTGATGGTGAGATAGATTTTGATGAGTTCATTAGGATGATGAGGAGGACTGGAT
  R N G D G E I D F D E F I R M M R R T G

ATGGTTACAAGCTTGCGGCCGCACTCGAGCACCACCACCACCACCAC**TGA**GATCCGGCTGCT
  Y G Y K L A A A L E H H H H H H

AACAAAGCCCGAAAGGAAGCTGAGTTGGCTGCTGCCACCGCTGAGCAATAACTAGCATAACC
CCTTGGGGCCTCTAAACGGGTCTTGAGGGGTTTTTTGCTGAAAGGAGGAACTATATCCGGAT

Figure 3.9 Nucleotide and deduced amino acid sequence of the *OsCML13* gene in the recombinant pET-21a. The red bold letters indicate start and stop codons. The green letters show a partial nucleotide sequence of the T7 promoter and the blue letters show the nucleotide sequence of the 6x His tag.
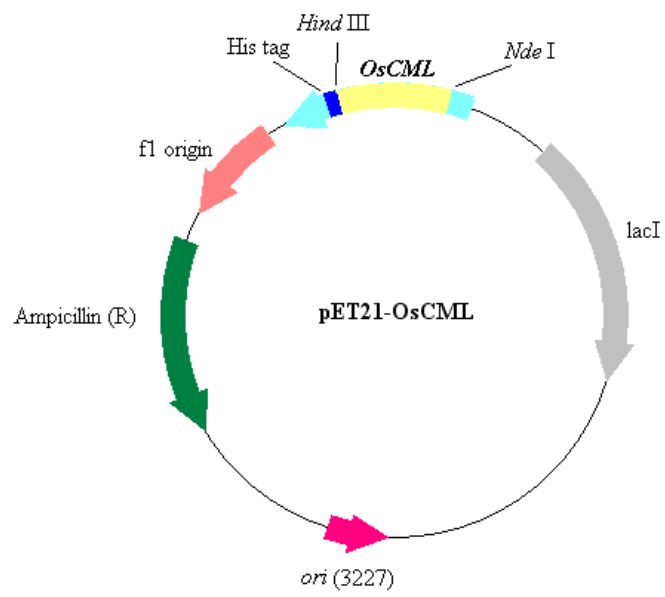
Figure 3.10 Direction of the *OsCML* genes inserted into pET21a containing His tag coding sequence.

Figure 3.11 SDS-PAGE of crude extracts of *E. coli* BL21(DE3) harboring pET21-OsCML9 clone induced at various IPTG concentrations

Lane M   = protein marker

Lane 1   = crude extract of *E. coli* BL21(DE3) harboring pET-21a

Lane 2   = crude extract of *E. coli* BL21(DE3) harboring pET-21a induced
          by 0.3 mM IPTG

Lane 3   = crude extract of *E. coli* BL21(DE3) harboring pET21-OsCML9

Lane 4   = crude extract of *E. coli* BL21(DE3) harboring pET21-OsCML9
          induced by 0.1 mM IPTG

Lane 5   = crude extract of *E. coli* BL21(DE3) harboring pET21-OsCML9
          induced by 0.3 mM IPTG

Lane 6   = crude extract of *E. coli* BL21(DE3) harboring pET21-OsCML9
          induced by 0.5 mM IPTG

Lane 7   = crude extract of *E. coli* BL21(DE3) harboring pET21-OsCML9

induced by 0.8 mM IPTG
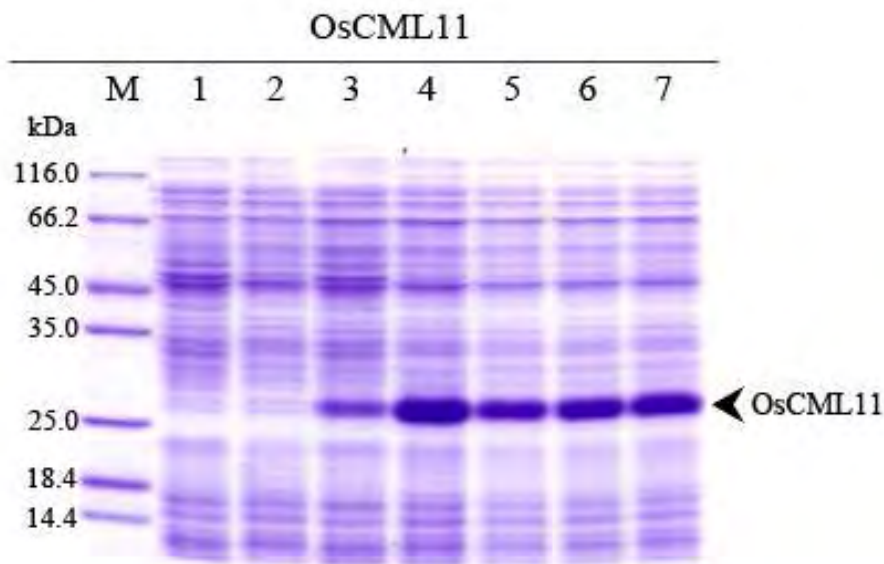
Figure 3.12 SDS-PAGE of crude extracts of *E. coli* BL21(DE3) harboring pET21-OsCML11 clone induced at various IPTG concentrations

Lane M   = protein marker

Lane 1   = crude extract of *E. coli* BL21(DE3) harboring pET-21a

Lane 2   = crude extract of *E. coli* BL21(DE3) harboring pET-21a induced
            by 0.3 mM IPTG

Lane 3   = crude extract of *E. coli* BL21(DE3) harboring pET21-OsCML11

Lane 4   = crude extract of *E. coli* BL21(DE3) harboring pET21-OsCML11
            induced by 0.1 mM IPTG

Lane 5   = crude extract of *E. coli* BL21(DE3) harboring pET21-OsCML11
            induced by 0.3 mM IPTG

Lane 6   = crude extract of *E. coli* BL21(DE3) harboring pET21-OsCML11
            induced by 0.5 mM IPTG

Lane 7   = crude extract of *E. coli* BL21(DE3) harboring pET21-OsCML11
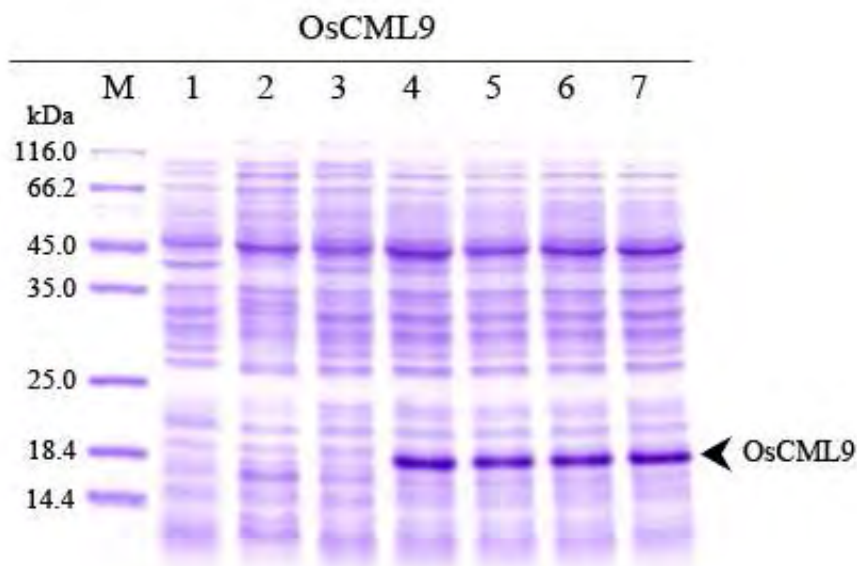   induced by 0.8 mM IPTG
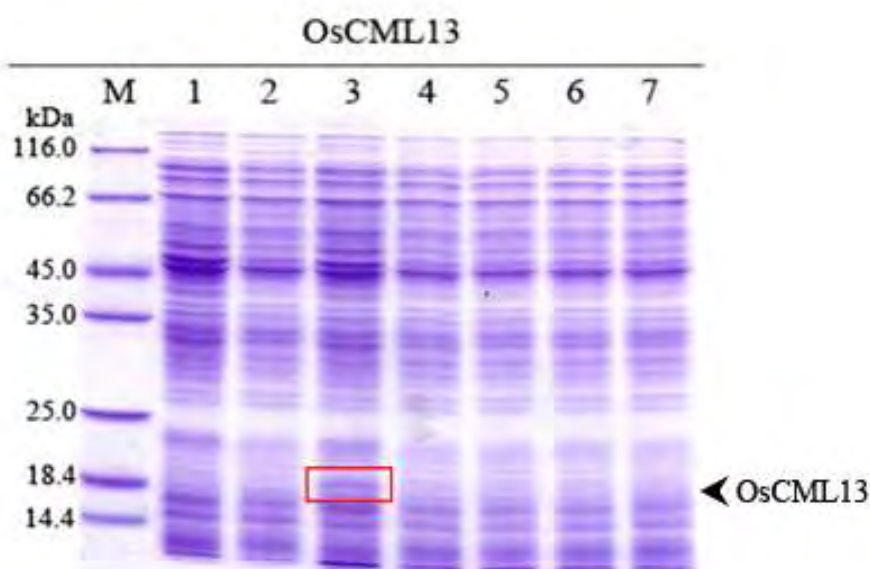
Figure 3.13 SDS-PAGE of crude extracts of *E. coli* BL21(DE3) harboring pET21-OsCML13 clone induced at various IPTG concentrations

Lane M = protein marker

Lane 1 = crude extract of *E. coli* BL21(DE3) harboring pET-21a

Lane 2 = crude extract of *E. coli* BL21(DE3) harboring pET-21a induced by 0.3 mM IPTG

Lane 3 = crude extract of *E. coli* BL21(DE3) harboring pET21-OsCML13

Lane 4 = crude extract of *E. coli* BL21(DE3) harboring pET21-OsCML13 induced by 0.1 mM IPTG

Lane 5 = crude extract of *E. coli* BL21(DE3) harboring pET21-OsCML13 induced by 0.3 mM IPTG

Lane 6 = crude extract of *E. coli* BL21(DE3) harboring pET21-OsCML13 induced by 0.5 mM IPTG

Lane 7 = crude extract of *E. coli* BL21(DE3) harboring pET21-OsCML13 induced by 0.8 mM IPTG

weights were estimated to be 26.1 kDa. In order to purify OsCML9, the crude extract was loaded into a Ni-Sepharose column prepared as described in section 2.3.9.2. Unbound proteins were washed from the column by Wash buffer II and the recombinant OsCML9 protein was eluted by Elution buffer II. Proteins from each step of purification were analyzed by SDS-PAGE as described in section 2.3.7. As a result, OsCML9 could be purified by Ni-Sepharose affinity chromatography. Figure 3.15 shows protein patterns of OsCML9 during purification. The molecular weight of OsCML9 was estimated to be 17.6 kDa by its mobility in SDS-PAGE when compared with those of standard proteins.

3.4 Characterization of OsCaM and OsCML proteins

3.4.1 Amino acid sequence analysis

Three *OsCam* (*OsCam1*, *OsCam2*, and *OsCam3*) and five *OsCML* (*OsCML1*, *OsCML3*, *OsCML4*, *OsCML5*, *OsCML8*) genes previously cloned in the pET-21a expression vector together with the three *OsCML* (*OsCML9*, *OsCML11* and *OsCML13*) genes cloned in this work were used for protein characterization. The deduced amino acid sequences of these OsCaM and OsCML proteins were compared. Figure 3.16 shows the primary structures of OsCaM and OsCML proteins using OsCaM1 as a standard. Amino acids are presented in the single-letter IUPAC nomenclature and sequences are aligned to illustrate the relationships of the four Ca^{2+}-binding domains. Table 3.1 shows characteristics of 12 OsCaM and OsCML proteins. Ca^{2+}-coordinating residues among OsCaMs and OsCMLs are invariable with those of the plant CaM consensus sequence. From pair-wise alignments, OsCaM2, OsCaM3, OsCML1, OsCML3, OsCML4, OsCML5, OsCML7, OsCML8, OsCML9, OsCML11

Figure 3.14 Protein patterns of *E. coli* BL21(DE3) harboring pET21-OsCML13 detected by SDS-PAGE during recombinant protein purification by a phenyl-Sepharose column

Lane M	= protein marker
Lane 1	= crude extract
Lane 2	= flow through
Lane 3	= eluted OsCML13

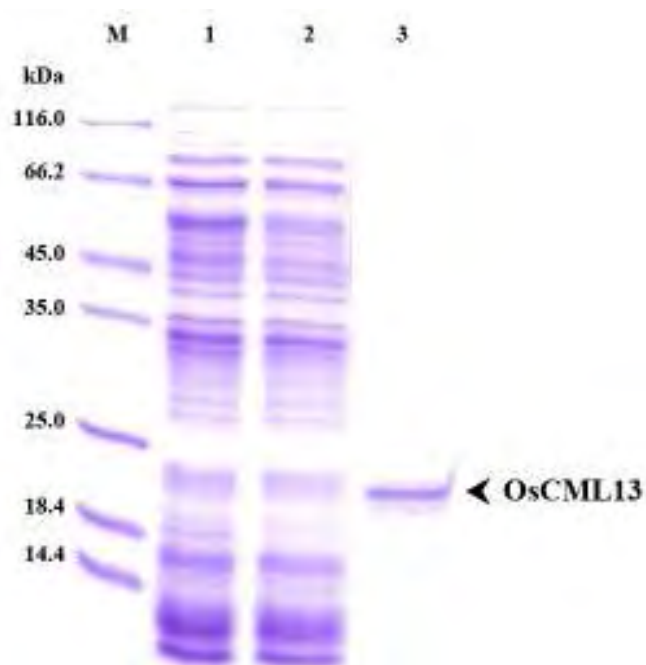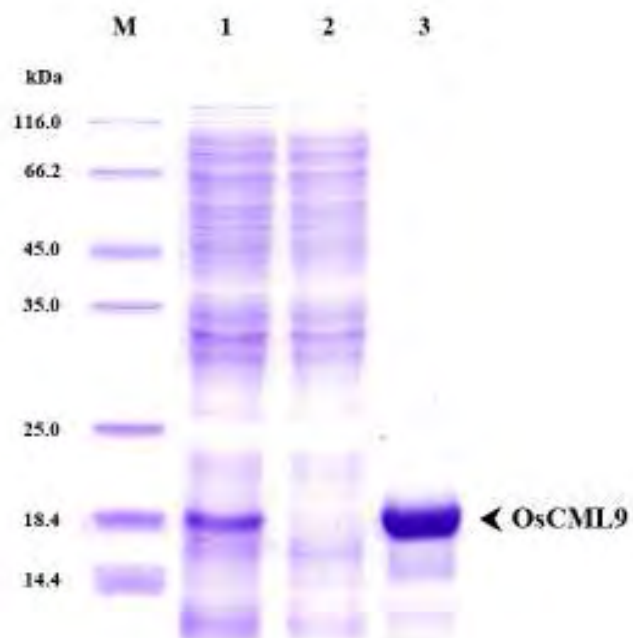**Figure 3.15 Protein patterns of *E. coli* BL21(DE3) harboring pET21-OsCML9 detected by SDS-PAGE during recombinant protein purification by a Ni-Sepharose column**

Lane M   = protein marker

Lane 1   = crude extract

Lane 2   = flow through

Lane 3   = eluted OsCML9

and OsCML13 have amino acid identities with OsCaM1 of 98.7, 98.7, 84.6, 68.9, 68.9, 62.2, 47.7, 47.0, 46.1, 44.1 and 43.6 %, respectively. All of the conserved nine methionine (M) and nine phenylalanine (F) residues among plant CaMs are present in all OsCaMs. The OsCML1 and OsCML3, containing a C-terminally extended 38 and 35 amino acid tail compared with an OsCaM1, respectively. However, the OsCML8, OsCML11 and OsCML13 have 35, 52 and 16 amino acid extensions in the N-terminus, respectively. All OsCaM and OsCML proteins have two pairs of identifiable EF hands except OsCML9 which has a single EF hand and OsCML7 which appears to have two separate EF hands.

3.4.2 Ca^{2+} binding properties of OsCaM and OsCML proteins

To produce recombinant proteins from the eight previously cloned genes, the recombinant clones were transformed into *E. coli* BL21(DE3) and protein production was induced by IPTG followed by protein purification by Ca^{2+}-dependent Phenyl-Sepharose hydrophobic chromatography using the protocols similar to those used for the *OsCML* genes cloned in this work as described above. These proteins as well as those produced from the genes cloned in this work would then be used for the characterization of the Ca^{2+}-binding properties as well as for all other experiments described below.

One of the characteristics of CaM is its ability to bind Ca^{2+} in the presence of SDS, which increases its electrophoretic mobility relative to CaM in the absence of Ca^{2+}. Figure 3.17 shows that all recombinant OsCaMs (OsCaM1, OsCaM2 and OsCaM3) and OsCMLs (OsCML1, OsCML3, OsCML4, OsCML5, OsCML8, OsCML9, OsCML11 and OsCML13) displayed this characteristic mobility shift when

Table 3.1 Characteristics of 12 OsCaM and OsCML proteins.

Proteins	Amino acids (a)	Number of EF-hand (b)	Number of Met residues (c)	Percentage of Met residues (d)	Identity to CaM1 (%) (e)
OsCaM1	149	4	9	6.0	100
OsCaM2	149	4	9	6.0	98.7
OsCaM3	149	4	9	6.0	98.7
OsCML1	187	4	8	4.3	84.6
OsCML3	183	4	9	4.9	68.9
OsCML4	154	4	10	6.5	68.9
OsCML5	166	4	8	4.8	62.2
OsCML7	148	2	4	2.8	47.7
OsCML8	191	4	10	5.2	47.0
OsCML9	155	1	5	3.2	46.1
OsCML11	211	4	3	1.4	44.1
OsCML13	169	4	9	5.3	43.6

(a) Number of amino acids of the deduced amino acid sequence. (b) Number of EF hands based on the prediction by InterProScan. (c) Number of methionine (M) residues in the deduced amino acid sequence. (d) Percentage of methionine (M) residues in the deduced amino acid sequence. (e) Number of identical residues divided by the total number of amino acids that have been aligned expressed in percentage.
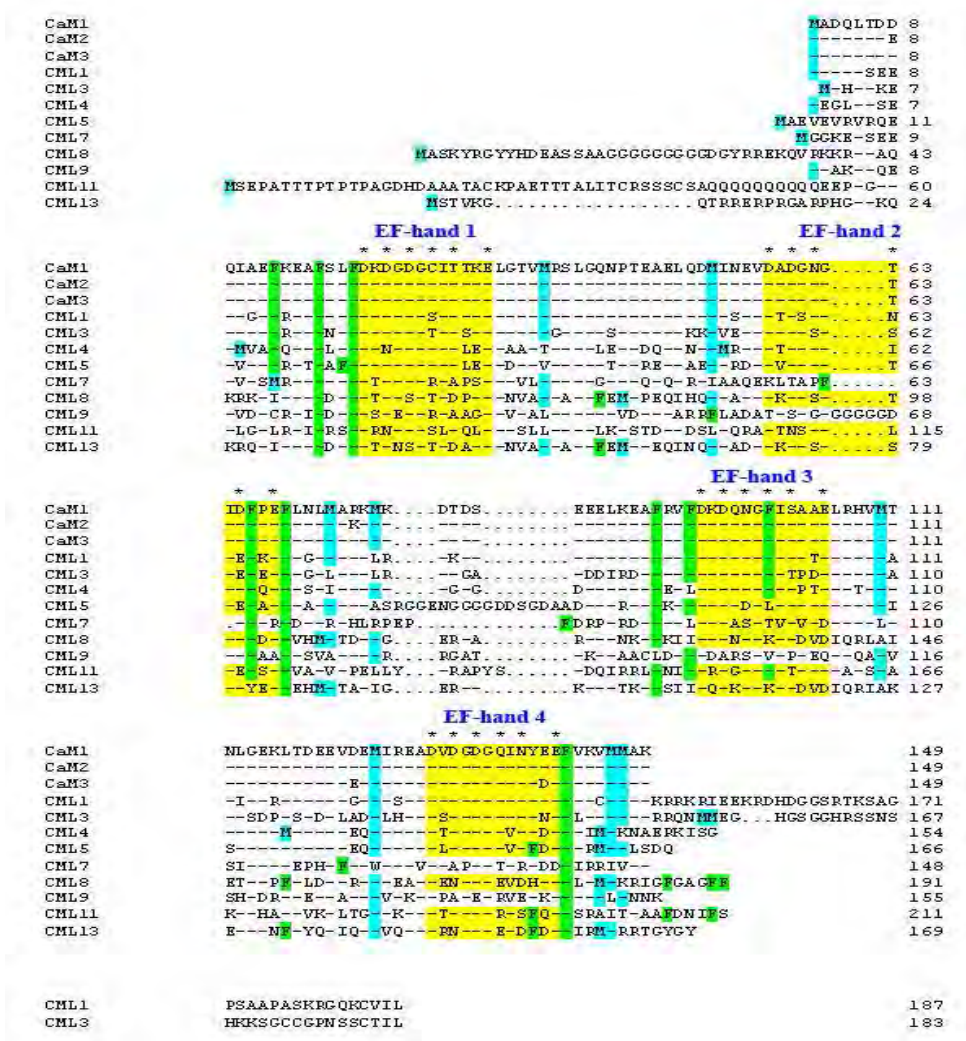
Figure 3.16 Comparison of the primary structures of OsCaM and OsCML proteins. Comparison of the deduced amino acid sequences of the OsCaM and OsCML proteins. The sequences are compared using OsCaM1 as a standard; identical residues in other sequences are indicated by a dash (-), and a gap introduced for alignment purposes is indicated by a dot (.). . The EF-hand calcium binding motifs are marked in yellow color and residues serving as Ca^{2+}-binding ligands are marked with asterisks (*). Methionine (M) and Phenylanine (F) residues are highlighted in blue and green, respectively.

incubated with 1 mM Ca^{2+} compared with 3 mM EGTA prior to electrophoresis. Even though the degree of mobility shift varied among different recombinant proteins with OsCML4 and OsCML13 exhibiting the highest degree of mobility shift, and OsCML9 and OsCML11 only displaying a subtle difference; these results indicate that the recombinant OsCaM and OsCML proteins produced in *E. coli* and purified by these methods are likely to be functional Ca^{2+}-binding proteins.

3.4.3)   CaMKII peptide binding properties of OsCaM and OsCML proteins

To further examine the properties of the OsCaM and OsCML proteins, its ability to bind the peptide derived from CaM kinase II (CaMKII) was assessed by gel mobility shift assay. Since CaM kinase II is a CaM-binding protein, examination of the ability to interact with its CaM-binding domain of particular CaM-related proteins would suggest whether they likely function similarly to and share similar sets of binding proteins with CaM. Incubation of 100 picomoles of recombinant proteins in the presence of 1 mM Ca^{2+} or 3 mM EGTA with different amounts of the peptide prior to PAGE-4 M urea resolution was performed.

All OsCaM proteins (OsCaM1, OsCaM2 and OsCaM3) displayed a peptide-protein complex whose electrophoretic mobility could be distinguished from that of the free proteins shown by the representative results of OsCaM2 in Figure 3.18. The clear band shift indicated that they bound the CaMKII peptide and suggested that mechanisms of action of these proteins were likely to be similar to those from known typical CaMs. On the contrary, under the same conditions, all OsCML proteins did not form complexes with CaMKII peptides that could be resolved from the free
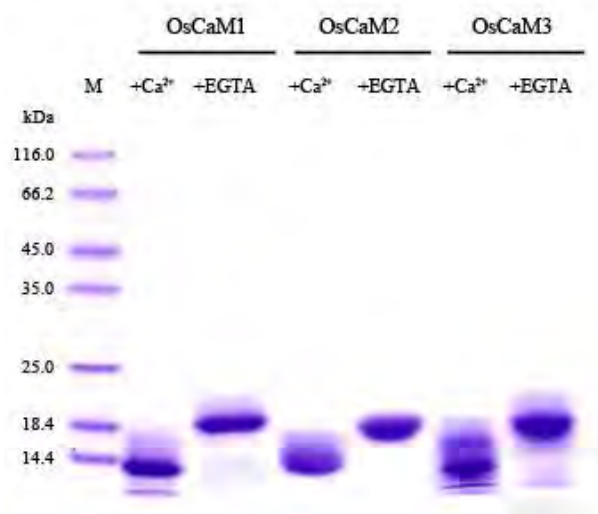
(a)
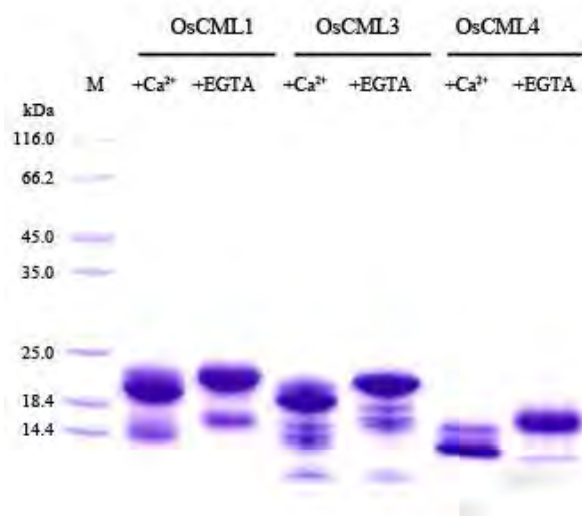
(b)
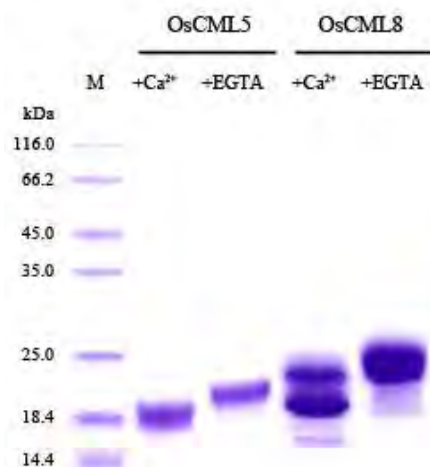
(c)
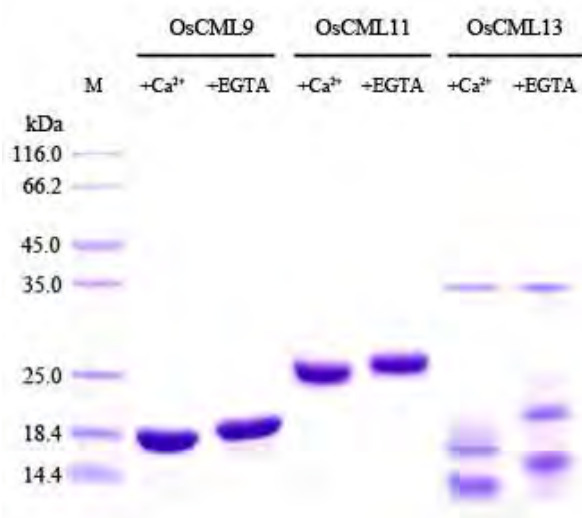
(d)

Figure 3.17 Ca^{2+}-induced electrophoretic mobility shift analyses of recombinant OsCaMs and OsCMLs in the presence of Ca^{2+} (lane + CaCl$_2$) or EGTA (lane +EGTA). Lane marked M contained molecular mass standard proteins. Gel electrophoretic mobility shift of recombinant OsCaM1, OsCaM2 and OsCaM3, (a); OsCML1, OsCML3 and OsCML4, (b); OsCML5 and OsCML8, (c); OsCML9, OsCML11 and OsCML13, (d).

proteins by gel electrophoresis as represented by the results of OsCML5 as shown in Figure 3.19.

3.4.4) Analysis of structural changes from circular dichroism spectroscopy

Far-ultraviolet circular dichroism (far-UV CD) spectroscopy was used to determine the secondary structures of all recombinant OsCaM and OsCML proteins and whether any structural changes occurred upon Ca^{2+}-binding. For CaM, major conformational changes including an increase in α-helicity upon Ca^{2+}-binding have been documented whereas very little structural information is available for the CML proteins. Figure 3.20 shows that the far-UV CD spectra of all proteins in the presence of 1 mM $CaCl_2$ or 1 mM EGTA have two minima near 208 and 222 nm indicating that these proteins contain substantial α-helical secondary structure. $[\theta]_n$ is molar ellipticity per residue for a residue of n amino acid residues. Table 3.1 summarizes values of $-[\theta]_n$ at 208 and 222 nm from the spectra of all proteins in the presence of 1 mM $CaCl_2$ or 1 mM EGTA and their changes upon Ca^{2+} addition, where Δ is the difference of molar ellipticity per residue between the presence and absence of Ca^{2+} and %Δ is the ratio of Δ and the molar ellipticity per residue in the presence of Ca^{2+} expressed in percentage form. Upon Ca^{2+} addition, an increase in molar ellipticity per residue at 208 and 222 nm was clearly observed for all recombinant OsCaMs and some OsCMLs (OsCML4, OsCML5 and OsCML8) with the percentage of change in $-[\theta]_n$ at 222 nm in the presence of Ca^{2+} ranging from 22 to 134 while OsCML1, OsCML3 and OsCML9 displayed very little change in the molar elipticity. As expected, all OsCaM proteins (OsCaM1, OsCaM2 and OsCaM3) displayed a large
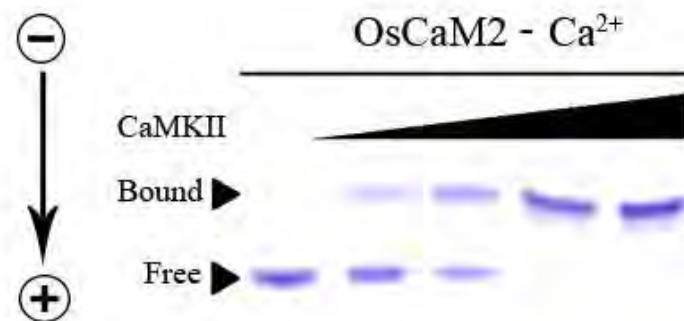
(a)
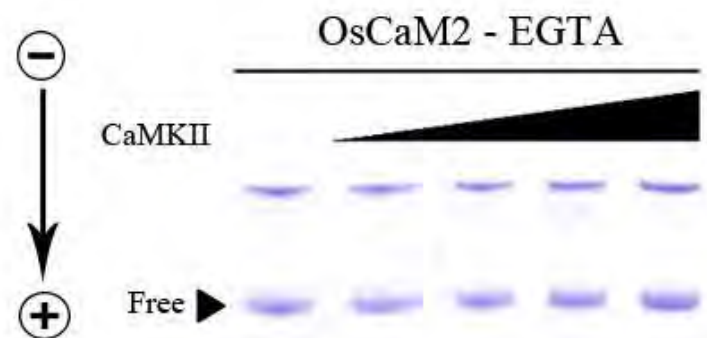
(b)

Figure 3.18 Gel mobility shift analysis of OsCaM2 interaction with a peptide from CaMKII. (a) Peptide binding assay in the presence of Ca^{2+} (b) Peptide binding assay in the presence of EGTA
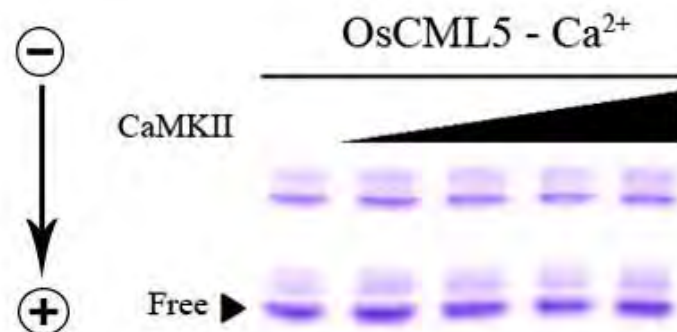
(a)
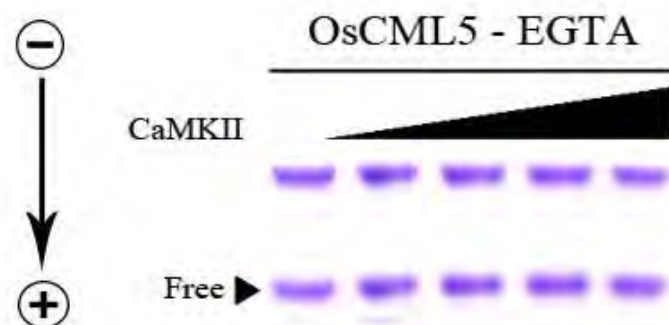
(b)

Figure 3.19 Gel mobility shift analysis of OsCML5 interaction with a peptide from CaMKII. (a) Peptide binding assay in the presence of Ca^{2+} (b) Peptide binding assay in the presence of EGTA

(a)

(b)
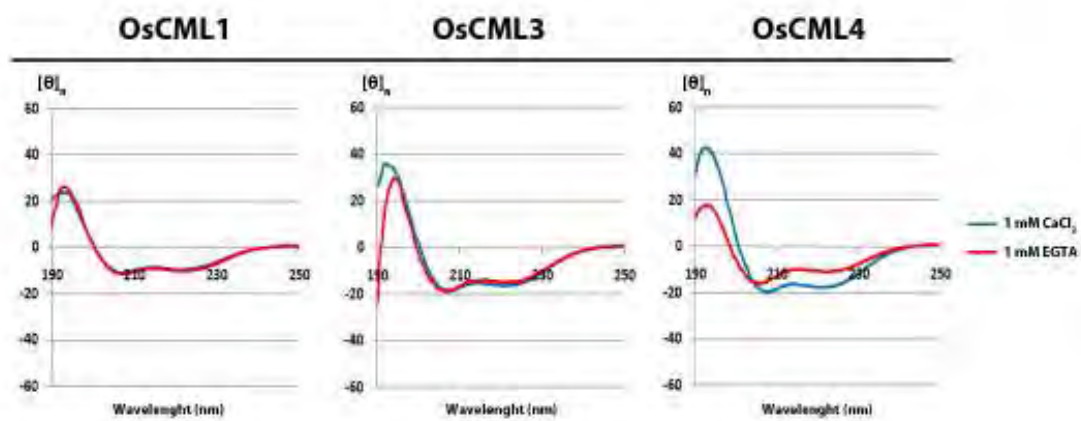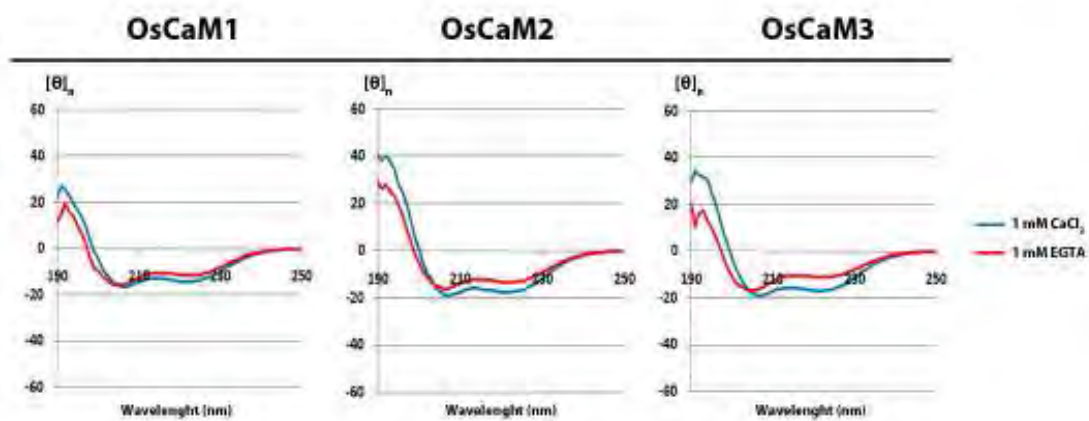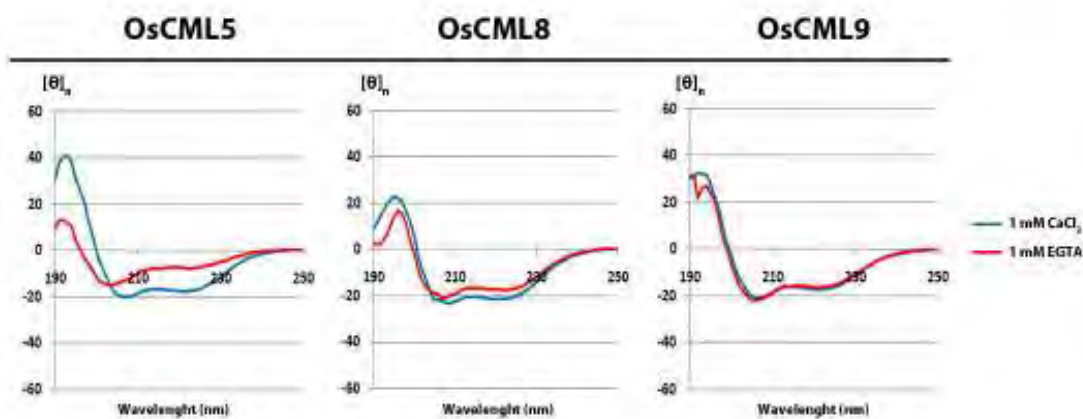
(c)
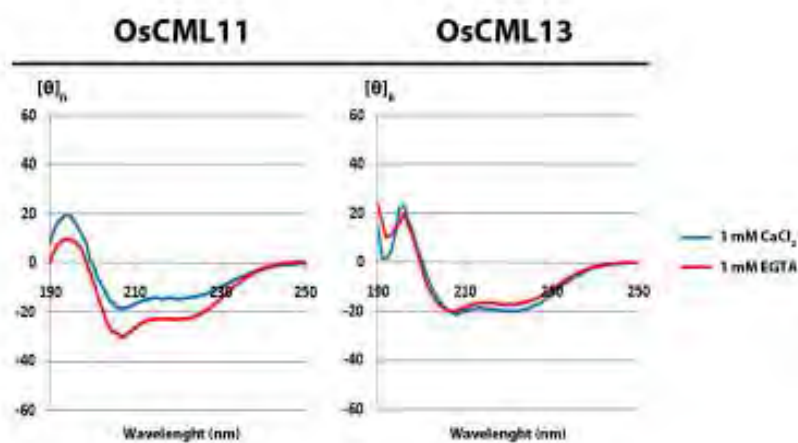
(d)

Figure 3.20 Ca^{2+}-induced conformational changes of the OsCaM and OsCML proteins   measured by Far-UV CD spectroscopy. Represents the difference far-UV CD spectra in the presence of Ca^{2+} or EGTA of OsCaM1, OsCaM2 and OsCaM3, (a); OsCML1, OsCML3 and OsCML4, (b); OsCML5 and OsCML8, (c); OsCML9, OsCML11 and OsCML13, (d).

Table 3.1 Summarizes values of $-[\theta]_n$ at 208 and 222 nm from the spectra of OsCaM and OsCML proteins in the presence of 1 mM CaCl$_2$ or 1 mM EGTA and their changes upon Ca^{2+} addition.

Recombinant protein	$-[\theta]_{n(208)}x10^{-2}$ (deg.cm^2 /dmol.residues)		Δ	$\%\Delta$	$-[\theta]_{n(222)}$ x10^{-2} (deg.cm^2 /dmol.residues)		Δ	$\%\Delta$
	$-Ca^{2+}$	$+Ca^{2+}$			$-Ca^{2+}$	$+Ca^{2+}$		
OsCaM1	14.29	15.65	1.36	9.5	11.44	14.13	2.69	23.5
OsCaM2	15.26	18.45	3.19	20.9	13.25	17.5	4.25	32.1
OsCaM3	15.07	18.77	3.7	24.5	10.96	16.88	5.92	54.0
OsCML1	11.48	11.01	-0.47	-4.1	10.09	9.5	-0.59	-5.8
OsCML3	18.4	18.53	0.13	0.7	14.76	16.32	1.56	10.6
OsCML4	14.78	19.68	4.9	33.1	11.03	17.82	6.79	61.6
OsCML5	11.85	19.93	8.08	68.2	7.53	17.62	10.09	134
OsCML8	20.71	23.41	2.7	13.0	17.42	21.34	3.92	22.5
OsCML9	21.02	20.66	-0.36	-1.7	16.43	17.17	0.74	4.5
OsCML11	29.15	18.37	-10.78	-37.0	22.82	14.30	-8.52	-37.3
OsCML13	19.78	21.17	1.39	7.0	17.19	19.94	2.75	16.0

increase in the $[\theta]_n$ of more than 20% (24%, 32% and 54%, respectively) when compared with the value in the absence of Ca^{2+}, which indicates that the helical content was highly increased in these proteins upon Ca^{2+} binding. Similar percentage was observed in OsCML8 (22%) while OsCML 4 and OsCML5 exhibited an even larger change in $-[\theta]_{n(222)}$ (62% and 134%, respectively) than OsCaMs. In addition, all OsCaMs, OsCML4, OsCML5 and OsCML8 also displayed a large change of spectrum in the interval of 190-200 nm. On the contrary, OsCML1, which share a high amino acid identity (84.6%) with typical CaM proteins, did not exhibit this induction while OsCML3 whose sequence is 64.9% identical to that of typical CaM proteins exhibited only small amount of increase in the $-[\theta]_{n(222)}$ (10.6%). However, it should be noted that a larger change of spectrum in the interval of 190-195 nm was observed for OsCML3 when Ca^{2+} was added. In contrast with the other proteins, the CD spectrum in the presence of Ca^{2+} of OsCML11 displayed a decrease in $[\theta]_n$ at 208 and 222 nm of more than 37%. Interestingly, the height of the peak at the interval of 190-200 nm of OsCML11 significantly increased in the presence of Ca^{2+}.

3.5.5) 8-Anilino-1-naphthalenesulphonate (ANS) fluorescence measurements

8-Anilino-1-naphthalenesulphonate (ANS) is a fluorescent probe that displays a blue shift when its environment is changed from an aqueous to a nonpolar medium. In addition, while its fluorescence in water is usually weak, ANS shows an enhanced fluorescence intensity in nonpolar medium. Therefore, ANS is a useful probe for Ca^{2+}-induced exposure of hydrophobic patches in the globular domains of CaMs

because its fluorescence spectrum is changed and can be monitored when it binds to the accessible hydrophobic surface of the proteins. To examine Ca^{2+}-induced exposure of the hydrophobic surfaces of the recombinant OsCaM and OsCML proteins, emission spectra of 100 μM ANS in the presence of each protein were monitored with the excitation wavelength set at 370 nm. Figure 3.21 shows representative emission spectra of 100 μM ANS in an aqueous buffer mixed with 1 μM of recombinant OsCaMs and OsCMLs in the presence of 3 mM EGTA or 1 mM Ca^{2+}. When mixed with each protein in the presence of EGTA, ANS displayed a relatively weak fluorescence with a maximum wavelength near 520 nm, which is almost identical to that of ANS alone (data not shown). Table 3.2 summarizes the changes in ANS fluorescence in the presence of each recombinant protein upon Ca^{2+} addition. In the presence of Ca^{2+}, the fluorescence spectrum of ANS mixed with each of the three OsCaM proteins or either of the two most highly conserved OsCMLs, OsCML1 and OsCML3, exhibited significant blue shifts in the maximum emission wavelengths (from 37 to 46 nm) and relatively large concomitant increases in the intensity (4.6 to 5.0 fold). The rest of the OsCML proteins upon Ca^{2+} addition have also caused similar changes to the ANS fluorescence, however, with smaller blue shifts and lower levels of intensity increment. Nonetheless, even with the smaller overall changes in ANS emission spectra, these changes indicate the exposure of hydrophobic patches on the surface of these OsCML proteins upon Ca^{2+} binding.
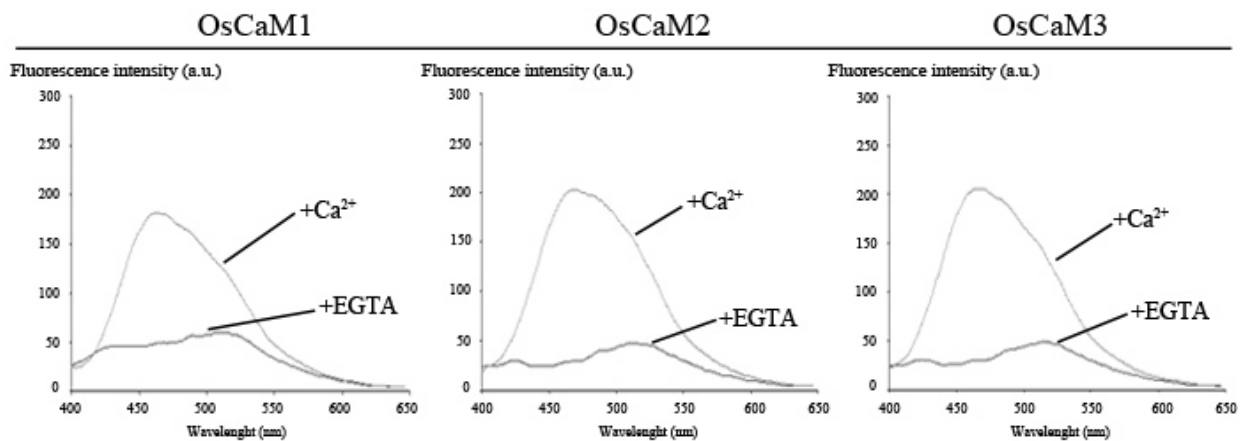
(a)
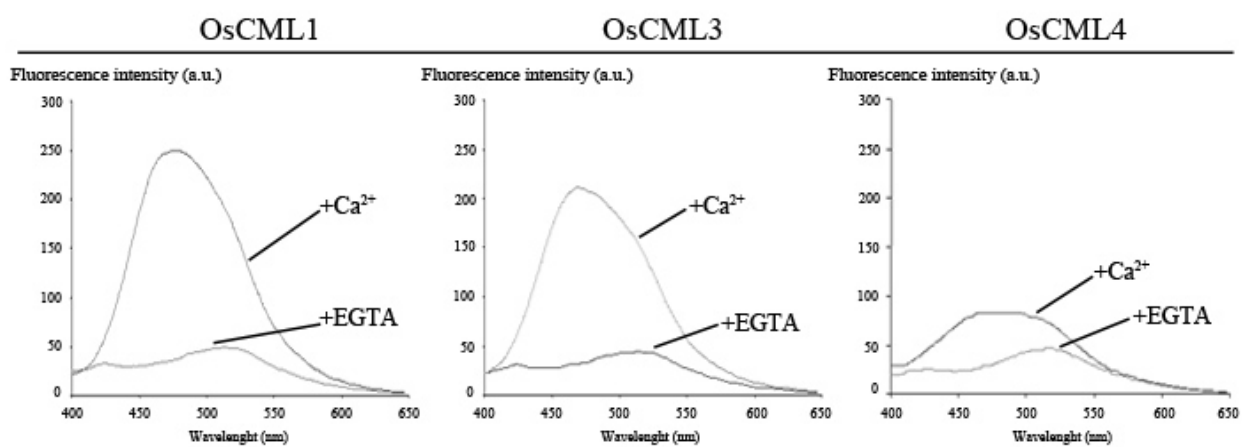
(b)
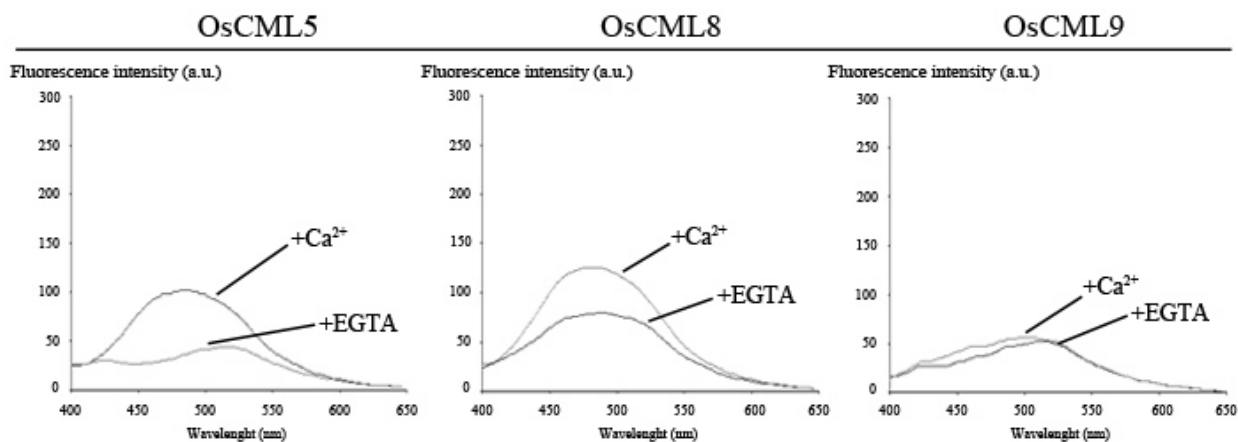
(c)
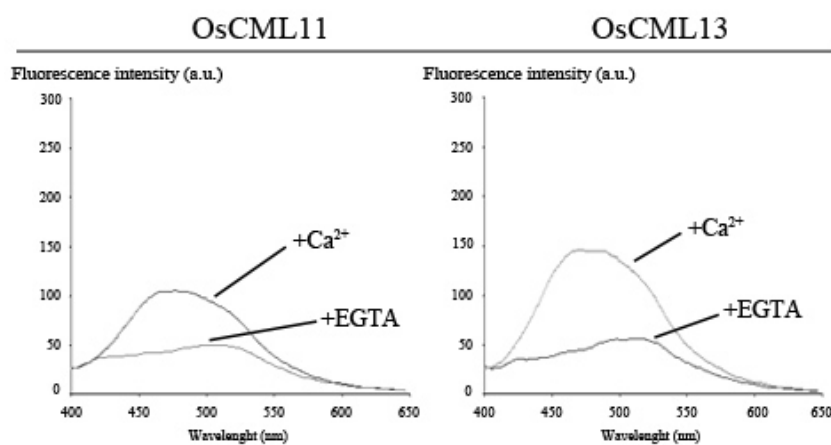
(d)

Figure 3.21 Conformational changes of the OsCaM and OsCML proteins measured by ANS fluorescence. Represents the conformation change in the presence of Ca^{2+} or EGTA of OsCaM1, OsCaM2 and OsCaM3, (a); OsCML1, OsCML3 and OsCML4, (b); OsCML5, OsCML8, and OsCML9, (c); OsCML11 and OsCML13, (d).

Table 3.2 The changes in ANS fluorescence in the presence of each of the OsCaM and OsCML proteins upon Ca^{2+} addition. $\Delta\lambda_{max}$ indicates the difference of maximum fluorescence emission of ANS in the presence and in the absence of Ca^{2+}. $I_{max}(+Ca^{2+})/I_{max}(-Ca^{2+})$ means the ratio of the maximum fluorescence intensity of ANS in the presence of Ca^{2+} to that in the absence of Ca^{2+}.

Recombinant Protein	Emission maximum(nm)	$\Delta\lambda_{max}$	$I_{max}(+Ca^{2+})/I_{max}(-Ca^{2+})$
OsCaM1	464	45	3.02
OsCaM2	469	44	4.28
OsCaM3	466	48	4.26
OsCML1	475	37	5.02
OsCML3	468	46	4.75
OsCML4	480	34	1.81
OsCML5	484	33	2.28
OsCML8	480	8	1.59
OsCML9	502	8	1.08
OsCML11	476	30	2.08
OsCML13	477	38	2.57

CHAPTER IV

DISCUSSION

Amino acid sequence analysis of OsCaM and OsCML proteins

The deduced amino acid sequences of 12 calmodulin (CaM) and calmodulin-like (CML) proteins were compared. OsCaM2 and OsCaM3 encode a protein of only two amino acid differences from OsCaM1 and their sequences share 98.7% identity with that of OsCaM1 protein. Hydrophobic residues contributing to hydrophobic interaction in the mechanism of CaM-target protein complex formation which are critical to CaM function are highly conserved. All of the conserved nine methionine (M) and nine phenylalanine (F) residues among plant CaMs are present in all OsCaMs. Due to its considerable conformational flexibility (Gellman, 1991) and being weakly polarized, methionine residues which are estimated to contribute nearly half of the accessible surface area of the hydrophobic patches of CaM allow it to interact with target proteins in a sequence-independent manner (O'Neil and DeGrado, 1990). Sequence conservation related to functionality of plant CaMs also includes lysine (K) at position 116 which is assumed to be trimethylated. All OsCaM proteins possess a lysine residue at this position. Lysine 116 trimethylation is believed to be a posttranslational modification that helps regulate CaM activity. All three OsCaM proteins have two pairs of EF hands with characteristic residues commonly found in plant CaMs. Ca^{2+}-coordinating residues among OsCaMs are invariable with those of the plant CaM consensus sequence.

The OsCML proteins under investigation have two pairs of identifiable EF hands except OsCML9 which has a single EF hand and OsCML7 which appears to have two separate EF hands. OsCML7 and OsCML9 are interesting because of their high amino acid identities with OsCaM1 (47.7% and 46.1%) but they possess only 2 and 1 EF hands; and have relatively low methionine (M) content (2.8% and 3.2%) compared with other OsCML proteins, respectively. Pairing of EF-hand motifs in the CaM molecule helps increase its affinity for Ca^{2+}, therefore an unpaired EF hand in OsCML7 and OsCML9 may bind Ca^{2+} with a lower affinity, or may be non-functional. Moreover, the OsCML1 and OsCML3 have 38 and 35 amino acid extensions, respectively in the C-terminus containing a polybasic domain in addition to the 149 amino acids OsCaM1. Previously, the published report shows that OsCML1 activated CaM-binding protein kinases (OsCBKs) in a Ca^{2+}-dependent manner, while the extended C-terminal domain was not required for the modulation. Conversely, the OsCMl8, OsCMl11 and OsCMl13 have 35, 52 and 16 amino acid extensions, respectively in the N-terminus in addition to the 149 amino acids OsCaM1. Interestingly, the OsCML11 has ten repeats glutamine (Q) residues in the N-terminus, which may be important to its function. The amino acid extensions in both termini may play regulatory roles for the Ca^{2+}-modulated activity of these OsCML proteins.

Ligands for Ca^{2+} coordination in the EF-hand motifs of OsCML proteins are highly conserved. Most residues in the Ca^{2+}-binding loops are conserved among OsCML proteins, thus suggesting that most of them are functional EF hands. Similar to OsCaMs, residues 1(+X) are exclusively filled with aspartate (D); and residues 3(+Y) and 5(+Z) are usually aspartate (D) or asparagine (N). Even though they are not

coordinating residues, glycine (G) at position 6 is absolutely conserved and hydrophobic residues (I, V, or L) are always found at position 8 in all 43 EF hands in all of the OsCaM and OsCML proteins examined. Residues 12(-Z) are mostly glutamate (E) with the exceptions of an EF hand in OsCML7, OsCML8, and OsCML13 which have aspartate (D) instead. While OsCML8 and OsCML13 have two pairs of EF-hand motifs, OsCML7 possess two separate EF hands with D at residue 12 in the EF-hand motif at the carboxyl terminus. Cates and colleagues (Cates *et. al*., 2005), previously reported that mutation of E12 to D reduced the affinity of EF hands for Ca^{2+} in parvalbumin by 100-fold and raised the affinity for Mg^{2+} by 10-fold. It is likely that these EF hands bind Mg^{2+} rather than Ca^{2+} but the physiological significance of Mg^{2+}-binding CaM-like activity is still not known.

Cloning and expression of *OsCam* and *OsCML* genes

In this research, four *OsCML* genes (*OsCML7*, *OsCML9*, *OsCML11* and *OsCML13*) were cloned into *E. coli* BL21(DE3) using plasmid pET-21a. For PCR amplification, one pair of primers specific for each gene was designed. The sense primer contained an *Nde*I site, while the antisense primer consisted of a *Hin*dIII site. The *Nde*I site within the sense primer allowed each gene fragment to be placed at an appropriate distance behind the T7 promoter and the ribosome binding site from the phage T7 major capsid protein in pET-21a (Novagen, 2002). Therefore, these *OsCML* genes as well as the other previously cloned genes used in this work (*OsCam1*, *OsCam2*, *OsCam3*, *OsCML1*, *OsCML3*, *OsCML4*, *OsCML5* and *OsCML8*) could be transcribed under the control of the T7 promoter and effectively translated using the

highly efficient ribosome binding site within the *E. coli* BL21(DE3) cell. The antisense primer, which contained a *Hind*III site, was designed to replace the stop codon in some of these genes with an amino acid and allow the gene fragment to fuse in-frame with the sequence encoding His-tag within pET-21a. Thus, after translation, the resulting fusion protein would consist of an encoded protein of interest and a His-tag interrupted by a few extra amino acids. The molecular weight of this fusion protein would be about 1,537 Da higher than the unfused protein. The His-tag behind the interested genes could be used to facilitate the purification and detection of the recombinant proteins. The $(His)_6$ fusion protein can easily be bound with Ni-Sepharose and then eluted with buffer containing imidazole.

pET system has been developed for tightly-regulated expression of recombinant proteins in *E. coli* cells. The approach to control basal expression is the use of vectors that contain what is termed a T7*lac* promoter (Studier *et al.*, 1990; Dubendorff and Studier, 1991). These plasmids contain a *lac* operator sequence just downstream of the T7 promoter. They also carry the natural promoter and coding sequence for the *lac* repressor (*lacI*), oriented so that the T7*lac* and *lacI* promoters diverge. When this type of vector is used in DE3 lysogens, the *lac* repressor acts both at the *lacUV5* promoter in the host chromosome to repress transcription of the T7 RNA polymerase gene by the host polymerase and at the T7*lac* promoter in the vector to block transcription of the target gene by any T7 RNA polymerase that is made. For protein production under this system control, addition of IPTG to a growing culture of the lysogen induces T7 RNA polymerase production, which in turn transcribes the target DNA in the plasmid. The result indicates that the *OsCML7* gene was not expressed by all final concentrations of IPTG. One possible explanation is the

secondary structure in the mRNA transcript, which may interfere with the AUG translation codon and/or the ribosome binding site. In the case of *OsCML9* and *OsCML11* genes expression, it was clearly expressed in the presence of IPTG. The expression levels of *OsCML9* were similar in all concentrations of IPTG. For *OsCML11*, the expression was also detected in the absence of IPTG and its level was highest at 0.1 mM IPTG. In the case of increasing over 0.1 mM IPTG concentration, it was found that the protein expression levels decreased. It is possible that the overexpressed protein may result in an accumulated misfolding protein leading to formation of inactive aggregates of protein known as inclusion bodies, or the overexpressed protein not involving in cellular mechanisms may interfere with a number of metabolic enzymes causing toxicity to the cell. For OsCML13, even in the absence of IPTG, its expression was detected. This might be due to some expression of T7 RNA polymerase from the *lacUV5* promoter in the DE3 lysogen from the *E. coli* genome (Novagen, 2002). Therefore, final concentrations of IPTG seem to influence the optimization of individual gene expression level. Variation in the expression level of the recombinant OsCMLs may be succeeding from mRNA secondary structure, protein misfolding and protein toxicity.

Purification of OsCaM and OsCML proteins

In this work, all OsCaMs and OsCMLs could be expressed as an intracellular soluble protein with the exception of OsCML7. Mechanical disruption methods are usually necessary to break down the cell wall in order to release intracellular protein prior to purification. The cell disintegration technique involved cell lysis by ultrasonication or high pressure sound waves, which causes cell breakage by

cavitations and shear forces, so in this work, cell wall was disrupted by ultrasonication. As a result, the control of metabolic regulation mechanism is lost when the cell is disrupted. However, several potential problems may arise during the disruption, due to the destruction of intracellular compartmentation. In this work, ethylenediamine tetraacetic acid (EDTA) was used in the extraction buffer as a metalloprotease inhibitor. This reagent protected the desired protein from the degradation by the proteolytic enzymes. Addition of a reagent containing a thiol group such as dithiothreitol (DTT) and also a chelating agent such as EDTA to chelate metal ions in the extraction buffer will minimize the oxidation damage (Bollag *et al.,* 1996).

The protein purification was carried out using Ca^{2+}-dependent hydrophobic chromatography on Phenyl-Sepharose, which is a medium for hydrophobic interaction chromatography (HIC). Substances are separated on the basic of their varying strength of their hydrophobic interaction with phenyl groups attached to the uncharged matrix. It widely used in the purification of recombinant CaM and CaM-like proteins from other sources such as CaM from *Nicotiana. tabacum* (Karita *et al.,* 2004), CML from *Pinctada fucata* (Li *et al.,* 2006) and CML37, CML38, CML39 from *Arabidopsis thaliana* (Vanderbeld and Snedden*,* 2007).

In the results, all OsCaM and OsCML proteins except OsCML9 could be purified by Ca^{2+}-dependent Phenyl-Sepharose hydrophobic chromatography. Binding to the column was dependent on the presence of Ca^{2+} suggesting that the proteins adopts an open conformation with nearly perpendicular interhelical angles between the globular domains, which exposes hydrophobic regions in the Ca^{2+} bound state. Successful purification of these proteins by the Ca^{2+}-dependent hydrophobic

chromatography suggests that they are functional Ca^{2+}-binding proteins. For OsCML9, it could be purified by Ni-Sepharose affinity chromatography. OsCML9 possesses only one EF hand and has relatively low methionine (M) content (3.2%). Pairing of EF-hand motifs in the CaM molecule helps increase its affinity for Ca^{2+}, therefore an unpaired EF hand in OsCML9 may bind Ca^{2+} with lower affinity. These characteristics agree well with the observation that it could not be purified by Ca^{2+}-dependent Phenyl-Sepharose hydrophobic chromatography.

Characterization of OsCaM and OsCML proteins

Even though, biophysical and structural properties of CaMs have been known in several organisms including some plant species, their related calcium sensors, CMLs, which have recently been extensively identified from Arabidopsis and rice, have not been characterized. Although the broad significance of these proteins can be postulated to be important in distinguishing between the Ca^{2+} signals from different stimuli and thus aid in eliciting the correct response, the actual significance is, however, not clearly understood, but nevertheless accumulating evidence suggests that each of the different *Cam* and *CML* genes may have distinct and significant functions. This work reports the molecular properties of CaM and CML proteins encoded by 11 genes from the rice genome. Based on the results of Ca^{2+}-dependent hydrophobic chromatography and Ca^{2+}-induced gel mobility shift as well as analyses of structural changes from CD spectroscopy and ANS fluorescence, all OsCaMs and OsCMLs under investigation appear to bind Ca^{2+} and undergo certain changes in their structures. By motif searches using InterProScan, two pairs of EF hands have been

detected in all of these proteins, with the exception of OsCML9. Most of these proteins exhibited the characteristic gel mobility shift in the presence of Ca^{2+} as expected because they contain all four EF hands with characteristic residues commonly found in plant CaMs except OsCML8/13, which have aspartate (D) in their third EF hands at residues 12(-Z), a position which normally contain a highly conserved glutamate (E) giving bidentate or monodentate metal ion chelation. Nonetheless, OsCML8/13 proteins appeared to bind Ca^{2+} in the conditions assayed and acquire α helical structure upon Ca^{2+} binding. Although OsCML9, which contain only one EF hand motif did not exhibit a similar gel mobility shift, CD spectra and ANS fluorescence have shown that OsCML9 binds to Ca^{2+} and undergoes some structural alterations, though of smaller degrees.

Arbitrarily, five genes which encode three different proteins that share the highest degree of amino acid sequence identity (>98%) with known typical plant CaMs have been classified as *OsCam* genes and the remaining rice CaM-related calcium sensors as CaM-like (*OsCML*) genes. To examine possible differential target-binding characteristic which is indicative of how they can be classified, their ability to bind the peptide derived from CaM kinase II in the presence of Ca^{2+} was assessed. All OsCaM proteins (OsCaM1, OsCaM2, and OsCaM3) exhibited this ability confirming their likely functionality as typical CaMs. Conversely, all OsCML proteins examined did not bind the peptide even though some of them share as high as 70-85% amino acid identity with OsCaMs. Even though what defines a "true" CaM and distinguishes it from a related Ca^{2+}-binding protein that serves a distinct role *in vivo* will still be an open question, these results suggest that target proteins of OsCMLs are likely

different from those of OsCaMs and possibly serve distinct roles, and support the classification of the proteins encoded by the five highly conserved *OsCam* genes as "true" CaM.

Among the OsCMLs under investigation, excluding their C-terminal extension, OsCML1 and OsCML3 share the highest amino acid identities with OsCaM1 (84.6% and 68.9%, respectively) and contain relatively high percentage of conserved methionine (M) residues (4.3% and 4.9%, respectively). These characters reflect in the results of ANS fluorescence in which their emission maximum significantly shifted and increased in the presence of Ca^{2+} similar to those from OsCaMs. However, the CD spectrum of OsCML1 and OsCML3 did not reveal an obvious increase in the helical content upon Ca^{2+}-binding suggesting that structural changes occur were not exactly the same as those of OsCaM proteins. It is interesting to know whether the C-terminal extensions in OsCML1 and OsCML3 play any roles in these differences. OsCML8 and OsCML13, which share lower amino acid identity percentages with OsCaM1 (47.0% and 43.6%, respectively) exhibited a smaller degree of increases in molar ellipticity per residue at 208 and 222 nm of the CD spectrum as well as a smaller blue shift and intensity increment of ANS fluorescence even though they possess a very high percentage (5.2% and 5.3%, respectively) of methionine (M) residues (most of them are in the same positions as OsCaM1) in their molecules. Interestingly, both proteins also contain extra amino acid sequences, though on the N-terminal end, of which their regulatory functions can be speculated.

The other two OsCMLs, OsCML4 and OsCML5 that share very high amino acid identities with OsCaM1 (68.9% and 66.2%) and contain very high methionine

content (6.5% and 4.8%, respectively) were found to behave very similarly to OsCaM proteins except only that, upon Ca^{2+}-binding, their emission maximum in ANS fluorescence did not increase as much. Among the proteins examined, OsCML5 displayed the highest degree of change in its molar ellipticity per residue at 208 nm (68.2%) when binds to Ca^{2+}, even more so than OsCaM proteins. OsCML5 has some interesting feature which is the extra region rich in glycine (G) between the two pair of its two EF-hand pairs. This structure likely affects the conformational change upon Ca^{2+}-binding of OsCML5 as well as how this protein interacts with its target proteins because it interrupts the central helix, of which its flexibility is key to the mechanism of action of CaM.

Finally, OsCML11, which share only 44.1% amino acid identity with OsCaM1, caused similar changes in the ANS fluorescence as OsCML4 and OsCML5 but displayed a decrease in molar ellipticity per residue at 208 and 222 nm in the presence of Ca^{2+} by CD spectroscopy suggesting that OsCML11 was more helical in the Ca^{2+}-free conformation than in the Ca^{2+}-bound state. In contrast to the other proteins, OsCML11 did not clearly exhibit the gel mobility shift when mixed with Ca^{2+}. Interestingly, OsCML11 contain a relatively low percentage of methionine (M) residues compared to the other OsCML proteins and when its amino acid sequence was closely inspected, aliphatic amino acids (leucine, valine and isoleucine) were found at the corresponding methionine positions in typical CaMs. Methionines have conformational flexibility compared with leucine, valine and isoleucine and are weakly polarized allowing them to interact with highly polarized solvent water and target proteins in a sequence-independent manner. The presence of aliphatic amino

acids would likely cause the exposed surface to be less flexible and only able to interact with a target protein in a more specific manner.

OsCML proteins are a novel family of Ca^{2+}-binding proteins which possibly play critical roles in Ca^{2+}-mediated stress responses in plants. In rice, nearly all of these proteins have not been studied, both structurally and functionally. This report has shown that OsCML proteins exhibit a spectrum of structural and functional characteristics of typical CaM proteins suggesting that OsCMLs represent novel sensor proteins whose modes of actions are probably different from or overlapping with those of OsCaMs and possibly serve distinct roles. The results will guide us in an attempt to undercover the identities and functional characteristics of CML proteins from rice by further investigation into the molecular functions and physiological significance of these OsCML proteins.

CHAPTER V

CONCLUSIONS

1. From alignments of their deduced amino acid sequences, OsCaM2, OsCaM3, OsCML1, OsCML3, OsCML4, OsCML5, OsCML7, OsCML8, OsCML9, OsCML11 and OsCML13 shared 98.7, 98.7, 84.6, 68.9, 68.9, 62.2, 47.7, 47.0, 46.1, 44.1 and 43.6 % amino acid identities with OsCaM1, respectively. All OsCaM and OsCML proteins have two pairs of identifiable EF hands except OsCML9 which had a single EF hand and OsCML7 which has two separate EF hands.

2. cDNA sequences of *OsCML7*, *OsCML9*, *OsCML11* and *OsCML13* were engineered by PCR amplification to facilitate cloning in the T7-based expression plasmid, pET-21a(+). The recombinant expression plasmids were introduced into *E. coli* strain BL21 (DE3) cells and successfully used to produce the recombinant OsCML9, OsCML11 and OsCML13 proteins.

3. All OsCaM and OsCML proteins except OsCML9 could be purified by Ca^{2+} dependent hydrophobic chromatography and exhibited the characteristic electrophoretic mobility shift in the presence of calcium ion indicating that they were functional Ca^{2+}-binding proteins.

4. All OsCaM proteins (OsCaM1, OsCaM2, and OsCaM3) exhibited the ability to bind the peptide from CaM kinase II confirming their likely functionality as typical

CaMs. Conversely, all OsCML proteins examined did not bind the peptide suggesting that they likely have distinct target proteins from typical CaMs.

5. Far-ultraviolet circular dichroism (far-UV CD) spectroscopy indicated that all OsCaM and OsCML proteins under investigation contained substantial α-helical secondary structure. Upon Ca^{2+} addition, an increase in molar ellipticity per residue $[\theta]_n$ at 208 and 222 nm was clearly observed for all recombinant OsCaMs and some OsCMLs (OsCML4, OsCML5 and OsCML8) indicating that the helical content was highly increased in these proteins upon Ca^{2+} binding. In contrast, OsCML11 displayed a decrease in $[\theta]_n$ while OsCML1, OsCML3 and OsCML9 displayed very little change in $[\theta]_n$.

6. In the presence of Ca^{2+}, the fluorescence spectrum of ANS mixed with each of the three OsCaM proteins or either of the two most highly conserved OsCMLs, OsCML1 and OsCML3, exhibited significant blue shifts in the maximum emission wavelengths and relatively large concomitant increases in the intensity, while the other OsCMLs exhibited smaller blue shifts and lower levels of intensity increment. Nonetheless, these results suggested that the hydrophobic patches on the surface of these proteins were exposed upon Ca^{2+} binding.

7. OsCML proteins exhibited a spectrum of both structural and functional characteristics differ from typical CaM proteins. These results suggested that OsCMLs represent novel sensor proteins whose modes of action were probably different from or overlapping with those of OsCaMs and possibly served distinct roles.

REFERENCES

Allen, G. J., Chu, S. P., Harrington, C. L., Schumacher, K., and Hoffmann, T. (2001). A defined range of guard cell calcium oscillation parameters encodes stomatal movements. *Nature*. 411: 1053-1057.

Allen, G. J., Chu, S. P., Schumacher, K., Shimazaki, C. T., Vafeados, D., and Kemper, A. (2000). Alteration of stimulus-specific guard cell calcium oscillations and stomatal closing in *Arabidopsis* det3 mutant. *Science*. 289: 2338-2342.

Babu, Y. S., Bugg, C. E., and Cook, W. J. (1988). Structure of calmodulin refined at 2.2 A resolution. *J Mol Biol.* 204: 191-204.

Beckingham, K. (1991). Use of site-directed mutations in the individual Ca^{2+}-binding sites of calmodulin to Ca^{2+}-induced conformational changes. *J Biol Chem*. 266: 6027-6030.

Bollag, D. M., Rozycki, M. D., and Edelstein, S. J. (1996). *Protein methods*. 2nd ed. New York: Wiley-Liss, Inc.

Bologna, G., Yvon, C., Duvaud, S., and Veuthey, A.-L. (2004). N-terminal myristoylation predictions by ensembles of neural networks. *Proteomics*. 4: 1626-1632.

Boonburapong, B., and Buaboocha, T. (2007). Gonome-wide identification and analyses of the rice calmodulin and related potential calcium sensor proteins. *BMC Plant Biol.* 7: 1-17.

Brokx, R. D., Scheek, R. M., Weljie, A. M., and Vogel, H. J. (2004). Backbone dynamic properties of the central linker region of calcium-calmodulin in 35% trifluoroethanol. *Journal of structural biology*. 146: 272-280.

Cates, M. S., Teodoro, M. L., Phillips, G. N. Jr., McCormack, E., Tsai, Y.C., and Braam, J. (2005). Handling calcium signaling: Arabidopsis CaMs and CMLs. *Trends Plant Sci*. 10: 383-389.

Chattopadhyaya, R., Meador, W. E., and Means, A. R., (1992). Calmodulin structure refined at 1.7 A° resolution. *J.Mol.Biol*. 228: 1177–1192.

Chiasson, D., Ekengren, S. K., Martin, G. B., Dobney, S. L., and Snedden, W.A. (2005) Calmodulin-like proteins from Arabidopsis and tomato are involved in host defense against *Pseudomonas syringae* pv. tomato *Plant Mol Biol*. 58: 887–897.

Delk, N. A., Johnson, K. A., Chowdhury, N. I., and Braam, J. (2005). CML24, regulated in expression by diverse stimuli, encodes a potential Ca^{2+} sensor that functions in responses to abscisic acid, daylength, and ion stress. *Plant Physiology*. 139: 240-253.

Dong, A., Xin, H., Yu, Y., Sun, C., Cao, K., and Shen, W-H. (2002). The subcellular localization of an unusual rice calmodulin isoform, OsCaM61, depends on its prenylation status. *Plant Mol Biol*. 48: 203-210.

Dubendorff, J. W., and Studier, F. W. (1991**).** Controlling basal expression in an inducible T7 expression system by blocking the target T7 promoter with lac repressor. *J. Mol. Biol*. 219: 45-59.

Emanuelsson, O., Nielson, H., Brunak, S., and Von Heijne, G. (2000). Predicting subcelluar localization of proteins based on their N-terminal amino acid sequence. *J Mol Biol*. 300: 1005-1016.

Evans, N. H., McAinsh, M. R., and Hetherington, A. M. (2001). Calcium oscillations in higher plants. *Curr Opin Plant Biol*. 4: 415-420.

Falke, J. J., Drake, S. K., Hazard, A. L., and Peersen, O. B. (1994). Molecular tuning of ion binding to calcium signaling proteins. Quart. *Rev. Biophys*. 27: 219-290.

Gellman, S. H. (1991). On the role of methionine residues in the sequence-independent recognition of nonpolar protein surfaces. *Biochemistry*. 30: 6633-6636.

Haiech, J., Kilhoffer, M. C., Lukas, T. J., Craig, T. A., Roberts, D. M., and Watterson, D. M. (1991). Restoration of the calcium binding activity of mutant calmodulins toward normal by the presence of a calmodulin binding structure. *J Biol Chem*. 266: 3427-3431.

Harmon, A. C. (2003). Calcium-Regulated protein kinase of plants. *Gravitational and Space Biology Bulletin*. 16.

Heo, W. D., et al. (1999). Involvement of specific calmodulin isoforms in salicylic acid-independent activation of plant disease resistance responses, *Proc Natl Acad Sci*. 19: 766-771.

Ikura, M., Clore, G. M., Gronenborn, A. M., Zhu, G., Klee, C. B., and Bax, A. (1992). Solution structure of a calmodulin-target peptide complex by multidimensional NMR. *Science*. 256: 632-638.

Karita, E., Yamakawa, H., Mitsuhara, I., Kuchitsu, K., and Ohashi, Y. (2004). Three types of tobacco calmodulins characteristically activate plant NAD kinase at different Ca^{2+} concentrations and pHs. *Plant Cell Physiol*. 45: 1371-1379.

Klee, C. B., Ren, H., Wang, X. (1998). Regulation of calmodulinstimulated protein phosphatase, calcineurin. *J Biol Chem*. 273: 13367-13370.

Kohler, C., and Neuhaus, G. (2000). Characterisation of calmodulin binding to cyclic nucleotide-gated ion channels from *Arabiodpsis thaliana*. *FEBS Lett.* 4710: 133-136.

Kuboniwa, H., Tjandra, N., Grzesiek, S., Ren, H., Klee, C. B., and Bax, A. (1995). Solution structure of calcium-free calmodulin. *Nat Struct Biol*. 2: 768-776.

Kurokawa, H., et al. (2001). Target-induced conformational adaptation of calmodulin revealed by the crystal structure of a complex with nematode Ca(2+)/calmodulin-dependent kinase kinase peptide. *J. Mol. Biol.* 312: 59-68.

Lee, S. H., et al. (2000). Differential regulation of Ca^{2+}:calmodulin-dependent enzymes by plant calmodulin isoforms and free Ca^{2+}concentration. *Biochem J.* 350: 299-306.

Lee, S. H., et al. (1995). Identification of a novel divergent calmodulin isoform from soybean which has differential ability to activate calmodulin-dependent enzymes. *J Biol Chem*. 270: 21806-21812.

Lee, S. H., et al. (1999). Competetive binding of calmodulin isoforms to calmodulin-binding proteins: implications for the function of calmodulin isoforms in plant. *Biochim Biophys Acta.* 1433: 56-67.

Lee, S. H., et al. (1997). Differential activation of NAD kinaseby plant calmodulin isoforms. The critical role of domainI. *J Biol Chem.* 272: 9252-9259.

Li, D. F., Li, J., Ma, L., Zhang, L., and Lu, Y. T. (2006). Calmodulin isoform-specific activation of a rice calmodulin-binding kinase conferred by only three amino-acids of OsCaM61. *FEBS Letters.* 580: 4325-431.

Li, S., Xie, Li., Meng, Q., and Zhang, R. (2006). Significance of the extra C-terminal tail of CaLP, a novel calmodulin-like protein involved in oyster calcium metabolism. *Comparative Biochemistry and Physiology.* 144: 463-471.

Luan, S., Kudla, J., Rodriguez-Concepcion, M., Yalovsky, S., and Gruissem, W. (2002). Calmodulins and Calcineurin B–like Proteins: calcium sensors for specific signal response coupling in plants. *Plant Cell.* S389-S400.

Malhó, R., Moutinho, A., van dyer Luit, A., and Trewavas, A. J. (1998). Spatial characteristics to calcium signalling; the calcium wave as a basic unit in plant cell calcium signaling. *Philos Trans R Soc Lond B.* 353: 1463-1473.

McCormack, E., and Braam, J. (2003). Calmodulins and related potential calcium sensors of Arabidopsis. *New Phytologist.* 159: 585-598.

McCormack, E., Tsai, Y.-C., and Braam, J. (2005). Handling calcium signalling: Arabidopsis CaMs and CMLs. *Trends Plant Sci.* 10: 383-389.

Nayyar, H. (2003). Calcium as environmental sensor in plants. *Curr. Sci.* 84, 893-902.

Novagen. 2002. *pET system manual*, 10th ed. www.novagen.com. pp. 11-15.

O'Neil, K. T., and DeGrado, W. F. (1990). How calmodulin binds its targets: sequence independent recognition of amphiphilic alphahelices. *Trends Biochem Sci*. 15: 59-64.

Reddy, A. S. N. (2001). Review Calcium: silver bullet in signaling. *Plant Sci.* 160: 381-404.

Roberts, D. M., and Harmon, A. C. (1992). Calcium-modulated proteins targets of intracellular calcium signals in higher plants. *Annu Rev Plant Physiol Plant Mol Biol*. 43: 375-414.

Rodriguez-Concepcion, M., Yalovsky, S., Zik, M., Fromm, H., and Gruissem, W. (1999). The prenylation status of a novel plant calmodulin directs plasma membrane or nuclear localization of the protein. *EMBO J.* 18: 1996-2007.

Rudd, J. J., and Franklin-Tong, V. E. (2001). Unravelling response-specificity in Ca^{2+} signaling pathways in plant cells. *New Phytologist*. 151: 7-33.

Snedden, W. A., and Fromm, H. (2001). Calmodulin as a versatile calcium signal transducer in plants. *New Phytologist*. 151: 35-66.

Sistrunk, M. L., Antosiewicz, D. M., Purugganan, M. M., and Braam, J. (1994). Arabidopsis *TCH3* encodes a nove1 Ca^{2+}-binding protein and shows environmentally induced and tissue-specific regulation. *The Plant Cell*. 6: 1553-1565.

Song, J., Zhao, Q., Thao, S., Frederick, R. O., and Markley, J. L. (2004). Solution structure of a calmodulin-like calcium-binding domain from *Arabidopsis thaliana*. *J Biomol NMR*. 30: 451-456.

Strynadka, N. C., and James, M. N. (1989). Crystal structures of the helix-loop-helix calcium-binding proteins. *Annu Rev of Biochem*. 58: 951-998.

Studier, F. W., Rosenberg, A. H., Dunn, J. J., and Dubendorff, J. W. (1990). Use of T7 RNA polymerase to direct expression of cloned genes. *Methods. Enzymol*. 185: 60-89.

Takezawa, D., Liu, Z. H., An, G., and Poovaiah, B. W. (1995). Calmodulin gene family in potato: developmental and touch-induced expression of the mRNA encoding a novel isoform, *Plant Mol Biol*. 27: 693-703.

Vanderbeld, B., and Snedden, W. A. (2007). Developmental and stimulus-induced expression patterns of Arabidopsis calmodulin-like genes *CML37*, *CML38* and *CML39*. *Plant Mol Biol*. 64: 683-697.

Vetter, S. W., and Leclerc, E. (2003). REVIEW ARTICLE: Novel aspects of calmodulin target recognition and activation. *Eur J Biochem*. 270: 404-414.

Xiao, C., Xin, H., Dong, A., Sun, C., and Cao, K. (1999). A novel calmodulin-like protein gene in rice which has an unusual prolonged C-terminal sequence carrying a putative prenylation site. *DNA Res*. 6: 179-181.

Xiong, L., Lee, H., Ishitani, M., and Zhu, J. K. (2002). Regulation of osmotic stress-responsive gene expression by the *LOS6/ABA1* locus in Arabidopsis. *J Biol Chem*. 277: 8588-8569.

Yamaguchi, T., Aharon, G. S., Sottosanto, J. B., and Blumwald, E. (2005). Vacuolar Na^+/H^+ antiporter cation selectivity is regulated by calmodulin from within the vacuole in a Ca^{2+}- and pH-dependent manner. *Proc Natl Acad Sci USA*. 102: 16107–16112.

Yang, T., and Poovaiah, B. W. (2003). Calcium/calmodulin-mediated signal network in plants. *Trends Plant Sci*. 8: 505-512.

Yun, C. H., Bai, J., Sun, D. Y., Cui, D. F., Chang, W. R., and Liang, D. C. (2004). Structure of potato calmodulin PCM6: the first report of the three-dimensional structure of a plant calmodulin. *Acta Crystallogr D Biol Crystallogr*. 60: 1214-1219.

Zhang, L., Liu, B., Liang, S., Jones, R. L., and Lu, Y. T. (2002). Molecular and biochemical characterization of a calcium/calmodulin-binding protein kinase from rice. *Biochem J*. 15: 145–157.

Zhang, L., and Lu, Y. T. (2003). Calmodulin-binding protein kinases in plants. *Trends Plant Sci*. 8: 123-127.

Zhang, M., Tanaka, T., and Ikura, M. (1995). Calcium-induced conformational transition revealed by the solution structure of apocalmodulin. *Nat Struct Biol.* 2: 758-767.

Zielinski, R. E. (1998). Calmodulin and calmodulin binding proteins in plants. *Annu Rev Plant Physiol Plant Mol Biol.* 49: 697-725.

APPENDICES

APPENDIX A

Restriction map of pTZ57R/T

Restriction map of pET-21a (+)
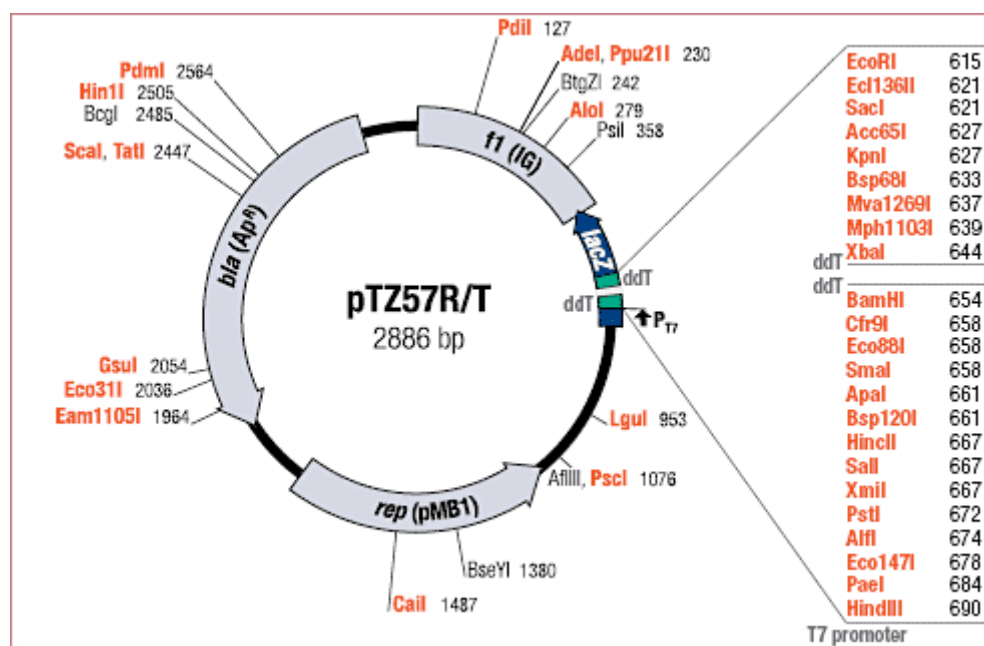
APPENDIX B

1. High Speed plasmid Mini kit protocol (Geneaid, USA)

1. Transfer 1.5 ml of cultured bacterial cells to a microcentrifuge tube. Centrifuge for 1 minute and discard the supernatant

2. Add 200 μl of PD1 Buffer (RNase A added) to the tube and resuspend the cell pellet by vortex or pipetting.

3. Add 200 μl of PD2 Buffer and mix gently by inverting the tube 10 times. Do not vortex to avoid shearing the genomic DNA. Let stand at room temperature for 2 minutes or until the lysate is homologous.

4. Add 300 μl of PD3 Buffer and mix immediately by inverting the tube 10 times. Centrifuge for 10 minutes and place a PD column in a 1.5 ml collection tube. Add the supernatant to the PD column and centrifuge for 1 minute. Discard the flow-through and place the PD column back in the collection tube.

5. Add 400 μl of W1 Buffer into the PD column. Centrifuge for 1 minute and discard the flow-through and place the PD column back in the collection tube. Add 600 μl of Wash Buffer (ethanol added) into the PD column.

6. Centrifuge for 1 minute and discard the flow-through and place the PD column back in the collection tube. Centrifuge again for 3 minutes to dry the column matrix.

7. Transfer the dried PD column to a new microcentrifuge tube. Add 50 μl of Elution Buffer or H_2O into the center of the column matrix. Let stand for 2 minutes and centrifuge for 2 minutes to elute the DNA.

APPENDIX C

Chemical solution

1. **Plasmid DNA isolation by alkaline lysis method**

   Lysis buffer (Buffer P1)

Tris base	1.51 g (50 mM)
Na$_2$EDTA·2H$_2$O	0.93 g (10 mM)
H$_2$O	200 ml

   Adjust pH to 8.0 with HCl, adjust the volume to 250 ml with distilled water then add 25 mg (100 µg/ml) RNaseA and store at 4°C

   Alkaline-SDS solution (Buffer P2)

1 M NaOH	50 ml (200 mM)
H$_2$O	150 ml

   Mix well and add 12.5 ml of 20% SDS then adjust volume to 250 ml with distilled water and store at room temperature

   High salt buffer (Buffer P3)

Potassium acetate	73.6 g (3 M)
H$_2$O	150 ml

Adjust pH to 5.5 with glacial acetic acid and adjust the volume to 250 ml with distilled water and and autoclave for 20 minutes at 121 °C

2. Preparation for protein determination by Bradford, M. M. (1976)

Bradford solution

Coomassie Brilliant Blue (G250)	100 mg
Absolute ethanol	50 ml

Stir the solution in a container protected from light for 2 hours and adjust 100 of 85% phosphoric acid. Bring the volume to 1 L with distilled water and filter through a sterile, 0.22 μm nitrocellulose filter. Store the solution in a brown glass bottle (usable for several weeks).

3. Preparation for polyacrylamide gel electrophoresis

Separating gel buffer 8X

Tris base	181.7 g
H_2O	250 ml

Adjust pH to 8.8 with conc. HCl, bring the volume to 500 ml with distilled water. Filter through a 0.22 μm nitrocellulose and store at room temperature.

Stacking gel buffer 4X

Tris base	15.1 g
H_2O	150 ml

Adjust pH to 6.8 with conc. HCl, bring the volume to 250 ml with distilled water. Filter through a 0.22 μm nitrocellulose and store at room temperature.

Acrylamide, 30% A: 0.8% B

Acrylamide	150 g
Bisacrylamide	4 g

Dissolve in final volume of 500 ml in distilled water. Filter through a 0.22 μm nitrocellulose and store at 4 °C in a dark bottle.

Reservoir buffer 10X

Tris base	60.5 g
Glycine	288 g

Dissolve in final volume of 2 L in distilled water. Store at room temperature. Before use, add 2 g of SDS (0.1% SDS).

20% (w/v) SDS

Sodium dodecylsulfate	20 g

Adjust the volumn to 100 ml with distilled water. Stir rapidly to dissolve completely and filter through a sterile, 0.22 μm nitrocellulose filter.

Sample buffer 5X

1M Tris-HCl, pH 6.9	60 μl
20% (w/v) SDS	100 μl

Glycerol	790 μl
2-mercaptoethanol	50 μl
Bromophenol blue	1 mg

Adjust the volume to 1 ml with distilled water. Store at -20 °C in 1 ml aliquots.

Sample buffer 5X for Urea-PAGE

1M Tris-HCl, pH 6.9	60 μl
Glycerol	790 μl
Bromophenol blue	1 mg

Adjust the volume to 1 ml with distilled water. Store at -20 °C in 1 ml aliquots.

10% (w/v) Ammonium Persulfate

Ammonium persulfate	0.5 g

Dissolve in a final volume of 5 ml in H_2O. Store at 4 °C. Prepare fresh every two weeks.

SDS-PAGE

12.5% Separating gel

Acrylamide, 30% A: 0.8% B	5 ml

Separating gel buffer 8X   1.5 ml

20% (w/v) SDS   30 µl

Distilled water   5.4 ml

10% (w/v) Ammonium persulfate   60 µl

TEMED   6 µl

4% Stacking gel

Acrylamide, 30% A: 0.8% B   0.65 ml

Stacking gel buffer 4X   1.25 ml

20% (w/v) SDS   12.5 µl

Distilled water   3 ml

10% (w/v) Ammonium persulfate   37.5 µl

TEMED   2.5 µl

Polyacrylamide gel containing 4 M urea

12.5% Separating gel

Acrylamide, 30% A: 0.8% B   5 ml

Separating gel buffer 8X   1.5 ml

Urea   2.88 g

100 mM CaCl$_2$ or   120 μl (final concentration 1 mM)

150 mM EGTA   240 μl (final concentration 3 mM)

Adjust the volumn to 12 ml with distilled water

10% (w/v) Ammonium persulfate   60 μl

TEMED   6 μl

4% Stacking gel

Acrylamide, 30% A: 0.8% B   0.65 ml

Stacking gel buffer 4X   1.25 ml

Urea   1.2 g

100 mM CaCl$_2$ or   50 μl (final concentration 1 mM)

150 mM EGTA   100 μl (final concentration 3 mM)

Adjust the volumn to 5 ml with distilled water

10% (w/v) Ammonium persulfate 37.5 μl

TEMED   2.5 μl

4. Protein staining solution

Staining solution, 1 litre

Coomassie Brilliant Blue R250	2.5 g
Methanol	500 ml
Glacial acetic acid	70 ml
H_2O	430 ml

Dissolve with rapid stirring and store at room temperature.

Destaining solution

Methanol	100 ml
Glacial acetc acid	70 ml
H_2O	830 ml

Dissolve with rapid stirring and store at room temperature.

BIOGRAPHY

Mr. Aumnart Chinpongpanich was born on June 20, 1983 in Bangkok. After he finished high school in 1999 from Bangkok Christian College School in Bangkok, he was enrolled in the Department of Biochemistry at Kasetsart University and graduated with the degree of Bachelor of Science in 2003. He has studied for the degree of Master of Science at the Department of Biochemistry, Faculty of Science, Chulalongkorn University since 2007.